Mathematik

An unfitted discontinuous Galerkin scheme for a phase-field approximation of pressurized fractures

Inaugural-Dissertation
zur Erlangung des Doktorgrades
der Naturwissenschaften im Fachbereich
Mathematik und Informatik
der Mathematisch-Naturwissenschaftlichen Fakultät
der Westfälischen Wilhelms-Universität Münster

vorgelegt von
Liesel Sommer, geb. Schumacher
aus Berlin, Deutschland
–2019–

Dekan:	Prof. Dr. Xiaoyi Jiang
Erster Gutachter:	Prof. Dr. Christian Engwer
Zweiter Gutachter:	Prof. Dr. Benedikt Wirth
Tag der mündlichen Prüfung:	26.11.2019
Tag der Promotion:	26.11.2019

Abstract

The simulation of the propagation of pressurized, fluid-filled fractures in the subsurface is of great interest since it allows to numerically evaluate the safety of modern techniques such as hydraulic fracturing and the extraction of geothermal energy. The main challenge for numerical experiments is the evolving domain, forcing standard finite element methods to require remeshing whenever fractures propagate. To overcome that problem unfitted methods as the unfitted discontinuous Galerkin (UDG) method and the extended finite element method (X-FEM) introduce new basis functions along the crack. Alternatively, phase-field approaches describe the crack implicitly and regularize it in the sense of Γ-convergence. In contrast to the former, the latter automatically deals with branching and joining of cracks as well as predicting the direction and velocity of a propagating crack. On the other hand, implicit methods are computationally far more expensive as the phase field must have a high resolution in the proximity of cracks. The present thesis combines a phase-field approach with the UDG method to exploit the advantages of both. Quasi-static evolution of fluid-filled, pressurized fractures is considered. The implicit representation of cracks predicts the propagation path and velocity and handles changes in the crack topology. An explicit representation of the crack is then reconstructed as medial axis of a level set of the phase field. Applying the UDG method allows for jumps of the displacement along the reconstructed cracks. The capability of our method to simulate the crack propagation is shown in some numerical experiments.

To present, the regularization of the implicit crack description was merely studied for pure linear elasticity. In this thesis Γ-convergence of the approximating functionals to the potential energy of the system in the presence of additional pressure terms is proven. As a result the inclusion of a pressurized fluid in phase-field approaches is justified.

Zusammenfassung

Um die Sicherheit modernen Techniken wie Hydraulic Fracturing und Geothermie zu untersuchen, ist die numerische Simulation von Rissen im Untergrund, die mit einer unter Druck stehenden Flüssigkeit gefüllt sind, von großer Bedeutung. Das größte Problem dabei ist das sich verändernde Gebiet. Standard Finite Elemente Methoden müssen das Gitter ständig an den propagierenden Riss anpassen. Nicht ans Gitter angepasste Methoden, wie die "unfitted discontinuous Galerkin" (UDG) Methode und die "extended finite element method" (X-FEM) führen zur Lösung dieses Problems neue Basisfunktionen entlang von Rissen ein. Alternativ stellen Phasenfeldansätze Risse nur implizit dar und regularisieren diese Darstellung im Sinne der Γ-Konvergenz. Im Gegensatz zu Ersteren ist bei Letzteren ein automatischer Umgang mit verzweigenden und zusammenwachsenden Rissen und die exakte Bestimmung der Ausbreitungsrichtung und -geschwindigkeit möglich. Dafür muss bei impliziten Methoden das Phasenfeld in der Umgebung von Rissen fein aufgelöst sein, wodurch sie wesentlich rechenintensiver sind. Die vorliegende Dissertation kombiniert deshalb einen Phasenfeldansatz mit einer UDG Methode um die Vorteile beider Methoden auszunutzen. Dabei wird die quasi-statische Entwicklung von flüssigkeitsgefüllten, unter Druck stehenden Rissen betrachtet. Die implizite Darstellung von Rissen wird verwendet, um Ausbreitungsrichtung und -geschwindigkeit zu prognostizieren und topologische Änderungen zu behandeln. Daraus wird eine explizite Darstellung der Risse als mediale Achse einer Niveaumenge des Phasenfeldes gewonnen. Die UDG Methode erlaubt dann Sprünge für die Verschiebung entlang der rekonstruierten Risse. Wir zeigen die Anwendbarkeit unserer Methode zur Simulation von Rissausbreitung in verschiedenen numerischen Experimenten.

Die Regularisierung der impliziten Rissdarstellung ist bis jetzt nur im Falle linearer Elastizität untersucht. In der vorliegenden Arbeit wird Γ-Konvergenz der approximierenden Funktionale gegen die potentielle Energie des Systems auch im Falle von zusätzlichen Drucktermen bewiesen. Dieses Ergebnis rechtfertigt die Einbeziehung einer unter Druck stehenden Flüssigkeit in Phasenfeldmodellen.

Acknowledgments

I would like to express my sincere gratitude to all people that made writing this thesis possible. First of all I am very grateful to my advisor Prof. Dr. Christian Engwer, who introduced me to this interesting and challenging subject. He always supported me and guided my way through scientific challenges and implementation problems. I would also like to thank Prof. Dr. Benedikt Wirth for co-advising my thesis and for his interest in my research topic. For fruitful discussions on Γ-convergence my deepest thanks go to Prof. Dr. Caterina Zeppieri and Annika Bach.
My profound gratitude goes to my colleagues at the "Institute of Applied Mathematics", especially René Milk for his help with technical questions and Andreas Nüssing for all the discussions on unfitted discontinuous Galerkin methods. For kindly proofreading my thesis I would like to thank Annika Bach, René Milk, Carolin Roßmanith, Jens Schumacher and Oliver Sommer.
Last but not least, this thesis would not have been possible without the ongoing support and understanding of my family and friends and I am very grateful for their help and patience.

Contents

List of Figures

List of Tables

1 Introduction

In recent years the interest in predicting the path fractures take in the subsurface has increased tremendously. Accurate and efficient predictions are one of the major challenges for new technologies in energy and environmental research. The best-known application might be the controversial technique of hydraulic fracturing. Injecting a pressurized liquid into the subsurface via wells induces and enlarges cracks in the rock. As a consequence the flow of oil or gas can be simplified. While the described technique allows to obtain such fossil resources from unconventional deposits, its risks for the environment, especially the ground water, yet remain to be investigated thoroughly. A similar process is used in enhanced geothermal systems. To increase the energy extraction from underground heat reservoirs, cold water is pumped into the rock at high pressure. By this process called hydro-shearing the permeability of the rock is enhanced. Both of these examples have in common that a fluid-filled fracture propagates due to high pressures. The contrary is the goal when geologically sequestrating carbon dioxide in the ground. While injecting CO_2 into geological storages one wants to keep the pressure at acceptable levels. Indeed, if the pressure were exceedingly high as to cause hydro-fracturing, the surrounding matrix could be harmed. As a result, the CO_2 would no longer be sealed properly.

All three described technologies have the potential to contribute substantially to the fight against climate change and play an important role for modern energy solutions. However, prior to being able to apply them safely, the risks for the environment and the population must be understood. In addition to direct impacts on the ground water, the changed fracture network and permeability might also affect earthquake probabilities. Due to the dangers and the large scales involved, it is rather difficult and expensive to conduct risk studies in-situ. As a consequence, numerical modeling of the propagation of fluid-filled fractures in the subsurface becomes an important prediction tool. Despite having the further advantage to enable long-term simulations, numerical studies face some challenges. First, very different length-scales are involved. While sometimes the complete discrete fracture network has to be considered, many processes happen on the significantly smaller scale of single cracks. The objective of the present thesis is to concentrate on the latter, the behavior of individual fractures, especially under the injection of a pressurized fluid.

However, even under restriction to one length-scale, the simulation of the propagation process gives rise to a second substantial numerical challenge. The behavior of cracks can be described by partial differential equations (PDEs). The standard approach to numerically solve these would include mesh based techniques like the finite element method (FEM). In any such method it is

not reasonable to assume that the evolving fracture will stick to element boundaries. We rather expect it to cut right through mesh cells. Any classical FEM would thus need a remeshing step whenever the crack propagates to regain an exact representation of the fracture by the mesh. As the fractures might not only change geometrically, but even topologically (for example if two cracks join) this process is rather demanding. Furthermore, it is not only the remeshing itself that is computationally expensive, the new mesh also leads to an increased amount of degrees of freedom. To overcome this problem, new methods avoiding the remeshing step have been developed.

In order to take the crack into account, one alternative approach is using unfitted methods that enrich the function space locally. In [MDB99] Moes et al. introduced the "extended finite element method" (X-FEM), the best-known strategy in this context. A similar approach is given by the "partition of unity method" [BM97]. Using X-FEM the crack is modeled by introducing new basis functions along the propagating fracture. Classically the basis is enriched by the sign function or the Heaviside function, thus reflecting the expected discontinuity at the crack. For an overview of successful applications of X-FEM we refer the interested reader to [FB10, Fri14]. One major problem in X-FEMs is the choice of enrichment functions at crack tips. At these points the induced stresses are singular. In particular it is rather challenging to determine the correct crack speed and direction [BCXZ03]. In addition, special treatment is needed for topological changes in the crack, such as the joining of two cracks or the branching of a single crack [BZMB04].

Alongside with remeshing techniques and the unfitted methods there exists a third approach overcoming these difficulties. In [FM98] Francfort and Marigo introduce a method that describes the crack implicitly. This means it automatically deals with topological changes and avoids the problems occurring at crack tips in unfitted methods. Based on Griffith's criterion [Gri21] an energy minimization problem characterizes the process of crack propagation. The resulting energy explicitly includes the shape of the crack and is therefore difficult to handle numerically. A solution to this problem is found noting the resemblance with the Mumford-Shah functional from image segmentation [MS89]. Ambrosio and Tortorelli [Amb89] proposed a regularization of the latter exploiting the concept of Γ-convergence. Transferring their ideas to the context of fracture propagation, a so-called phase field $0 \leq \varphi \leq 1$ is introduced to regularize the crack. As some regularization parameter ε goes to zero, φ becomes equal to one almost everywhere and approaches zero along the crack. The regularized energy thus converges to the discrete one in the sense of Γ-limits as $\varepsilon \to 0$. This implicit representation of the crack does not only avoid remeshing but is also capable of determining the propagation velocity and direction of fractures. Furthermore it automatically handles events such as the branching and joining of cracks. It was successfully applied in numerical studies [BFM00, BFM08, KM10, MHW10, MWW15b]. While the former studies only deal with the elastic behavior of the matrix surrounding the fracture, the latter introduce a pressure inside the fracture into the framework.

In recent years there were also developments combining the advantages of unfitted methods with phase-field approaches. For example an X-FEM approach can be combined with a phase-field model around the tip [GSF17]. Thus the phase field predicts propagation direction and velocity.

A reconstruction of the crack based on its regularization is then used to employ an X-FEM and thereby reduce computational complexity. Approaches coupling damage models, which implicitly describe the crack, with methods including explicit discontinuities for the surrounding bulk can be found in [RLS15] and [TMRF15].

The present thesis follows the path of combining a phase-field representation of the crack with an unfitted method. The novelty in the method lies in applying an unfitted discontinuous Galerkin (UDG) discretization [BE09] rather then the standard continuous Galerkin method as in X-FEM. As our goal is to simulate actual discontinuities along the crack this seems a rather natural approach. Furthermore the advantages of DG such as easy generalization to higher order, natural integration of conservation properties and simplification of parallelization could prove beneficial in the future. Starting with a discretization that combines a phase field with a DG discretization for the displacement, we reconstruct the crack and omit the weak enforcement of continuity along this crack. Allowing the fractures to cut through elements we end up with an UDG discretization for the displacement in the rock surrounding the fracture. In doing this, we do not only consider linear elastic behavior of the material but also include the pressure in the underlying energy formulation describing the fracture propagation process.

While it is not new to include pressure terms in the numerical treatment of fracture propagation, the regularization in analogy to the Mumford-Shah functional was not studied in detail to this day. Γ-convergence in the presence of pressure with respect to convergence in the strong L^1-topology is investigated in the present thesis. Further the circumstances under which the results obtained imply convergence of minimizers, and thereby justify the usage of the regularized energy functionals for numerical treatment, are discussed.

The present thesis consists roughly of three parts. First, Chapter 2 introduces some preliminaries. The energy used to describe the fracture propagation process is developed. Next a short introduction to Γ-convergence and the strongly related spaces of functions of bounded variation and bounded deformation is given. Finally the finite element method and its discontinuous variants DG and UDG are shortly recalled. Second, Chapter 3 proves Γ-convergence of the regularized energy functionals to the discrete energy functional. The special case of a one-dimensional situation is analyzed first, followed by the proof for higher dimensions. Finally convergence of minimizers based on criteria for the equi-coercivity of the underlying functionals is discussed. The third part of this thesis comprises the numerical treatment of the problem. In Chapter 4 the discretization scheme is derived. Starting from a DG scheme an unfitted version allowing for actual discontinuities along the crack is developed. Further the process of reconstructing the crack from the phase field is described in more detail. Chapter 5 deals with some implementational details. In particular it discusses how to implement the reconstruction of the crack and how to include it into the grid in a way suitable for the application of the UDG method. Chapter 6 closes the numerical part of this thesis with some validation studies. Finally, Chapter 7 summarizes our findings and discusses possible future research.

2 Preliminaries

2.1 Basic notation

In this section we fix some basic notation applied throughout the present thesis. Given a matrix $A \in \mathbb{R}^{n\times n}$ we write A^T for its transposed and $\operatorname{tr} A$ for its trace. If $A = A^T$, the matrix A is called symmetric and we write $A \in \mathbb{R}^{n\times n}_{\mathrm{sym}}$. Further we denote by $I \in \mathbb{R}^{n\times n}$ the n-dimensional identity matrix. For two matrices $A = (a_{ij})_{i,j=1}^{n} \in \mathbb{R}^{n\times n}$ and $B = (b_{ij})_{i,j=1}^{n} \in \mathbb{R}^{n\times n}$ the inner product is written as $A : B = \sum_{i,j=1}^{n} a_{ij} b_{ij}$.
For $x \in \mathbb{R}$, $v \in \mathbb{R}^n$ and $A \in \mathbb{R}^{N\times n}$ we denote by $|x|$, $|v|$ and $|A| = \sqrt{\operatorname{tr}(A^T A)}$ the absolute value, the Euclidean norm of a vector and the Frobenius norm of a matrix, respectively. For a set S we denote by $\#(S)$ its cardinality. Moreover, the distance of a point $x \in \mathbb{R}^n$ from a set $S \subset \mathbb{R}^n$ is given as $\operatorname{dist}(x, S) = \inf_{y\in S}(|x - y|)$. By $B_\rho(x) = \{y \in \mathbb{R}^n : |x - y| < \rho\} \subset \mathbb{R}^n$ we denote the n-dimensional ball of radius ρ and by $\mathbb{S}^{n-1} = \partial B_1(0) \subset \mathbb{R}^n$ the $(n-1)$-dimensional unit sphere.

Throughout this thesis Ω will be an open and bounded subset of $\mathbb{R}^n$ with Lipschitz boundary $\partial\Omega$. Moreover we define $\mathcal{A}(\Omega) = \{A \subset \Omega : A \text{ is open}\}$ and $\mathfrak{B}(\Omega) = \{B \subset \Omega : B \text{ is Borel}\}$. For any set $B \in \mathfrak{B}(\Omega)$ we denote the characteristic function of B by $\mathcal{X}_B$. For two sets A_1 and A_2 we write $A_1 \Subset A_2$ if A_1 is compactly embedded in A_2.
As usual $\mathcal{L}^n$ stands for the n-dimensional Lebesgue measure. Furthermore we adopt the standard notation for Lebesgue spaces. Namely for $1 \le p \le +\infty$ and any positive integer m we denote the L^p-spaces and their localized versions by

$$L^p(\Omega;\mathbb{R}^m) = \left\{u\colon \Omega \to \mathbb{R}^m : u \text{ is measurable and } \|u\|_{L^p(\Omega;\mathbb{R}^m)} < +\infty\right\} \text{ and}$$
$$L^p_{loc}(\Omega;\mathbb{R}^m) = \left\{u\colon \Omega \to \mathbb{R}^m : u \text{ is measurable and } \|u\|_{L^p(K;\mathbb{R}^m)} < +\infty \text{ for all } K \subset \Omega \text{ compact}\right\},$$

where we recall the p-norm for $A \subset \Omega$

$$\|u\|_{L^p(A;\mathbb{R}^m)} = \left(\int_A |u|^p \,\mathrm{d}x\right)^{\frac{1}{p}} \qquad \text{for } 1 \le p < +\infty$$
$$\|u\|_{L^\infty(A;\mathbb{R}^m)} = \operatorname*{ess\,sup}_{x\in A} |u(x)|.$$

Here ess sup denotes the essential supremum. In particular we consider L^p-functions with values in $\mathbb{R}$, $\mathbb{R}^n$ and $\mathbb{R}^{N\times n}$ and omit the $\mathbb{R}$ in the first case. To emphasize vector-valued functions we

use the notation $\mathbf{u}$ in the case $\mathbb{R}^n$ in contrast to u for functions with values in $\mathbb{R}$. Finally let us summarize the standard notation for Sobolev spaces. For $k \in \mathbb{N}$ and $1 \leq p \leq +\infty$ and $m \in \mathbb{N}$, $m > 0$ we recall

$$W^{k,p}(\Omega;\mathbb{R}^m) = \{u \in L^p(\Omega;\mathbb{R}^m) : D^\alpha u \in L^p(\Omega;\mathbb{R}^m) \text{ for all } |\alpha| < k\},$$

where $D^\alpha u$ denotes the weak partial derivative corresponding to the multi-index α. We equip these spaces with the Sobolev norm

$$\|u\|_{W^{k,p}(\Omega;\mathbb{R}^m)} = \left(\sum_{|\alpha|<k} \int_\Omega |D^\alpha u|^p \,\mathrm{d}x\right)^{\frac{1}{p}} \qquad \text{if } 1 \leq p < +\infty$$
$$\|u\|_{W^{k,\infty}(\Omega;\mathbb{R}^m)} = \sum_{|\alpha|<k} \operatorname*{ess\,sup}_{x\in\Omega} |D^\alpha u(x)|.$$

For a given function $\mathbf{u}_D \in W^{k,p}(\mathbb{R}^n;\mathbb{R}^m)$ we define the space with Dirichlet boundary conditions as

$$W_D^{k,p}(\Omega;\mathbb{R}^m) = \left\{\mathbf{u} \in W^{k,p}(\mathbb{R}^n;\mathbb{R}^m) : \operatorname{tr}\mathbf{u}|_{\partial\Omega} = \operatorname{tr}\mathbf{u}_D|_{\partial\Omega}\right\},$$

where $\operatorname{tr}\mathbf{u}$ denotes the trace of $\mathbf{u}$. For $p = 2$ we write $H^k(\Omega;\mathbb{R}^m) = W^{k,2}(\Omega;\mathbb{R}^m)$, $H_D^k(\Omega;\mathbb{R}^m) = W_D^{k,2}(\Omega;\mathbb{R}^m)$ and as before for $m = 1$ we omit the $\mathbb{R}$.

2.2 Pressurized fractures

The main aim of this thesis is to simulate the propagation of pressurized fractures in the subsurface. In this section we derive the governing equations describing the arising phenomena, following the approach of Griffith [Gri21]. His ideas inspired Francfort and Marigo [FM98] to study the phenomena of brittle fracture as an energy minimizing problem. Their work was the basis for a wide range of papers interested in the numerical simulation of fracture propagation in a poroelastic medium, see for example [BFM00, BFM08, KM10, MHW10, MWW15b]. We follow their modeling approach, resulting in a total potential energy which needs to be minimized. We start by decomposing the energy into bulk and surface parts. Subsequently we describe each of them in more detail.

2.2.1 Energy formulation

A well known principle in mechanics is the principle of minimal total potential energy, see [Red17]. It states that the equilibrium state of an elastic solid is at a state of minimal total energy. Griffith [Gri21] extends this principle to claim that a material will break, provided this final broken

equilibrium state can be reached by only decreasing the total potential energy of the system. Thus he provides us with a criterion for crack propagation. To derive the total potential energy of the system, we divide it into two components. The first part is given by the energy stored in the bulk. This bulk energy is defined on the domain $\Omega \setminus \overline{\mathcal{C}} \subset \mathbb{R}^n$ and denoted by $E_b(\mathbf{u}, \mathcal{C})$. Here $\mathbf{u}$ is the vector of displacement and $\mathcal{C}$ describes the crack. Following [MWW15a] we think of $\mathcal{C} \subset \mathbb{R}^n$ as an n-dimensional domain with sufficiently smooth boundary $\partial\mathcal{C}$. The second part of the energy describes the surface energy $E_s(\mathbf{u}, \mathcal{C})$ at the outer boundary $\partial\Omega$ and at the crack $\mathcal{C}$. Thus the total potential energy of the system is given by

$$E(\mathbf{u}, \mathcal{C}) = E_b(\mathbf{u}, \mathcal{C}) + E_s(\mathbf{u}, \mathcal{C}).$$

The problem of fracture propagation is then solved by minimizing $E(\mathbf{u}, \mathcal{C})$ with respect to $\mathcal{C}$ and $\mathbf{u}$. Furthermore we need to avoid healing of existing cracks. Therefore the minimization takes place under the constraint that the crack $\mathcal{C}$ can only grow, never shrink. This is called the irreversibility condition. In the remainder of this section we will the two parts of $E(\mathbf{u}, \mathcal{C})$ more closely.

2.2.2 Bulk energy

To derive an equation for the bulk energy we have to make some assumptions on the medium in which we want to describe the propagation of fractures. A classical assumption is to consider a linear porous medium in which the energy is described by linear elasticity. This approach can be found for example in the papers [MHW10, KM10]. There are two underlying equations which describe the phenomenon of linear elasticity. At first we need a description of the relation between the stress tensor σ and the strain tensor $e(\mathbf{u})$, where the latter denotes the symmetric gradient of $\mathbf{u}$. Second we need an equation of motion, derived from Newton's second law. With μ and λ denoting the material dependent Lamé parameters and $\mathbb{C}$ the fourth-order linear elasticity tensor for an isotropic material given by

$$\mathbb{C}A = 2\mu A + \lambda \operatorname{tr} A \quad \forall A \in \mathbb{R}^{n\times n}_{\text{sym}} \tag{2.1}$$

the stress-strain relation reads $\sigma = \mathbb{C}e(\mathbf{u})$ in $\Omega \setminus \mathcal{C}$. We recall that $\mathbb{C}$ satisfies for all $A \in \mathbb{R}^{n\times n}_{\text{sym}}$

$$2\mu |A|^2 \leq A : \mathbb{C}A \leq (2\mu + n\lambda) |A|^2, \tag{2.2}$$

a property that will prove beneficial in Chapter 3 and Section 4.1.1.

Let us start with Newton's second law, $F = ma$, stating that the total forces of the system equal mass times acceleration. We consider the quasi-static situation $a = 0$. In a first step we apply no external body forces, hence F is only given by internal body forces, boundary forces are then added in equation (2.4). According to Cauchy's first law of motion, see [Tru92], the equation of motion then becomes $\nabla \cdot \sigma = 0$ in $\Omega \setminus \mathcal{C}$.

As in the work of Mikelić et al. [MWW15b, MWW15a] we want to work in a poroelastic setting, considering some pressurized fluid in the porous medium. Therefore the pressure in the bulk and the fluid-filled fracture are called p_B and p_F, respectively. Denoting by α the Biot coefficient, the governing equations in the domain $\Omega \setminus \mathcal{C}$ in a poroelastic medium, taking pressure into account, are given by the quasi-static Biot equations [Bio55]

$$\begin{aligned} \sigma &= \mathbb{C}e(\mathbf{u}) - \alpha p_B I \quad && \text{in } \Omega \setminus \mathcal{C} \\ -\nabla \cdot \sigma &= 0 && \text{in } \Omega \setminus \mathcal{C}. \end{aligned} \tag{2.3}$$

For a detailed introduction to poroelasticity and an interpretation of α see for example [Mer16].

To include the crack in our situation we need to describe boundary conditions at its surface. We assume continuity of the contact force along the crack, that is $\sigma\nu = -p_F\nu$ on $\partial\mathcal{C}$, where ν denotes the normal vector to $\partial\mathcal{C}$. Further we assume continuity of the pressure on $\partial\mathcal{C}$, setting $p = p_B = p_F$. The exterior boundary $\partial\Omega$ is divided into a Dirichlet boundary Γ_D and a Neumann boundary Γ_N. On Γ_D we describe a fixed displacement $\mathbf{u}_D$ and on Γ_N a surface force τ is applied. Thus the strong equations for our problem are

$$\begin{aligned} -\nabla \cdot (\mathbb{C}e(\mathbf{u}) - \alpha p I) &= 0 && \text{in } \Omega \setminus \mathcal{C} \\ (\mathbb{C}e(\mathbf{u}) - \alpha p I)\,\nu &= \tau && \text{on } \Gamma_N \\ \mathbf{u} &= \mathbf{u}_D && \text{on } \Gamma_D \\ (\mathbb{C}e(\mathbf{u}) - \alpha p I)\,\nu &= -p\nu && \text{on } \partial\mathcal{C}. \end{aligned} \tag{2.4}$$

We now derive a weak formulation of these equations in terms of an energy minimization problem. According to Washizu [Was74] the bulk energy is $E_b(\mathbf{u}, \mathcal{C}) = \int\limits_{\Omega\setminus\mathcal{C}} \mathrm{dA}\,\mathrm{dx}$, where we can calculate the strain energy density dA as

$$\mathrm{dA} = \sum_{i,j=1}^{3} \sigma^{ij} \mathrm{d}\left(e(\mathbf{u})\right)_{ij}.$$

Using equation (2.3) we can derive the strain energy density in the case of Biot's equation as

$$\begin{aligned} \mathrm{dA} &= \sum_{i,j} \sigma^{ij} \mathrm{d}\left(e(\mathbf{u})\right)_{ij} \\ &= \sum_{i,j} \left(\mathbb{C}e(\mathbf{u}) - \alpha p I\right)^{ij} \mathrm{d}\left(e(\mathbf{u})\right)_{ij} \\ &= \sum_{i,j} \frac{1}{2}\left(2\mu \mathbb{C}\left(e(\mathbf{u})\right)_{ij}^2 + \lambda \left(e(\mathbf{u})\right)_{ii} \left(e(\mathbf{u})\right)_{jj}\right) - \sum_{i} \alpha p \left(e(\mathbf{u})\right)_{ii} \\ &= \frac{1}{2}\Big(e(\mathbf{u}) : (2\mu e(\mathbf{u})) + e(\mathbf{u}) : (\lambda I \operatorname{tr}(e(\mathbf{u})))\Big) - \alpha p \operatorname{tr}(e(\mathbf{u})) \\ &= \frac{1}{2}\left(e(\mathbf{u}) : \mathbb{C}e(\mathbf{u})\right) - \alpha p \nabla \cdot \mathbf{u}. \end{aligned} \tag{2.5}$$

Using the strain energy density as in equation (2.5) the bulk energy reads

$$E_b(\mathbf{u}, \mathcal{C}) = \int_{\Omega \setminus \mathcal{C}} \frac{1}{2} (e(\mathbf{u}) : \mathbb{C}e(\mathbf{u})) - \alpha p \nabla \cdot \mathbf{u} \, \mathrm{dx}. \tag{2.6}$$

2.2.3 Surface energy

There are two main contributions to the surface energy. The first part translates the boundary conditions in equation (2.4) to energies due to external surface forces. These yield the energy contribution

$$-\int_{\Gamma_N} \tau \cdot \mathbf{u} \, \mathrm{ds} + \int_{\partial \mathcal{C}} p\nu \cdot \mathbf{u} \, \mathrm{ds}. \tag{2.7}$$

The description of the second part of the surface energy goes back to Griffith [Gri21]. It describes the work that must be applied against the material for a crack to propagate. It is proportional to the length of the crack, that is $\mathcal{H}^{n-1}(\mathcal{C})$. Here $\mathcal{H}^{n-1}$ is the $(n-1)$-dimensional Hausdorff measure defined in Definition 2.4.3. Griffith now states that crack propagation occurs whenever some critical energy release rate G_c is reached. Hence he describes this crucial part of the surface energy as $G_c \mathcal{H}^{n-1}(\mathcal{C})$. Summing up equation (2.7) and the crack energy we get the total description of the surface energy as

$$E_s(\mathbf{u}, \mathcal{C}) = -\int_{\Gamma_N} \tau \cdot \mathbf{u} \, \mathrm{ds} + \int_{\partial \mathcal{C}} p\nu \cdot \mathbf{u} \, \mathrm{ds} + G_c \mathcal{H}^{n-1}(\mathcal{C}). \tag{2.8}$$

Together, equations (2.6) and (2.8) lead to the following total energy of the system.

$$E(\mathbf{u}, \mathcal{C}) = \int_{\Omega \setminus \mathcal{C}} \frac{1}{2} (e(\mathbf{u}) : \mathbb{C}e(\mathbf{u})) - \alpha p \nabla \cdot \mathbf{u} - \int_{\Gamma_N} \tau \cdot \mathbf{u} \, \mathrm{ds} + \int_{\partial \mathcal{C}} p\nu \cdot \mathbf{u} \, \mathrm{ds} + G_c \mathcal{H}^{n-1}(\mathcal{C}) \tag{2.9}$$

Finally we want to reduce the dependency of equation (2.9) on $\mathcal{C}$, which is a-priori unknown. An application of Gauss' theorem leads to our final energy formulation.

Definition 2.2.1 (Energy minimization problem)**:**
Given α, μ, λ, G_c as before as well as $p \in W^{1,\infty}(\Omega)$, $\mathbf{u}_D \in H^1_D(\Omega; \mathbb{R}^n)$ and $\tau \in L^\infty(\Omega)$ find $\mathbf{u}$, $\mathcal{C}$ *such that*

$$\begin{aligned} E(\mathbf{u}, \mathcal{C}) &= \min_{\mathbf{v}, K} E(\mathbf{v}, K) \\ &= \min_{\mathbf{v}, K} \left(\int_{\Omega \setminus K} \frac{1}{2} e(\mathbf{v}) : \mathbb{C}e(\mathbf{v}) \;\; + (1-\alpha) p \nabla \cdot \mathbf{v} + \nabla p \cdot \mathbf{v} \right. \\ &\qquad \left. - \int_{\Gamma_N} (\tau + p\nu) \cdot \mathbf{v} \, \mathrm{ds} - \int_{\Gamma_D} p\nu \cdot \mathbf{u}_D \, \mathrm{ds} + G_c \mathcal{H}^{n-1}(K) \right). \end{aligned} \tag{2.10}$$

The next section deals with the remaining dependencies on the crack $\mathcal{C}$.

2.2.4 Phase-field formulation

As our goal is the numerical simulation of crack propagation, we need to minimize equation (2.10) numerically. The unknown crack surface $\mathcal{C}$ is a tremendous challenge for this, since it may have a very complex geometry. During the propagation it might even change topologically, for example a crack could branch or two cracks could join. To overcome this problem, Bourdin, Francfort and Marigo [BFM00, Chapter 8] approximate the total energy derived in [FM98] by an elliptic functional. The corresponding underlying idea originates from the theory of Γ-convergence and goes back to an approximation of the Mumford-Shah functional by Ambrosio and Tortorelli. The Mumford-Shah functional [MS89] is used in the theory of image segmentation and reads

$$MS(u,K) = \int_{\Omega\setminus K} |\nabla u|^2 + \beta (u-g)^2 \,\mathrm{dx} + \alpha \mathcal{H}^{n-1}(K), \tag{2.11}$$

where $u \in H^1(\Omega \setminus K)$ and $K \subset \Omega$ closed. In [AT90] Ambrosio and Tortorelli approximate it in the sense of Γ-convergence by

$$AT_\varepsilon(u,z) = \int_\Omega \left(|\nabla u|^2 + |\nabla z|^2\right)\left(1-z^2\right)^{2h} + \frac{1}{4}\alpha^2 h^2 z^2 \,\mathrm{dx} + \beta \int_\Omega |u-g|^2 \,\mathrm{dx}. \tag{2.12}$$

Further the functionals are extended by $+\infty$ outside of suitable function spaces in a way that does not interfere with the solution of the minimization problem. Following their idea we approximate equation (2.10) by elliptic functionals in the sense of Γ-convergence. We discuss the basics of Γ-convergence in detail in Section 2.3 and the convergence of our formulation to equation (2.10) in Chapter 3. At this point we only state the approximated energy functional E_ε used for the simulations throughout this thesis, without further notes on the analysis. Following the work of Mikelić, Wheeler and Wick [MWW15b] E_ε generalizes the functionals in [BFM00] by taking the pressure into account. To approximate the crack $\mathcal{C}$ we introduce a variable φ called the phase field. It takes values between 0 and 1, where $\varphi = 0$ symbolizes the crack and $\varphi = 1$ stands for completely unbroken material. Thus the irreversibility condition can be assured by the requirement $\frac{\partial}{\partial t}\varphi \leq 0$. In a quasi-static setting this translates to $\varphi \leq \varphi_{\text{previous}}$. Furthermore we introduce a small regularization parameter ε and a small parameter $k_\varepsilon \ll \varepsilon$ to ensure coercivity. The minimization problem then reads as follows.

Definition 2.2.2 (Approximative energy minimization problem)**:**
Given α, μ, λ, G_c as before as well as $p \in W^{1,\infty}(\Omega)$, $\mathbf{u}_D \in H^1_D(\Omega;\mathbb{R}^n)$ and $\tau \in L^\infty(\Omega)$, find

$\mathbf{u} \in H^1_D(\Omega;\mathbb{R}^n)$ *and* $\varphi \in H^1(\Omega)$ *with* $0 \le \varphi \le 1$ *and* $\frac{\partial}{\partial t}\varphi \le 0$ *satisfying*

$$\begin{aligned} E_\varepsilon(\mathbf{u},\varphi) &= \min_{\mathbf{v},\psi} E_\varepsilon(\mathbf{v},\psi) \\ &= \min_{\mathbf{v},\psi} \left(\int_\Omega \frac{1}{2}\left(\psi^2 + k_\varepsilon\right) e(\mathbf{v}) : \mathbb{C}e(\mathbf{v}) + (1-\alpha)\,\psi p \nabla\cdot\mathbf{v} + \psi\,\nabla p\cdot\mathbf{v}\,\mathrm{dx} \right. \\ &\quad \left. - \int_{\Gamma_N} (\tau + p\nu)\cdot\mathbf{v}\,\mathrm{ds} - \int_{\Gamma_D} p\nu\cdot\mathbf{u}_D\,\mathrm{ds} + G_c \int_\Omega \frac{1}{2\varepsilon}(1-\psi)^2 + \frac{\varepsilon}{2}|\nabla\psi|^2\,\mathrm{dx} \right). \end{aligned} \tag{2.13}$$

2.3 Γ-convergence

In [DGF75, DG75, DG77] Ennio De Giorgi introduced a new notion of variational convergence called Γ-convergence. It became a frequently applied tool to study convergence of minimizers for various energy minimizing problems. In this section we recall its definition and state the main properties and results that will prove beneficial in the remainder of this thesis. For an exhaustive introduction to Γ-convergence we refer to the books of Dal Maso [DM12] and Braides [Bra02] on which the definitions and results in this sections are based.

We define Γ-convergence and Γ-limits in the setting of a metric space (X,d). Thus in the remaining part of this subsection continuity and convergence is always understood with respect to the metric d. Note that it is possible to define Γ-convergence for the more general category of topological spaces, as introduced in [DM12, Chapter 4], see also [Bra02, Section 1.4]. If one wants to emphasize the case of a metric space, the definition given here is sometimes called sequential Γ-convergence.

Definition 2.3.1 (Γ-limit)**:**
Let (X,d) *be a metric space and let* $F_j\colon X \to [-\infty,+\infty]$ *be a sequence of functions on* X*. A function* $F : X \to [-\infty,+\infty]$ *is called the* Γ*-limit of* F_j *and we write* $F = \Gamma\text{-}\lim_{j\to+\infty} F_j$ *if and only if for all* $x \in X$ *we have*

- (lim inf inequality) *for all sequences* $(x_j) \subset X$ *with* $x_j \to x$ *for* $j \to +\infty$ *holds*

$$F(x) \le \liminf_{j\to+\infty} F_j(x_j) \quad \text{and} \tag{2.14}$$

- (lim sup inequality) *for every* $x \in X$ *one can find a sequence* $(x_j) \subset X$ *with* $x_j \to x$ *for* $j \to +\infty$ *such that*

$$F(x) \ge \limsup_{j\to+\infty} F_j(x_j). \tag{2.15}$$

The function F *is uniquely determined by equations* (2.14) *and* (2.15)*.*

Note that the definition above depends on the metric d, that is on the sense of convergence of $x_\jmath \to x$. Further note that often the space X is a function space, hence sometimes $F_\jmath$ and F are called functionals and not functions.

Remark: Condition (2.15) is often referred to as the existence of a recovery sequence, as by equation (2.14) it is equivalent to the existence of a sequence $x_\jmath \to x$ in X such that

$$F(x) = \lim_{\jmath \to +\infty} F_\jmath(x_\jmath).$$

Γ-convergence can also be seen as the equality of lower and upper limits in the sense of the following definition.

Definition 2.3.2 (Γ-lower and Γ-upper limit)**:**
For a sequence of functions $F_\jmath \colon X \to [-\infty, +\infty]$ we define the Γ-lower limit at a point $x \in X$ as

$$\Gamma\text{-}\liminf_{\jmath \to +\infty} F_\jmath(x) = \inf\left(\liminf_{\jmath \to +\infty} F_\jmath(x_\jmath)\right),$$

where the infimum is taken over all sequences $x_\jmath$ with $x_\jmath \to x$. The Γ-upper limit at $x \in X$ is defined as

$$\Gamma\text{-}\limsup_{\jmath \to +\infty} F_\jmath(x) = \inf\left(\limsup_{\jmath \to +\infty} F_\jmath(x_\jmath)\right),$$

where the infimum is again taken over all sequences $x_\jmath$ with $x_\jmath \to x$. If for some $\lambda \in [-\infty, +\infty]$ it holds

$$\Gamma\text{-}\liminf_{\jmath \to +\infty} F_\jmath(x) = \lambda = \Gamma\text{-}\limsup_{\jmath \to +\infty} F_\jmath(x)$$

we call λ the Γ-limit of $F_\jmath$ at x and write $\lambda = \Gamma\text{-}\lim_{\jmath \to +\infty} F_\jmath(x)$.

Let us recall some important properties of Γ-limits.

Lemma 2.3.3 (Properties of Γ-limits)**:**

- (Equality of Definitions 2.3.1 and 2.3.2) *A function F is the Γ-limit of the sequence $F_\jmath$ at a point $x \in X$ if and only if $\lambda = \Gamma\text{-}\lim_{\jmath \to +\infty} F_\jmath(x)$ exists and $\lambda = F(x)$. Further $F = \Gamma\text{-}\lim_{\jmath \to +\infty} F_\jmath$ if and only if F is pointwise the Γ-limit of $F_\jmath$ for all $x \in X$.*
- (Lower semicontinuity) *For a sequence $F_\jmath$ the Γ-lower and Γ-upper limit $\Gamma\text{-}\liminf_{\jmath \to +\infty} F_\jmath$ and $\Gamma\text{-}\limsup_{\jmath \to +\infty} F_\jmath$ are lower semicontinuous functions.*
- (Stability under continuous perturbations) *Let $G \colon X \to [-\infty, +\infty]$ be a continuous function and let $F = \Gamma\text{-}\lim_{\jmath \to +\infty} F_\jmath$. Then*

$$F + G = \Gamma\text{-}\lim_{\jmath \to +\infty} (F_\jmath + G).$$

- (lim sup inequality by density) *Let $\mathcal{D} \subset X$ be a dense subset such that for all $\eta > 0$ and every $x \in X$ we can find an $x^\eta \in \mathcal{D}$ with $d(x^\eta - x) < \eta$ and $|F(x^\eta) - F(x)| < \eta$. Further let equation (2.15) hold for all $x \in \mathcal{D}$. Then equation (2.15) holds for every $x \in X$.*

- (Urysohn property of Γ-convergence) *$F = \Gamma\text{-}\lim_{j\to+\infty} F_j$ if and only if for every subsequence F_{j_k} there exists a further subsequence $F_{j_{k_l}}$ such that $F = \Gamma\text{-}\lim_{l\to+\infty} F_{j_{k_l}}$.*

In the context of the present thesis a broader definition of Γ-convergence, including uncountable families of functions, is often applied.

Definition 2.3.4 (Γ-limit of a family of functions)**:**
A family $F_\varepsilon \colon X \to [-\infty, +\infty]$ of functions depending on $\varepsilon > 0$ is said to converge for $\varepsilon \to 0$ to some $F \colon X \to [-\infty, +\infty]$ in the sense of Γ-convergence if and only if $F = \Gamma\text{-}\lim_{j\to+\infty} F_{\varepsilon_j}$ for every sequence $\varepsilon_j > 0$ with $\lim_{j\to+\infty} \varepsilon_j = 0$. Then we call F the Γ-limit of F_ε and write $F = \Gamma\text{-}\lim_{\varepsilon\to 0} F_\varepsilon$.

Remark: In view of Definition 2.3.4, throughout the remainder of this thesis $\varepsilon > 0$ is a positive parameter varying in a strictly decreasing sequence converging to zero.

As stated before, Γ-convergence is a useful tool for studying the convergence of minimizers of variational problems. To this end the functions must satisfy an additional coercivity condition. Therefore we recall the definitions of different notions of coercivity before stating the main result about convergence of minimizers under Γ-convergence.

Definition 2.3.5 (Equi-coercivity)**:**
We call the function $F \colon X \to [-\infty, +\infty]$ coercive if the set $\{F \leq t\}$ is precompact for all $t \in \mathbb{R}$. It is called mildly coercive if one can find a set $K \subset X$, with K non-empty and compact, satisfying $\inf_X F = \inf_K F$. A sequence F_j is called equi-mildly coercive or equi-coercive if there exists a compact non-empty set $K \subset X$ such that for all $j \in \mathbb{N}$ holds $\inf_X F_j = \inf_K F_j$.

Theorem 2.3.6 (Convergence of minimizers)**:**
Let X be a metric space and $F = \Gamma\text{-}\lim_{j\to+\infty} F_j$ for a sequence of equi-coercive functions F_j. Then there exists a solution of the minimization problem $\min_X F$ that satisfies

$$\min_{x\in X} F(x) = \lim_{j\to+\infty} \inf_{x\in X} F_j(x).$$

Furthermore for every precompact sequence x_j with $\lim_{j\to+\infty} F_j(x_j) = \lim_{j\to+\infty} \inf_{x\in X} F_j(x)$ every limit of a subsequence of x_j is a minimizer of the limit function F.

A proof of this result can be found in [Bra02, Section 1.5]. For more details on the convergence of minimizers in the context of Γ-convergence see also Chapter 7, especially Corollary 7.20, of [DM12].

2.4 Functions of bounded variation and bounded deformation

In the proof of Γ-convergence results for functionals of the form (2.10) and (2.11) the spaces of functions of bounded variation and bounded deformation play an important role. They turn out to be the natural choice of domain in which to state the energy minimization problem. In this section we first recall some measure-theoretic preliminaries. Second we introduce the space of functions of bounded variation, its generalizations and specializations, followed by its main properties. We close the section with an introduction to the space of functions of bounded deformation and its properties.

2.4.1 Measure theory

In this short summary we recall some properties of measures that will prove beneficial in the remainder of this thesis. We mainly follow Braides [Bra98]. For an advanced introduction to measure theory we refer the interested reader to [EG92], [AFP00] and [Fed14].

Definition 2.4.1 (Measures)**:**

- *We denote the set of Radon measures on Ω with values in $\mathbb{R}^m$, $m \in \mathbb{N}$, $m > 0$ by $\mathcal{M}(\Omega; \mathbb{R}^m)$. For bounded Radon measures, positive Radon measures and positive, bounded Radon measures we write $\mathcal{M}_b(\Omega; \mathbb{R}^m)$, $\mathcal{M}^+(\Omega; [0, +\infty])$ and $\mathcal{M}_b^+(\Omega; [0, +\infty])$ respectively. Usually we consider $\mathbb{R}^{n\times n}_{sym}$, $\mathbb{R}^N$ or $\mathbb{R}$, where in the last case we omit the $\mathbb{R}$ and write $\mathcal{M}(\Omega)$ etc.*

- *For a measure $\mu \in \mathcal{M}(\Omega; \mathbb{R}^N)$ the total variation of μ on a Borel set B is defined as*

$$|\mu|(B) = \sup_{B=\bigcup_{i\in\mathbb{N}} B_i} \left(\sum_{i\in\mathbb{N}} |\mu(B_i)| \right).$$

  It holds $|\mu| \in \mathcal{M}^+(\Omega)$.

In the proof of Γ-convergence in higher dimensions a technique called "slicing" is often applied. One key component therein is the following property of measures, see [Bra98, Proposition 1.16].

Proposition 2.4.2 (Supremum of measures)**:**
Let $\mu\colon \mathcal{A}(\Omega) \to [0, +\infty)$ be an open set function. Further for $A, B \in \mathcal{A}(\Omega)$ with $\overline{A} \cap \overline{B} = \emptyset$ and $\overline{A} \cup \overline{B} \Subset \Omega$ let μ satisfy $\mu(A \cup B) \geq \mu(A) + \mu(B)$. Let $\lambda \in \mathcal{M}^+(\Omega)$ and for a countable family of positive Borel functions ψ_i we set $\psi = \sup_i \psi_i$. Then

$$\mu(A) \geq \int_A \psi_i \,\mathrm{d}\lambda \quad \text{for all } A \in \mathcal{A}(\Omega) \text{ and for all } i$$
$$\Longrightarrow \mu(A) \geq \int_A \psi \,\mathrm{d}\lambda \quad \text{for all } A \in \mathcal{A}(\Omega).$$

As we will frequently use the Hausdorff measure, we recall its definition here.

Definition 2.4.3 (Hausdorff measure)**:**
Let $s \in [0, +\infty)$, $\delta \in [0, +\infty)$ and $A \subset \mathbb{R}^n$. The Hausdorff pre-measure of A is defined as

$$\mathcal{H}_\delta^s(A) = \frac{\alpha(s)}{2^s} \inf \left(\sum_{j \in \mathbb{N}} (\operatorname{diam} C_j)^s \right),$$

where the infimum is taken over all families C_j such that $A \subset \bigcup_{j \in \mathbb{N}} C_j$ and $\operatorname{diam} C_j \leq \delta$ for all $j \in \mathbb{N}$. The scalar factor $\alpha(s)$ is given by $\alpha(s) = (\pi)^{s/2} (\Gamma(1 + s/2))$, where $\Gamma(t) = \int_0^{+\infty} e^{-x} x^{t-1} \, \mathrm{dx}$. As $\mathcal{H}_\delta^s$ is decreasing for $\delta \to 0$ we can define the s-dimensional Hausdorff measure as

$$\mathcal{H}^s(A) = \sup_{\delta > 0} \mathcal{H}_\delta^s(A) = \lim_{\delta \to 0} \mathcal{H}_\delta^s(A). \tag{2.16}$$

Remark: The factor $\alpha(s)/2^s$ is chosen to guarantee equality of the n-dimensional Hausdorff measure and the n-dimensional Lebesgue measure in $\mathbb{R}^n$. Some authors (e.g. Halmos [Hal13]) define the Hausdorff measure without this factor.

2.4.2 Bounded variation

In the following we introduce the space of functions of bounded variation. As before we mainly follow Braides [Bra98], more details can be found in [AFP00] and [EG92].

Definition 2.4.4 (The space $BV(\Omega; \mathbb{R}^N)$)**:**
A function $\mathbf{u} \in L^1(\Omega; \mathbb{R}^N)$ is called a function of bounded variation if its distributional derivative $D\mathbf{u}$ is a measure on Ω with values in $\mathbb{R}^{N \times n}$ and has finite total variation $|D\mathbf{u}|(\Omega)$. In other words denoting $\mathbf{u} = (u^1, \ldots, u^N)$ and denoting the entries of $D\mathbf{u}$ by $D_i u^\alpha$, for every $\varphi \in C_c^1(\Omega; \mathbb{R}^N)$ holds

$$\sum_{\alpha=1}^{N} \int_\Omega u^\alpha \nabla \cdot \varphi^\alpha \, \mathrm{dx} = - \sum_{\alpha=1}^{N} \sum_{i=1}^{n} \int_\Omega \varphi_i^\alpha \, \mathrm{d} \, D_i u^\alpha.$$

For such $\mathbf{u}$ we write $\mathbf{u} \in BV(\Omega; \mathbb{R}^N)$. If $N = 1$ we omit the $\mathbb{R}$ and write $u \in BV(\Omega)$.

Characteristic functions are of special interest in the theory of BV functions. We call a set $A \subset \mathbb{R}^n$ a set of finite perimeter if $\mathcal{X}_A \in BV(\Omega)$ and call $|D\mathcal{X}_A|(\Omega)$ its perimeter in Ω, denoted by $\operatorname{Per}(A)$. Note that while in this introduction we distinguish between the dimension n of the domain and the dimension N of the image space, throughout the remainder of this thesis we typically consider the case $N = n$.

The following Lemma summarizes some properties of BV functions.

Lemma 2.4.5 (Properties of BV functions)**:**

- *Equipped with the norm*

$$\|\mathbf{u}\|_{BV(\Omega;\mathbb{R}^N)} = \|\mathbf{u}\|_{L^1(\Omega;\mathbb{R}^N)} + |D\mathbf{u}|(\Omega),$$

  $BV(\Omega;\mathbb{R}^N)$ *is a Banach space.*

- *Every Sobolev function* $\mathbf{u} \in W^{1,1}(\Omega;\mathbb{R}^N)$ *with weak derivative* $\nabla \mathbf{u}$ *is a function of bounded variation with* $|D\mathbf{u}|(\Omega) = \int_\Omega |\nabla \mathbf{u}| \, \mathrm{dx}$.

- *The space* $\mathcal{C}^\infty(\Omega;\mathbb{R}^N)$ *is dense in* $BV(\Omega;\mathbb{R}^N)$ *with respect to* $\|\cdot\|_{BV(\Omega;\mathbb{R}^N)}$.

- *For every sequence* $(\mathbf{u}_j) \subset BV(\Omega;\mathbb{R}^N)$ *with* $\sup_{j\in\mathbb{N}} \|\mathbf{u}\|_{BV(\Omega;\mathbb{R}^N)} < +\infty$ *there exists a subsequence that converges in* $L^1_{loc}(\Omega;\mathbb{R}^N)$ *to some* $\mathbf{u} \in BV(\Omega;\mathbb{R}^N)$.

The subsequent generalization of the coarea formula to the case of BV functions goes back to [FR60], a proof can be found in [Bra98, Theorem 1.51].

Proposition 2.4.6 (Fleming-Rishel coarea formula)**:**
For $u \in L^1(\Omega)$ *it holds*

$$|Du|(\Omega) = \int_{-\infty}^{+\infty} \left|D\mathcal{X}_{\{u>t\}}\right|(\Omega) \, \mathrm{dt}.$$

Further $u \in BV(\Omega)$ *if and only if* $|Du|(\Omega)$ *is finite.*

For examining the structure of BV functions in more detail, the notion of approximate limits plays an important role. An overview in the N-dimensional setting can be found in [DM13, Section 2].

Definition 2.4.7 (Approximate limit)**:**
Let $\mathbf{u}\colon A \to \mathbb{R}^N$ *be an* $\mathcal{L}^n$*-measurable function, let* $A \subset \mathbb{R}^n$ *and* $x \in A$. *We call* $a \in \mathbb{R}^N \cup \{+\infty\}$ *the approximate limit of* $\mathbf{u}$ *for* $y \to x$ *and write* $a = \operatorname{ap\,lim}_{y\to x} \mathbf{u}(y)$ *if for all* $\delta > 0$ *it holds*

$$\lim_{\rho\to 0} \frac{\mathcal{L}^n(\{y \in A \cap B_\rho(x) : |\mathbf{u}(y) - a| > \delta\})}{\rho^n} = 0.$$

If $a = \operatorname{ap\,lim}_{y\to x} \mathbf{u}(y) \in \mathbb{R}^N$ *exists we write* $\tilde{\mathbf{u}}(x) = a$ *and say that* $\mathbf{u}$ *is approximately continuous at* x. *We define the approximate discontinuity set of* $\mathbf{u}$ *as*

$$S_{\mathbf{u}} = \{x \in A : \mathbf{u} \text{ is not approximately continuous at } x\}.$$

Further we define the approximate jump set of $\mathbf{u}$ *as*

$$J_{\mathbf{u}} = \left\{ x \in A : \exists\, a, b \in \mathbb{R}^N,\ a \neq b,\ \nu \in \mathbb{S}^{n-1} \text{ s.t. } \operatorname*{ap\,lim}_{\substack{(y-x)\cdot\nu>0 \\ y\to x}} \mathbf{u}(y) = a \text{ and } \operatorname*{ap\,lim}_{\substack{(y-x)\cdot\nu<0 \\ y\to x}} \mathbf{u}(y) = b \right\}.$$

Up to change of sign of ν and permutation of a and b, the triplet (a, b, ν) is uniquely determined and denoted by $(\mathbf{u}^+(x), \mathbf{u}^-(x), \nu_{\mathbf{u}}(x))$ for $x \in J_{\mathbf{u}}$. With this notation we can define the jump of $\mathbf{u}$ at $x \in J_{\mathbf{u}}$ as $[\![\mathbf{u}]\!](x) = \mathbf{u}^+(x) - \mathbf{u}^-(x)$ and write

$$J_{\mathbf{u}}^1 = \{x \in J_{\mathbf{u}} : |[\![\mathbf{u}]\!](x)| \geq 1\}.$$

Note that by Lebesgue's differentiation theorem $\mathbf{u} = \tilde{\mathbf{u}}$ holds $\mathcal{L}^n$-almost everywhere in A and $\mathcal{L}^n(S_{\mathbf{u}}) = 0$. Further $J_{\mathbf{u}}^1 \subset J_{\mathbf{u}} \subset S_{\mathbf{u}}$.

Definition 2.4.8 (Approximate gradient)**:**
We say that an $\mathcal{L}^n$-measurable function $\mathbf{u}\colon A \to \mathbb{R}^N$ is approximately differentiable at $x \in A$ if a matrix $M \in \mathbb{R}^{N \times n}$ exists such that

$$\operatorname*{ap\,lim}_{y \to x} \frac{|\mathbf{u}(y) - \tilde{\mathbf{u}}(x) - M \cdot (y - x)|}{|y - x|} = 0.$$

We call M the approximate gradient of $\mathbf{u}$ at x and write $\nabla \mathbf{u}(x) = M$. For $N = n$ suppose that for $x \in A$ there exists a matrix $L \in \mathbb{R}^{n \times n}_{sym}$ such that

$$\operatorname*{ap\,lim}_{y \to x} \frac{(\mathbf{u}(y) - \tilde{\mathbf{u}}(x) - L \cdot (y - x)) \cdot (y - x)}{|y - x|^2} = 0. \tag{2.17}$$

Then we say that $\mathbf{u}$ has an approximate symmetric gradient at x and denote it by $e(\mathbf{u})(x) = L$.

According to the Radon-Nikodym theorem we can decompose the measure $D\mathbf{u}$ as $D\mathbf{u} = D^a\mathbf{u} + D^s\mathbf{u}$ where $D^a\mathbf{u}$ is the absolute continuous part of $D\mathbf{u}$ with respect to $\mathcal{L}^n$ and $D^s\mathbf{u}$ is the singular part of $D\mathbf{u}$ with respect to $\mathcal{L}^n$. We further decompose $D^s\mathbf{u}$ as $D^s\mathbf{u} = D^J\mathbf{u} + D^c\mathbf{u}$, where the restrictions $D^J\mathbf{u} = D^s\mathbf{u} \llcorner S_{\mathbf{u}}$ and $D^c\mathbf{u} = D^s\mathbf{u} \llcorner (\Omega \setminus S_{\mathbf{u}})$ are called the jump part and the cantor part respectively.

Theorem 2.4.9 (Properties of $D^a\mathbf{u}$, $D^J\mathbf{u}$ and $D^c\mathbf{u}$)**:**
Let $\mathbf{u} \in BV(\Omega; \mathbb{R}^N)$ and let $D\mathbf{u} = D^a\mathbf{u} + D^J\mathbf{u} + D^c\mathbf{u}$ be its distributional derivative, decomposed as above. Then

- *$\mathbf{u}$ is approximately differentiable for $\mathcal{L}^n$-a. e. $x \in \Omega$ and $\nabla \mathbf{u}$ is the density of $D^a\mathbf{u}$ with respect to $\mathcal{L}^n$.*
- *If $A \in \mathfrak{B}(\Omega)$ and $\mathcal{H}^{n-1}(A) < +\infty$ then $|D^c\mathbf{u}|$ vanishes on A.*
- *$\mathcal{H}^{n-1}(S_{\mathbf{u}} \setminus J_{\mathbf{u}}) = 0$, the discontinuity set $S_{\mathbf{u}}$ is countably $\mathcal{H}^{n-1}$-rectifiable and for every $A \in \mathfrak{B}(\Omega)$ it holds*

$$D^J\mathbf{u}(A) = \int_{A \cap J_{\mathbf{u}}} (\mathbf{u}^+ - \mathbf{u}^-) \otimes \nu_{\mathbf{u}} \, \mathrm{d}\mathcal{H}^{n-1}.$$

The decomposition of $D\mathbf{u}$ motivates the definition below.

Definition 2.4.10 ($SBV\left(\Omega;\mathbb{R}^N\right)$)**:**
Let $\mathbf{u} \in BV\left(\Omega;\mathbb{R}^N\right)$. *If* $D^c\mathbf{u} = 0$ *we call* $\mathbf{u}$ *a special function of bounded variation and write* $\mathbf{u} \in SBV\left(\Omega;\mathbb{R}^N\right)$. *If in addition* $\nabla\,\mathbf{u} \in L^p\left(\Omega;\mathbb{R}^{N\times n}\right)$ *for some* $p \in (1,+\infty)$ *and* $\mathcal{H}^{n-1}\left(J_{\mathbf{u}}\right) < +\infty$ *we say* $\mathbf{u} \in SBV^p\left(\Omega;\mathbb{R}^N\right)$.

In Section 2.4.3 it will prove beneficial to have localized versions of BV and SBV defined.

Definition 2.4.11 ($BV_{loc}\left(\Omega;\mathbb{R}^N\right)$ and $SBV_{loc}\left(\Omega;\mathbb{R}^N\right)$)**:**
If $\mathbf{u} \in L^1_{loc}\left(\Omega;\mathbb{R}^N\right)$ *and* $\mathbf{u} \in BV\left(A;\mathbb{R}^N\right)$ *for every open, compactly embedded subset* $A \Subset \Omega$, *we call* $\mathbf{u}$ *a function of locally bounded variation and write* $\mathbf{u} \in BV_{loc}\left(\Omega;\mathbb{R}^N\right)$.

If $\mathbf{u} \in BV_{loc}\left(\Omega;\mathbb{R}^N\right)$ *and* $D^c\mathbf{u} = 0$ *we call* $\mathbf{u}$ *a special function of locally bounded variation and write* $\mathbf{u} \in SBV_{loc}\left(\Omega;\mathbb{R}^N\right)$.

For the sake of completeness let us also define the space of generalized special functions of bounded variation.

Definition 2.4.12 ($GSBV\left(\Omega;\mathbb{R}^N\right)$)**:**
Let $\mathbf{u}\colon \Omega \to \mathbb{R}^N$ *be a Borel function. We say that* $\mathbf{u}$ *is a generalized special function of bounded variation if* $g(\mathbf{u}) \in SBV(\Omega)$ *holds for every* $g \in \mathcal{C}^1\left(\mathbb{R}^N\right)$ *with* ∇g *having compact support. The set of these functions is denoted by* $GSBV\left(\Omega;\mathbb{R}^N\right)$. *In analogy with* $SBV^p\left(\Omega;\mathbb{R}^N\right)$ *we define for* $p \in (1,+\infty)$

$$GSBV^p\left(\Omega;\mathbb{R}^N\right) = \left\{\mathbf{u} \in GSBV\left(\Omega;\mathbb{R}^N\right) : \nabla\,\mathbf{u} \in L^p\left(\Omega;\mathbb{R}^{N\times n}\right),\ \mathcal{H}^{n-1}\left(J_{\mathbf{u}}\right) < +\infty\right\}.$$

Remark: Note that $GSBV$ inherits most of the properties of SBV. For example $S_{\mathbf{u}}$ is countably $\mathcal{H}^{n-1}$ rectifiable, $\mathcal{H}^{n-1}\left(S_{\mathbf{u}} \setminus J_{\mathbf{u}}\right) = 0$ and the approximate gradient $\nabla\,\mathbf{u}$ exists $\mathcal{L}^n$-almost everywhere, see [Amb90, Proposition 1.3 and Proposition 1.4].

As mentioned previously a common technique to prove the lim inf inequality of Γ-convergence in higher dimensions is known as "slicing", which connects the directional derivatives of BV functions with their one-dimensional sections. It goes back to Ambrosio [Amb89], see also [Bra98, Theorem 4.1]. In order to understand this technique let us introduce some notation. For given $\xi \in \mathbb{S}^{n-1}$ we denote by $\Pi^\xi = \{y \in \mathbb{R}^n : \xi \cdot y = 0\}$ the hyperplane orthogonal to ξ passing through the origin. For every $y \in \Pi^\xi$ and $A \subset \mathbb{R}^n$ we define $A^\xi_y = \{t \in \mathbb{R} : y + t\xi \in A\}$ and finally for $u\colon \Omega \to \mathbb{R}$ we set $u^\xi_y\colon \Omega^\xi_y \to \mathbb{R}$ as $u^\xi_y(t) = u(y + t\xi)$.

Theorem 2.4.13 (Slicing theorem in $GSBV(\Omega)$)**:**
Let $u \in GSBV(\Omega)$. *For all* $\xi \in \mathbb{S}^{n-1}$ *and for* $\mathcal{H}^{n-1}$*-almost every* $y \in \Pi^\xi$ *we have* $u^\xi_y \in GSBV\left(\Omega^\xi_y\right)$ *and*

- $\left(u^\xi_y\right)'(t) = \nabla\,u(y + t\xi)\cdot\xi$ *for* $\mathcal{L}^1$*-almost every* $t \in \Omega^\xi_y$,
- $S_{u^\xi_y} = \{t \in \mathbb{R} : y + t\xi \in S_u\}$,

- $\left(u_y^\xi\right)^+(t) = u^+(y+t\xi)$ *and* $\left(u_y^\xi\right)^-(t) = u^-(y+t\xi)$ *up to the sign of* $\nu_u \cdot \xi$.

In addition, for any Borel function g *it holds*

$$\int_{\Pi^\xi} \sum_{t \in S_{u_y^\xi}} g(t)\, \mathrm{d}\mathcal{H}^{n-1}(y) = \int_{S_u} g(x)\, |\nu_u \cdot \xi|\, \mathrm{d}\mathcal{H}^{n-1}(x),$$

which we often apply in the special case $g = \mathcal{X}_B$, *where* $B \in \mathfrak{B}(\Omega)$.

On the other hand, let $u \in L^1(\Omega)$. *Let* $(\xi_i)_{i=1,\dots,n}$ *be a basis of* $\mathbb{S}^{n-1}$. *Assume that for every direction* ξ_i *and* $\mathcal{H}^{n-1}$*-almost every* $y \in \Pi^\xi$ *holds* $u_y^\xi \in SBV\left(\Omega_y^\xi\right)$ *and*

$$\int_{\Pi^\xi} \left|Du_y^\xi\right|\left(\Omega_y^\xi\right) \mathrm{d}\mathcal{H}^{n-1}(y) < +\infty.$$

Then $u \in SBV(\Omega)$.

Let us finish this introduction to functions of bounded variation with a density result obtained by Cortesani [Cor97]. It turns out to be beneficial in the proof of an upper bound for the Γ-limit. Note that there exists a generalization of the following result to anisotropic energies by Cortesani and Toader [CT99].

Definition 2.4.14 (Piecewise smooth SBV functions)**:**
Let $\mathbf{u} \in SBV\left(\Omega;\mathbb{R}^N\right)$. *We call* $\mathbf{u}$ *piecewise smooth and write* $\mathbf{u} \in \mathcal{W}\left(\Omega;\mathbb{R}^N\right)$ *if*

- $\mathbf{u} \in W^{k,\infty}\left(\Omega \setminus \overline{S_\mathbf{u}};\mathbb{R}^N\right)$ *for all* $k \in \mathbb{N}$,
- $\mathcal{H}^{n-1}\left(\overline{S_\mathbf{u}} \setminus S_\mathbf{u}\right) = 0$, *that is* $S_\mathbf{u}$ *is essentially closed,*
- $\overline{S_\mathbf{u}}$ *is a polyhedral set, that is* $\overline{S_\mathbf{u}} = \Omega \cap \bigcup_{i=1,\dots,m} K_m$, *where the* K_m *are* $(n-1)$*-dimensional simplices.*

Theorem 2.4.15 (Density of $\mathcal{W}\left(\Omega;\mathbb{R}^N\right)$ in $GSBV^p\left(\Omega;\mathbb{R}^N\right) \cap L^p\left(\Omega;\mathbb{R}^N\right)$)**:**
Let $\Omega \subset \mathbb{R}^n$ *be open and bounded with locally Lipschitz boundary* $\partial\Omega$. *Further let* $\mathbf{u} \in GSBV^p\left(\Omega;\mathbb{R}^N\right) \cap L^p\left(\Omega;\mathbb{R}^N\right)$. *Then for every* $\delta > 0$ *we can find a function* $\mathbf{v} \in \mathcal{W}\left(\Omega;\mathbb{R}^N\right)$ *such that*

$$\begin{aligned} \|\mathbf{u} - \mathbf{v}\|_{L^p(\Omega;\mathbb{R}^N)} &< \delta, \\ \|\nabla \mathbf{u} - \nabla \mathbf{v}\|_{L^p(\Omega;\mathbb{R}^{N\times n})} &< \delta, \\ \left|\mathcal{H}^{n-1}(S_\mathbf{u}) - \mathcal{H}^{n-1}(S_\mathbf{v})\right| = \left|\mathcal{H}^{n-1}(J_\mathbf{u}) - \mathcal{H}^{n-1}(J_\mathbf{v})\right| &< \delta. \end{aligned}$$

2.4.3 Bounded deformation

In the case of brittle fracture we no longer have any direct control over the approximate gradient $\nabla \mathbf{u}$. The energy (2.10) only depends on the symmetric gradient $e(\mathbf{u})$. Therefore the natural spaces in which to state the energy minimizing problem (2.13) do not control $\nabla \mathbf{u}$ but only $e(\mathbf{u})$. These are called spaces of functions of bounded deformation and are the subject of the current section. They were introduced in [MSC79] and [Suq78] in the context of plasticity problems and further studied in [TS80] and [Koh79]. For additional literature on the subject we refer the interested reader to the bibliography of [DM13]. The present chapter follows [ACDM97] for the introduction of functions of bounded deformation and special functions of bounded deformation and for the statement of their main properties. For further properties see for example [BCDM98]. The generalization of these function spaces follows [DM13] and [CC19].

Definition 2.4.16 ($BD(\Omega;\mathbb{R}^n)$)**:**
Let $\mathbf{u} \in L^1(\Omega;\mathbb{R}^n)$ and let $D\mathbf{u}$ be its distributional derivative. We define the symmetric part of its distributional derivative by

$$E\mathbf{u} = \frac{1}{2}\left(D\mathbf{u} + (D\mathbf{u})^T\right).$$

We say that $\mathbf{u}$ is a function of bounded deformation and write $\mathbf{u} \in BD(\Omega;\mathbb{R}^n)$ if $E\mathbf{u}$ is a Radon measure on Ω with values in $\mathbb{R}^{n\times n}_{sym}$ and finite total variation $|E\mathbf{u}|(\Omega)$.

Note that the definition of the symmetrized distributional derivative does only make sense in the case $N = n$, hence from now on we only consider functions $\mathbf{u}\colon \mathbb{R}^n \supset \Omega \to \mathbb{R}^n$. Let us summarize some properties of BD functions.

Theorem 2.4.17 (Properties of BD functions)**:**

- *$BD(\Omega;\mathbb{R}^n)$ is a Banach space if equipped with the norm*

$$\|\mathbf{u}\|_{BD(\Omega;\mathbb{R}^n)} = \|\mathbf{u}\|_{L^1(\Omega;\mathbb{R}^n)} + |E\mathbf{u}|(\Omega).$$

- *It can easily be seen that $BV(\Omega;\mathbb{R}^n) \subset BD(\Omega;\mathbb{R}^n)$.*

In analogy to BV functions we decompose the measure $E\mathbf{u}$ and write $E\mathbf{u} = E^a\mathbf{u} + E^j\mathbf{u} + E^c\mathbf{u}$. $E^a\mathbf{u}$ is again the absolute continuous part of $E\mathbf{u}$ with respect to $\mathcal{L}^n$ while $E^s\mathbf{u} = E^j\mathbf{u} + E^c\mathbf{u}$ is the singular part of $E\mathbf{u}$ with respect to $\mathcal{L}^n$ according to the Radon-Nikodym decomposition. Furthermore, the jump part $E^j\mathbf{u} = E^s\mathbf{u}\llcorner J_{\mathbf{u}}$ is the restriction of the singular part to the jump set and the Cantor part $E^c\mathbf{u} = E^s\mathbf{u}\llcorner(\Omega \setminus J_{\mathbf{u}})$ is the restriction to its complement.

Theorem 2.4.18 (Properties of $E^a\mathbf{u}$, $E^j\mathbf{u}$ and $E^c\mathbf{u}$)**:**
Let $\mathbf{u} \in BD(\Omega;\mathbb{R}^n)$ and let $E\mathbf{u} = E^a\mathbf{u} + E^j\mathbf{u} + E^c\mathbf{u}$ be its symmetrized distributional derivative, decomposed as above. Then the following holds.

- *For $\mathcal{L}^n$-a. e. $x \in \Omega$, the function $\mathbf{u}$ has an approximate symmetric gradient $e(\mathbf{u})$ at x and $e(\mathbf{u})$ is the density of $E^a\mathbf{u}$ with respect to $\mathcal{L}^n$.*
- *If $A \in \mathfrak{B}(\Omega)$ and $\mathcal{H}^{n-1}(A) < +\infty$ then $|E^c\mathbf{u}|$ vanishes on A.*
- *The jump set $J_\mathbf{u}$ is countably $\mathcal{H}^{n-1}$-rectifiable and for every $A \in \mathfrak{B}(\Omega)$ it holds*

$$E^j\mathbf{u}(A) = \int_{A \cap J_\mathbf{u}} \left(\mathbf{u}^+ - \mathbf{u}^-\right) \otimes \nu_\mathbf{u} \, \mathrm{d}\mathcal{H}^{n-1}.$$

- *$\mathcal{H}^{n-1+\varepsilon}(S_\mathbf{u} \setminus J_\mathbf{u}) = 0$ for every $\varepsilon > 0$ (see [Koh79]), but for $\varepsilon = 0$ this is still an open question.*

Motivated by the decomposition of $E\mathbf{u}$ we define specialized functions of bounded deformation.

Definition 2.4.19 ($SBD(\Omega;\mathbb{R}^n)$)**:**
Let $\mathbf{u} \in BD(\Omega;\mathbb{R}^n)$. If $E^c\mathbf{u} = 0$ we call $\mathbf{u}$ a special function of bounded deformation and write $\mathbf{u} \in SBD(\Omega;\mathbb{R}^n)$. If in addition $e(\mathbf{u}) \in L^p(\Omega;\mathbb{R}^{n\times n})$ for some $p \in (1,+\infty)$ and $\mathcal{H}^{n-1}(J_\mathbf{u}) < +\infty$ we write $\mathbf{u} \in SBD^p(\Omega;\mathbb{R}^n)$.

In analogy to BV functions, see Theorem 2.4.13, the functions of bounded deformation can be characterized by their one-dimensional sections. The two subsequent theorems are taken from [ACDM97, Proposition 3.2 and Theorem 4.5]. Before stating the results of Ambrosio et al. we need to introduce some additional notation. For given $\xi \in \mathbb{S}^{n-1}$ let $\hat{\mathbf{u}}_y^\xi = \mathbf{u}_y^\xi \cdot \xi = \mathbf{u}(y+t\xi)\cdot\xi$ and $J_\mathbf{u}^\xi = \{x \in J_\mathbf{u} : (\mathbf{u}^+(x) - \mathbf{u}^-(x))\cdot\xi \neq 0\}$. Note that $\mathcal{H}^{n-1}\left(J_\mathbf{u} \setminus J_\mathbf{u}^\xi\right) = 0$. Further denote the pointwise variation of an integrable function u on an interval $I \subset \mathbb{R}$ by $Vu(I) = \sup\left(\sum_{t=1}^{k-1} |u(t_{t+1}) - u(t_t)|\right)$ where the supremum is taken over all decompositions $t_1 < t_2 < \cdots < t_k$ of I.

Theorem 2.4.20 (Slicing theorem in $BD(\Omega;\mathbb{R}^n)$)**:**
For $\mathbf{u} \in BD(\Omega;\mathbb{R}^n)$, $\xi \in \mathbb{S}^{n-1}$ and $\mathcal{H}^{n-1}$-almost every $y \in \Omega^\xi$ the following holds.

- $\left(\widetilde{\hat{\mathbf{u}}}\right)_y^\xi = \hat{\mathbf{u}}_y^\xi$ *holds $\mathcal{L}^1$-almost everywhere in Ω_y^ξ,*
- $\hat{\mathbf{u}}_y^\xi \in BV\left(\Omega_y^\xi\right)$ *and* $\left|D\hat{\mathbf{u}}_y^\xi\right| = V\left(\left(\widetilde{\hat{\mathbf{u}}}\right)_y^\xi\right)$ *on Ω_y^ξ,*
- $E\mathbf{u}\,\xi\cdot\xi = \int_{\Pi^\xi} D\hat{\mathbf{u}}_y^\xi \, \mathrm{d}\mathcal{H}^{n-1}(y)$ *and* $|E\mathbf{u}\,\xi\cdot\xi| = \int_{\Pi^\xi} \left|D\hat{\mathbf{u}}_y^\xi\right| \mathrm{d}\mathcal{H}^{n-1}(y)$.

On the other hand, let $\mathbf{u} \in L^1_{loc}(\Omega;\mathbb{R}^n)$. Let $(\xi_i)_{i=1,\dots,n}$ be a basis of $\mathbb{S}^{n-1}$. Assume that every direction $\xi = \xi_i + \xi_j$ and $\mathcal{H}^{n-1}$-almost every $y \in \Pi^\xi$ satisfy $\hat{\mathbf{u}}_y^\xi \in BV\left(\Omega_y^\xi\right)$ and

$$\int_{\Pi^\xi} \left|D\hat{\mathbf{u}}_y^\xi\right|\left(\Omega_y^\xi\right) \mathrm{d}\mathcal{H}^{n-1}(y) < +\infty.$$

Then $\mathbf{u} \in BD(\Omega;\mathbb{R}^n)$.

Theorem 2.4.21 (Structure theorem in $BD(\Omega;\mathbb{R}^n)$)**:**
Let $\mathbf{u} \in BD(\Omega;\mathbb{R}^n)$ and $\xi \in \mathbb{S}^{n-1}$. Recall the decomposition $E\mathbf{u} = E^a\mathbf{u} + E^j\mathbf{u} + E^c\mathbf{u}$. Then

- $E^\times \mathbf{u}\,\xi\cdot\xi = \int\limits_{\Pi^\xi} D^\times \hat{\mathbf{u}}_y^\xi \,\mathrm{d}\mathcal{H}^{n-1}(y)$ *and* $|E^\times \mathbf{u}\,\xi\cdot\xi| = \int\limits_{\Pi^\xi} \left|D^\times \hat{\mathbf{u}}_y^\xi\right| \mathrm{d}\mathcal{H}^{n-1}(y)$ *for* $\times \in \{a, j, c\}$,
- $e(\mathbf{u})(y+t\xi)\,\xi\cdot\xi = \nabla\,\hat{\mathbf{u}}_y^\xi(t) = \left(\left(\widetilde{\hat{\mathbf{u}}}\right)_y^\xi\right)'(t)$ *for $\mathcal{L}^1$-almost every $t \in \Omega_y^\xi$.*
- *Let the normal vectors to $J_{\hat{\mathbf{u}}_y^\xi}$ and $J_{\mathbf{u}}$ be such that $\nu_{\hat{\mathbf{u}}_y^\xi} = 1$ and $\nu_{\mathbf{u}}\cdot\xi > 0$. Then for every $t \in \left(J_{\mathbf{u}}^\xi\right)_y^\xi$ and $\mathcal{H}^{n-1}$-almost every $y \in \Omega^\xi$ we have*

$$\mathbf{u}^+(y+t\xi)\cdot\xi = \left(\hat{\mathbf{u}}_y^\xi\right)^+(t) = \lim_{s\to t^+}\left(\widetilde{\hat{\mathbf{u}}}\right)_y^\xi(s) \text{ and } \mathbf{u}^-(y+t\xi)\cdot\xi = \left(\hat{\mathbf{u}}_y^\xi\right)^-(t) = \lim_{s\to t^-}\left(\widetilde{\hat{\mathbf{u}}}\right)_y^\xi(s).$$

Note that by Theorem 2.4.21 a function $\mathbf{u} \in BD(\Omega;\mathbb{R}^n)$ is also in $SBD(\Omega;\mathbb{R}^n)$ if and only if for some basis $(\xi_i)_{i=1,\dots,n}$ of $\mathbb{S}^{n-1}$ we have $\hat{\mathbf{u}}_y^\xi \in SBV\left(\Omega_y^\xi\right)$ for every $\xi = \xi_i + \xi_j$ and for $\mathcal{H}^{n-1}$-almost every $y \in \Omega^\xi$ (see [ACDM97, Proposition 4.7]).

As Dal Maso discusses in the introduction of [DM13], it is not reasonable to define the generalized space of special functions of bounded deformation, $GSBD(\Omega;\mathbb{R}^n)$, in analogy to $GSBV(\Omega;\mathbb{R}^n)$, as the result would not contain $SBD(\Omega;\mathbb{R}^n)$. Instead he incorporates the characterization via one-dimensional sections for the definition and we follow his approach in the upcoming section on $GSBD(\Omega;\mathbb{R}^n)$. For any function $v \in L^1_{loc}(\Omega)$ we denote its corresponding directional derivative by $D_\xi v = Dv\cdot\xi$.

Definition 2.4.22 ($GBD(\Omega;\mathbb{R}^n)$)**:**
Let $\mathbf{u}\colon \Omega \to \mathbb{R}^n$ be $\mathcal{L}^n$-measurable. We say that $\mathbf{u}$ is a generalized function of bounded deformation and write $\mathbf{u} \in GBD(\Omega;\mathbb{R}^n)$ if we can find $\lambda \in \mathcal{M}_b^+(\Omega)$ such that for every $\xi \in \mathbb{S}^{n-1}$ the following equivalent conditions hold.

- *For every $\tau \in \mathcal{C}^1(\mathbb{R})$ with $-\frac{1}{2} \le \tau \le \frac{1}{2}$ and $0 \le \tau' \le 1$ and for every $B \in \mathfrak{B}(\Omega)$ it holds*

$$D_\xi(\tau(\mathbf{u}\cdot\xi)) \in \mathcal{M}_b(\Omega) \text{ and } |D_\xi(\tau(\mathbf{u}\cdot\xi))|(B) \le \lambda(B).$$

- *For $\mathcal{H}^{n-1}$-almost every $y \in \Pi^\xi$ and for every $B \in \mathfrak{B}(\Omega)$ it holds*

$$\hat{\mathbf{u}}_y^\xi \in BV_{loc}\left(\Omega_y^\xi\right) \text{ and } \int_{\Pi^\xi} \left|D\hat{\mathbf{u}}_y^\xi\right|\left(B_y^\xi \setminus J^1_{\hat{\mathbf{u}}_y^\xi}\right) + \mathcal{H}^0\left(B_y^\xi \cap J^1_{\hat{\mathbf{u}}_y^\xi}\right)\mathrm{d}\mathcal{H}^{n-1}(y) \le \lambda(B).$$

Definition 2.4.23 ($GSBD(\Omega;\mathbb{R}^n)$)**:**
Let $\mathbf{u} \in GBD(\Omega;\mathbb{R}^n)$. We say that $\mathbf{u}$ is a generalized special function of bounded deformation and write $\mathbf{u} \in GSBD(\Omega;\mathbb{R}^n)$ if $\hat{\mathbf{u}}_y^\xi \in SBV_{loc}\left(\Omega_y^\xi\right)$ holds for every $\xi \in \mathbb{S}^{n-1}$ and $\mathcal{H}^{n-1}$-almost every $y \in \Pi^\xi$.

Note that Theorem 2.4.21 and the subsequent remark yield $BD(\Omega;\mathbb{R}^n) \subset GBD(\Omega;\mathbb{R}^n)$ and

$SBD(\Omega;\mathbb{R}^n) \subset GSBD(\Omega;\mathbb{R}^n)$. In the theorem below we collect some important properties of GBD and $GSBD$ functions. The corresponding proofs can be found in [DM13].

Theorem 2.4.24 (Properties of GBD and $GSBD$ functions)**:**

- *For every* $\mathbf{u} \in GBD(\Omega;\mathbb{R}^n)$ *and for* $\mathcal{H}^{n-1}$*-almost every* $x \in \partial\Omega$ *the trace* $\operatorname{tr}\mathbf{u}(x) = \operatorname{ap}\lim_{\substack{y\to x\\ y\in\Omega}} \mathbf{u}(y)$ *exists.*
- *For* $\mathbf{u} \in GBD(\Omega;\mathbb{R}^n)$ *the jump set* $J_{\mathbf{u}}$ *is countably* $\mathcal{H}^{n-1}$*-rectifiable.*
- *For every* $\mathbf{u} \in GBD(\Omega;\mathbb{R}^n)$ *and* $\mathcal{L}^n$*-almost every* $x \in \Omega$ *there exists a matrix* $e(\mathbf{u}) \in L^1\left(\Omega;\mathbb{R}^{n\times n}_{sym}\right)$ *satisfying equation* (2.17)*. We call* $e(\mathbf{u})$ *the approximate symmetric gradient of* $\mathbf{u}$*.*
- *For* $\mathcal{H}^{n-1}$*-almost every* $y \in \Pi^\xi$ *and for every* $\xi \in \mathbb{S}^{n-1}$ *it holds*

$$(e(\mathbf{u}))^\xi_y \xi \cdot \xi = \nabla \hat{\mathbf{u}}^\xi_y$$

  $\mathcal{L}^1$*-almost everywhere on* Ω^ξ_y*.*
- $\left(J^\xi_{\mathbf{u}}\right)^\xi_y = J_{\hat{\mathbf{u}}^\xi_y}$.

Note that the existence of an approximate symmetric gradient justifies the use of the divergence operator by setting $\nabla \cdot \mathbf{u} = \operatorname{tr}(e(\mathbf{u}))$. This definition is consistent with the usual notation of the gradient for (weakly) differentiable functions, see also [ACDM97, Theorem 7.4, Remark 7.5]. Note further that Jensen's inequality implies $|\nabla \cdot \mathbf{u}|^2 \leq n\,|e(\mathbf{u})|^2$, an estimate that we apply several times throughout this thesis. Moreover the space $GSBD(\Omega;\mathbb{R}^n)$ is compact in the sense of [DM13, Theorem 11.3]. We give a simplified version here, tailored to our needs.

Theorem 2.4.25 (Compactness in $GSBD(\Omega;\mathbb{R}^n)$)**:**
Given a sequence $\mathbf{u}_k \in GSBD(\Omega;\mathbb{R}^n)$ *suppose that we can find* $C > 0$ *such that*

$$\int_\Omega |\mathbf{u}_k|\,\mathrm{d}x + \int_\Omega |e(\mathbf{u}_k)|^2\,\mathrm{d}x + \mathcal{H}^{n-1}(J_{\mathbf{u}_k}) < C$$

for all $k \in \mathbb{N}$*. Then there exists* $\mathbf{u} \in GSBD(\Omega;\mathbb{R}^n)$ *and a subsequence* $\mathbf{u}_{k_j}$ *such that*

$$\begin{aligned} \mathbf{u}_{k_j} &\to \mathbf{u} \text{ pointwise } \mathcal{L}^n\text{-a. e. on } \Omega,\\ e\left(\mathbf{u}_{k_j}\right) &\rightharpoonup e(\mathbf{u}) \text{ weakly in } L^1\left(\Omega;\mathbb{R}^{n\times n}_{sym}\right),\\ \mathcal{H}^{n-1}(J_{\mathbf{u}}) &\leq \liminf_{j\to 0} \mathcal{H}^{n-1}\left(J_{\mathbf{u}_{k_j}}\right). \end{aligned}$$

We close this section with a density theorem for functions in $GSBD(\Omega;\mathbb{R}^n)$. It is a version of [CC19, Theorem 1.1] for functions in $L^1_{loc}(\Omega;\mathbb{R}^n)$ adapted to our needs and can be combined with Theorem 2.4.15.

Theorem 2.4.26 (Density in $GSBD(\Omega;\mathbb{R}^n)$)**:**
Let $\Omega \subset \mathbb{R}^n$ be an open, bounded set with locally Lipschitz boundary $\partial\Omega$. For $p \in (1,+\infty)$ let $\mathbf{u} \in GSBD^p(\Omega;\mathbb{R}^n) \cap L^1(\Omega;\mathbb{R}^n)$. Then we can find a sequence $\mathbf{u}_k \in SBV^p(\Omega;\mathbb{R}^n) \cap L^\infty(\Omega;\mathbb{R}^n)$ such that $J_{\mathbf{u}_k} \subset \Omega$ is closed and contained in a finite union of closed $\mathcal{C}^1$ curves and $\mathbf{u}_k \in W^{1,\infty}(\Omega \setminus J_{\mathbf{u}_k};\mathbb{R}^n)$. Further $\mathbf{u}_k$ satisfies

$$
\begin{aligned}
&e(\mathbf{u}_k) \to e(\mathbf{u}) \ \text{ in } L^p\left(\Omega;\mathbb{R}^{n\times n}_{sym}\right),\\
&\mathcal{H}^{n-1}(J_{\mathbf{u}_k} \Delta J_{\mathbf{u}}) \to 0,\\
&\lim_{k\to+\infty} \int_\Omega |\mathbf{u}_k - \mathbf{u}|\,\mathrm{dx} = 0.
\end{aligned}
$$

Moreover, if $\mathbf{u} \in GSBD^2(\Omega;\mathbb{R}^n) \cap L^2(\Omega;\mathbb{R}^n)$ the sequence $\mathbf{u}_k$ can be chosen such that

$$
\lim_{k\to+\infty} \|\mathbf{u}_k - \mathbf{u}\|_{L^2(\Omega;\mathbb{R}^n)} = 0.
$$

2.5 Discretization methods

In the previous sections we focused on the preliminaries for the analytical derivation of a weak formulation of the problem of fracture propagation. Now we concentrate on the numerical treatment of such an equation.

Given a partial differential equation (PDE) that cannot be solved exactly, there exist multiple possibilities to discretize it and solve it numerically. An extensive overview of discretization methods can be found in [SdBH04]. The most common ones are finite difference methods (FDM), finite volume methods (FVM) and finite element methods (FEM). While FDM are comparably easy to implement, they are also the least flexible of the aforementioned methods. They rely on the approximation of derivatives by finite differences and thus are most efficient on structured grids. For an introduction we refer the interested reader to [GR07] and [SdBH04, Chapter 2].

The FVM has the substantial advantage that it directly poses conservation laws on the discrete level. Thus it is a very common discretization approach for example when simulating equations from fluid mechanics, meteorology, electromagnetics and other research areas that deal with conservation laws. It relies on the discretization of the domain into small volumes called cells. On each cell the solution is approximated by its average. This cell average is then modified through the numerical flux across its boundary. An introduction to FVM methods can be found in [LeV02] and [SdBH04, Chapter 15].

In the present work we choose FEM as discretization method for our problem. It is more flexible than the other two and has better approximation properties. Nevertheless the flexibility comes with more complexity, analytically as well as concerning the implementation. Indeed FVM are

described as a special case of FEM sometimes, see for example [GR07, Chapter 4.5.4]. We describe the basic ideas of FEM and introduce some important notation in Section 2.5.1, followed by the introduction of a special FEM, the so-called discontinuous Galerkin method in Section 2.5.2. This method can be seen as a generalization of an FVM, it is conservative and well suited to handle discontinuities [DPE12]. Finally in Section 2.5.3 we recall a method called unfitted discontinuous Galerkin method (UDG) that was first established in [BE09].

2.5.1 Finite element methods

Let us shortly recall the main ideas of finite element methods and fix some definitions and notation. For a more detailed introduction to FEM we refer the reader to [Cia02] and [SdBH04, Chapter 4], see also [BS08, Bra07]. For illustration we use the example of the Poisson equation with homogeneous Dirichlet boundary conditions, given in its strong form as follows.

Find $u \in C^2(\Omega)$ *such that*

$$\begin{aligned} -\Delta u &= f \text{ in } \Omega \\ u &= 0 \text{ on } \partial\Omega. \end{aligned} \tag{2.18}$$

Here Ω is some given open domain, typically with Lipschitz boundary $\partial\Omega$ and $f \in L^2(\Omega)$ is some given function called the right-hand side (RHS).

For the derivation of the FEM formulation we assume that we have a partial differential equation given in its variational (weak) form. For the Poisson problem we can derive the weak form in the weak solution space $V = H_0^1(\Omega)$ if we test equation (2.18) with a function $v \in C_c^\infty(\Omega)$ and integrate by parts.

Let $a: V \times V \to \mathbb{R}$ *be given by* $a(u,v) = \int_\Omega \nabla u \nabla v \,\mathrm{dx}$ *and* $F: V \to \mathbb{R}$ *by* $F(v) = \int_\Omega fv \,\mathrm{dx}$. *Find* $u \in V$ *such that*

$$a(u,v) = F(v) \tag{2.19}$$

for all $\varphi \in V$.

Note that $a(\cdot,\cdot)$ is a continuous, symmetric, positive definite bilinear form and $F(\cdot)$ is a continuous linear form, thus by the Lax-Milgram theorem there exists a unique solution of equation (2.19).

Theorem 2.5.1 (Lax-Milgram)**:**
Let V *be a Hilbert-space and* $a: V \times V \to \mathbb{R}$ *a continuous and coercive bilinear form. Let further* $F: V \to \mathbb{R}$ *be a bounded linear form. Then there exists a unique function* $u \in V$ *such that*

$$a(u,v) = F(v) \quad \forall\, v \in V.$$

For a proof of Theorem 2.5.1 see [Eva10, section 6.2.1].

While a solution of equation (2.18) always solves equation (2.19), the reverse is obviously false, but a solution of equation (2.19) satisfies equation (2.18) almost everywhere.

Following [Cia02], the discretization of equation (2.19) now consists of three main parts. First, a discretization of the domain Ω. Second a finite-dimensional solution space V_h and the discrete analogues of $a(\cdot,\cdot)$ and $F(\cdot)$, $a_h(\cdot,\cdot)$ and $F_h(\cdot)$ respectively. Third, the choice of an appropriate basis for V_h.

For the discretization of Ω we demand that it is a regular triangulation in the sense of [Cia02].

Definition 2.5.2 (Regular triangulation)**:**
We say that a set of elements $\mathcal{T} = \{T\}$ is a regular triangulation of Ω if

- $\overline{\Omega} = \bigcup_{T\in\mathcal{T}} T$,
- *for all $T \in \mathcal{T}$ holds $T = \overline{\mathring{T}}$ and $\mathring{T} \neq \emptyset$,*
- *for all $T \in \mathcal{T}$ holds ∂T is Lipschitz continuous,*
- *for all $T_1, T_2 \in \mathcal{T}$ with $T_1 \neq T_2$ holds $\mathring{T}_1 \cap \mathring{T}_2 = \emptyset$,*
- *for all $T_1, T_2 \in \mathcal{T}$ with $T_1 \neq T_2$ holds $T_1 \cap T_2$ is either empty, a single point or a common face F.*

Note that it is not mandatory to choose triangles as the elements T to construct a regular triangulation. It is also quite common to choose quadrangles and further generalizations for example to elements bounded by NURBS (non-Uniform Rational B-Splines) are possible [HCB05].

Definition 2.5.3 (Mesh parameter h)**:**
Let $\mathcal{T}$ be a regular triangulation. For every element $T \in \mathcal{T}$ we set $h_T = \operatorname{diam} T$, the diameter of the element. Then the mesh parameter h is defined as $h = \max_{T\in\mathcal{T}} h_T$. For every face $F = \partial T_1 \cap \partial T_2$ with $T_1,\ T_2 \in \mathcal{T}$ we set $h_F = \frac{|T_1|_d + |T_2|_d}{2|F|_{d-1}}$, where $|\cdot|_d$ and $|\cdot|_{d-1}$ denote the volume and surface measure, respectively.

The discrete solution space V_h is often chosen as a subset of the weak solution space V, the method is then called a conforming FEM. Typical examples are continuous functions that are piecewise polynomial. Denoting the space of polynomials of degree $\leq k$ on a domain T by $\mathcal{P}_k(T)$ and setting

$$\mathcal{P}_k(\mathcal{T}) = \left\{u \in L^2(\Omega) : \forall T \in \mathcal{T} \text{ holds } u|_T \in \mathcal{P}_k(T)\right\},$$

we define $V_h = \mathcal{P}_k(\mathcal{T}) \cap \mathcal{C}(\Omega)$. Defining a_h and F_h as the restrictions of a and F to this subspace, the discrete problem becomes the following.

Let $a_h \colon V_h \times V_h \to \mathbb{R}$ *be given by* $a_h(u,v) = \int_\Omega \nabla u \cdot \nabla v \,\mathrm{dx}$ *and* $F_h \colon V_h \to \mathbb{R}$ *by* $F_h(v) = \int_\Omega fv \,\mathrm{dx}$. *Find* $u \in V_h$ *such that*

$$a_h(u,v) = F_h(v) \tag{2.20}$$

for all $v \in V_h$.

To finally solve equation (2.20) we choose a finite basis $(v_i)_{i=0}^{N-1}$ for the N-dimensional space V_h. Setting $u_h = \sum_{i=0}^{N-1} u_i v_i$ and testing equation (2.20) with all basis functions v_i we obtain a system of N linear equations to solve for the coefficient vector $(u_i)_{i=0}^{N-1}$.

2.5.2 Discontinuous Galerkin methods

In the case of fracture propagation we have to deal with a displacement vector, that becomes discontinuous at the crack. Therefore it seems natural to already include this discontinuity in the discrete function space V_h. Thus given a triangulation $\mathcal{T}$ of Ω as above we choose $V_h = \mathcal{P}_k(\mathcal{T})$ as discrete function space, no longer requiring continuity. Nevertheless in the rest of the domain, away from the crack, continuity is desired. To achieve it, discontinuous Galerkin (DG) methods punish discontinuity at element boundaries with a penalty term. In the literature different possibilities exist to accommodate this. In the ongoing chapter we present the symmetric interior penalty Galerkin (SIPG) method followed by a short overview of well-known analytical results. In doing this, we mainly follow [DPE12]. For a more detailed treatise on the subject we refer the reader to the aforementioned book, where one can also find a brief overview of the development of DG methods. An analytic overview defining a common framework for different DG methods can be found in [ABCM02].

For the definition of DG methods we need two important quantities, the jump and the average of a function over a face. In order to define them we fix some additional notation.

Definition 2.5.4 (Skeleton, jump and average)**:**
Let $\mathcal{T}$ *be a regular triangulation of some domain* $\Omega \subset \mathbb{R}^n$. *We define its inner skeleton* $\mathcal{F}_{int}$ *as*

$$\mathcal{F}_{int} = \left\{ F : F = \partial T_1 \cap \partial T_2 \text{ where } T_1, T_2 \in \mathcal{T} \text{ and } 0 < \mathcal{H}^{n-1}(F) < +\infty \right\}.$$

Its outer skeleton is defined as

$$\mathcal{F}_{ext} = \left\{ F : F = \partial T \cap \partial\Omega \text{ where } T \in \mathcal{T} \text{ and } 0 < \mathcal{H}^{n-1}(F) < +\infty \right\}$$

and the union $\mathcal{F} = \mathcal{F}_{int} \cup \mathcal{F}_{ext}$ *is called the skeleton.*

We now consider a scalar-valued function $\varphi \colon \Omega \to \mathbb{R}$ *and a vector-valued function* $\mathbf{v} \colon \Omega \to \mathbb{R}^n$. *Assume that* φ *and* $\mathbf{v}$ *are sufficiently smooth such that their restrictions* $\varphi|_T$ *and* $\mathbf{v}|_T$ *are well*

defined up to the boundary ∂T for every $T \in \mathcal{T}$. Then their jump across a face F is defined by

$$[\![\varphi]\!] = \begin{cases} \varphi|_{T_1} - \varphi|_{T_2} & F \in \mathcal{F}_{int}, F = \partial T_1 \cap \partial T_2, \\ \varphi|_T & F \in \mathcal{F}_{ext}, F = \partial\Omega \cap \partial T, \end{cases}$$

$$[\![\mathbf{v}]\!] = \begin{cases} \mathbf{v}|_{T_1} - \mathbf{v}|_{T_2} & F \in \mathcal{F}_{int}, F = \partial T_1 \cap \partial T_2, \\ \mathbf{v}|_T & F \in \mathcal{F}_{ext}, F = \partial\Omega \cap \partial T. \end{cases}$$

Note that this definition depends on the ordering of T_1 and T_2. In what follows we always fix the orientation such that the unit normal to the face $F = \partial T_1 \cap \partial T_2$ is the outer unit normal to T_1, hence we write $\nu = \nu_F = \nu_1 = -\nu_2$, where ν_1 and ν_2 denote the outer normals to T_1 and T_2 respectively. The average of φ and $\mathbf{v}$ is defined as

$$\{\!\{\varphi\}\!\} = \begin{cases} \frac{1}{2}\left(\varphi|_{T_1} + \varphi|_{T_2}\right) & F \in \mathcal{F}_{int}, F = \partial T_1 \cap \partial T_2, \\ \varphi|_T & F \in \mathcal{F}_{ext}, F = \partial\Omega \cap \partial T, \end{cases}$$

$$\{\!\{\mathbf{v}\}\!\} = \begin{cases} \frac{1}{2}\left(\mathbf{v}|_{T_1} + \mathbf{v}|_{T_2}\right) & F \in \mathcal{F}_{int}, F = \partial T_1 \cap \partial T_2, \\ \mathbf{v}|_T & F \in \mathcal{F}_{ext}, F = \partial\Omega \cap \partial T. \end{cases}$$

Note that depending on the author the definitions of the jump might slightly differ. Sometimes it is defined as $\varphi|_{T_1}\nu_1 + \varphi|_{T_2}\nu_2$, see for example [ABCM02]. While this definition is independent of an ordering of T_1 and T_2 it makes the jump of a vector-valued function become a scalar-valued function. In addition the definition at the boundary might be slightly different from source to source. Note further that for any scalar function φ and any vector-valued functions $\mathbf{v}$ and $\mathbf{w}$ as above it holds $[\![\varphi\mathbf{v}]\!] = \{\!\{\varphi\}\!\}\,[\![\mathbf{v}]\!] + \{\!\{\mathbf{v}\}\!\}\,[\![\varphi]\!]$ and $[\![\mathbf{w}\cdot\mathbf{v}]\!] = \{\!\{\mathbf{w}\}\!\}\cdot[\![\mathbf{v}]\!] + \{\!\{\mathbf{v}\}\!\}\cdot[\![\mathbf{w}]\!]$.

Having discontinuous basis functions, the partial integration we used in Section 2.5.1 can only be carried out on each element $T \in \mathcal{T}$. Thus we get contributions along the boundaries ∂T of elements. Consequently the discontinuous Galerkin discretization of equation (2.19) includes additional terms along $\mathcal{F}_{int}$ in comparison to equation (2.20). Moreover Nitsche's method [Nit71] is used to weakly enforce continuity of the discrete solution along $\mathcal{F}_{int}$ and homogeneous boundary conditions. The SIPG method applied here goes back to [Arn82].

Definition 2.5.5 (SIPG discretization of the Poisson model problem (2.18), see [DPE12])**:**
Let $a_h^{DG}\colon V_h \times V_h \to \mathbb{R}$ and $F_h^{DG}\colon V_h \to \mathbb{R}$ be given by

$$a_h^{DG}(u,v) = \sum_{T\in\mathcal{T}} \int_T \nabla u \nabla v \,\mathrm{d}x - \sum_{F\in\mathcal{F}} \int_F \{\!\{\nabla u\}\!\}\cdot\nu\,[\![v]\!] + \{\!\{\nabla v\}\!\}\cdot\nu\,[\![u]\!]\,\mathrm{d}s + \sum_{F\in\mathcal{F}} \frac{\eta}{h_F}[\![u]\!]\,[\![v]\!]\,\mathrm{d}s,$$

$$F_h^{DG}(v) = \sum_{T\in\mathcal{T}} \int_T fv\,\mathrm{d}x\,.$$

Here the gradient ∇ has to be taken elementwise. This is sometimes written as broken gradient $\nabla_h u$ defined by $(\nabla_h u)|_T = \nabla u|_T$. The discrete problem can then be formulated as follows. Find

$u \in V_h$ such that

$$a_h^{DG}(u,v) = F_h^{DG}(v) \tag{2.21}$$

for all $v \in V_h$.

Remark: The term $-\sum_{F\in\mathcal{F}} \int_F \{\!\{\nabla u\}\!\}\cdot\nu\,[\![v]\!]$ is called *consistency term* as it ensures that any solution u of equation (2.18) with $u \in H^2(\Omega)$ satisfies equation (2.21). The term $-\sum_{F\in\mathcal{F}} \int_F \{\!\{\nabla v\}\!\}\cdot\nu\,[\![u]\!]\,\mathrm{ds}$ is not necessary for consistency, since for any function $u \in H_0^1(\Omega)\cap H^2(\Omega)$ it holds $[\![u]\!] = [\![\nabla u]\!]\cdot\nu = 0$ along any edge $F \in \mathcal{F}_{int}$ [DPE12, Lemma 4.3]. It is called the *symmetry term* as it ensures symmetry of the bilinear form a_h^{DG}. Finally the term $\sum_{F\in\mathcal{F}} \frac{\eta}{h_F}[\![u]\!][\![v]\!]\,\mathrm{ds}$ is called the *penalty term* and weakly forces the solution to become continuous along faces. It does not interfere with consistency and symmetry. The penalty parameter $\eta > 0$ is a numerical parameter that must be adjusted according to the problem. If η is chosen sufficiently large it ensures discrete coercivity of a_h^{DG}. For the proofs of consistency and discrete coercivity we refer the interested reader to [DPE12, Lemma 4.8 and Lemma 4.12]. Additionally in [DPE12, Lemma 4.16] a boundedness result for a_h^{DG} can be found. According to Theorem 2.5.1 these guarantee the unique existence of a discrete solution of equation (2.21).

2.5.3 Unfitted discontinuous Galerkin methods

As described previously, a common technique to simulate fracture propagation is to implement unfitted finite element methods. Our choice of method is the unfitted discontinuous Galerkin (UDG) method that we present subsequently. This introduction goes along the lines of the original publications [BE09, Eng09] that first presented the UDG method. Let us assume that the domain Ω is partitioned into a set $\mathcal{G}$ of N sub-domains as follows.

Definition 2.5.6 (Sub-domains):
Let $\Omega \subset \mathbb{R}^n$ be a domain as before. Let $\mathcal{G}(\Omega) = \{\Omega^0,\dots,\Omega^{N-1}\}$ be such that $\Omega^i \subset \Omega$ for all $0 \le i < N$ and $\Omega^i \cap \Omega^j = \emptyset$ for all $0 \le i < j < N$. Further we require $\overline{\Omega} = \bigcup_{i=0}^{N-1}\overline{\Omega^i}$. Then we call $\mathcal{G}$ a disjoint partition of Ω into sub-domains. We call $\Gamma^{i,j} = \partial\Omega^i \cap \partial\Omega^j$ the interface between Ω^i and Ω^j.

Next we need to define the restriction of the mesh to these sub-domains.

Definition 2.5.7:
Let $\mathcal{T}$ and $\mathcal{G}$ be given as above. Then the sub-domain mesh is defined as

$$\mathcal{T}^i = \mathcal{T}(\Omega^i) = \left\{T^i : T^i = \Omega^i \cap T \text{ for some } T \in \mathcal{T} \text{ and } T^i \neq \emptyset\right\}.$$

We further define the internal and external skeleton corresponding to a sub-domain. In the internal skeleton we distinguish between edges connecting elements in the same domain, $\mathcal{F}_{int}^i$, and edges

connecting different domains, $\mathcal{F}_{int}^{i,j}$ for $i \neq j$.

$$\mathcal{F}_{int}^{i,i} = \left\{F_{1,2} : F_{1,2} = \partial T_1^i \cap \partial T_2^i \text{ where } T_1^i, T_2^i \in \mathcal{T}^i \text{ and } 0 < \mathcal{H}^{n-1}(F_{1,2}) < +\infty\right\},$$
$$\mathcal{F}_{int}^{i,j} = \left\{F_{1,2} : F_{1,2} = \partial T_1^i \cap \partial T_2^j \text{ where } T_1^i \in \mathcal{T}^i, T_2^j \in \mathcal{T}^j, i \neq j \text{ and } 0 < \mathcal{H}^{n-1}(F_{1,2}) < +\infty\right\},$$
$$\mathcal{F}_{ext}^{i} = \left\{F_1 : F_1 = \partial T^i \cap \partial\Omega \text{ where } T^i \in \mathcal{T}^i \text{ and } 0 < \mathcal{H}^{n-1}(F_1) < +\infty\right\}.$$

To shorten notation we define $\mathcal{F}_{int}^{i} = \bigcup_{j<i} \mathcal{F}_{int}^{i,j} \cup \mathcal{F}_{int}^{i,i}$ and $\mathcal{F}^i = \mathcal{F}_{int}^{i} \cup \mathcal{F}_{ext}^{i}$.

Having a notion for the mesh of a sub-domain we can define the basis functions for the UDG method and the resulting finite element space for the discretization in a sub-domain Ω^i. As before we consider the space of piecewise polynomials, this time for each sub-domain, defining $V_h^i = \mathcal{P}_k(\mathcal{T}^i)$. For the construction of the basis functions of these spaces we start with the basis functions v_i of $V_h = \mathcal{P}_k(\mathcal{T})$ and restrict their support to the so-called cut-cells $T^i \in \mathcal{T}^i$. That is, for any $T_n^i \in \mathcal{T}^i$ we set

$$v_{j,n}^i = \begin{cases} v_j & \text{inside of } T_n^i, \\ 0 & \text{outside of } T_n^i. \end{cases}$$

Thus the UDG discretization of the Poisson model problem using SIPG as underlying DG method looks similar to Definition 2.5.5, using cut-cells instead of the elements of $\mathcal{T}$ and taking into account the additional inter-domain interfaces $\Gamma^{i,j}$.

Definition 2.5.8 (UDG discretization of the Poisson model problem, see [DPE12])**:**
Let $a_h^{UDG} : V_h \times V_h \to \mathbb{R}$ and $F_h^{UDG} : V_h \to \mathbb{R}$ be given by

$$\begin{aligned} a_h^{UDG}(u,v) = &\sum_{i=0}^{N-1} \sum_{T \in \mathcal{T}^i} \int_T \nabla u \nabla v \,\mathrm{dx} \\ &+ \sum_{i=0}^{N-1} \sum_{F \in \mathcal{F}^i} \left(- \int_F \{\!\{\nabla u\}\!\} \cdot \nu \,[\![v]\!] + \{\!\{\nabla v\}\!\} \cdot \nu \,[\![u]\!] \,\mathrm{ds} + \int_F \frac{\eta}{h_F} [\![u]\!] [\![v]\!] \,\mathrm{ds} \right), \\ F_h^{UDG}(v) = &\sum_{i=0}^{N-1} \sum_{T \in \mathcal{T}^i} \int_T f v \,\mathrm{dx}. \end{aligned}$$

Once again the gradient ∇ has to be taken elementwise. The discrete problem can then be formulated as follows. Find $u \in V_h$ such that

$$a_h^{UDG}(u,v) = F_h^{UDG}(v) \tag{2.22}$$

for all $v \in V_h$.

Integrations on an element $T^i \in \mathcal{T}^i$ are carried out using a local triangulation. As the local triangulation is only used for finding decent quadrature points, its quality has no influence on

the condition number of the resulting system. Thus for example arbitrarily small angles are not problematic. What does influence the condition number of the system is the size of the cut-cells $T^i \in \mathcal{T}^i$. To counter the effect of small cut-cells we follow [Eng09], wherein the authors propose a scaling of the corresponding local basis functions to the bounding box. Another approach would be to use ghost penalty terms as done by [GM].

3 Γ-convergence of the energy functional

The present chapter deals with the Γ-convergence of the energy functional derived in Section 2.2. Namely we investigate the Γ-convergence of functionals of the type (2.13) to functionals of the type (2.10). We start by an examination of the one-dimensional case in Section 3.1 and consider the higher dimensional case in Section 3.2. We end our treatise of Γ-convergence with some notes on the conditions under which we obtain convergence of minimizers in Section 3.3.

3.1 One-dimensional case

We first consider one-dimensional versions of the energy functionals in the case of a one-dimensional open bounded domain $\Omega \subset \mathbb{R}$. In the following we consider a domain $\Omega = (a, b)$. The general case can be treated by repeating the arguments on each connected component. Note that the results presented in this section were previously published in [ES17]. Let us start by the definition of some functionals. The corresponding higher-dimensional functionals are defined in Definition 3.2.1.

Definition 3.1.1:
Considering only the surface part of the energy we define $\widetilde{G}_\varepsilon \colon L^1((a,b)) \to [0,+\infty]$ *by*

$$\widetilde{G}_\varepsilon(\varphi) = \begin{cases} \frac{G_c}{2} \int_a^b \varepsilon |\varphi'|^2 + \frac{1}{\varepsilon}(1-\varphi)^2 \,\mathrm{dt} & \text{if } \varphi \in H^1((a,b)),\ 0 \le \varphi \le 1, \\ +\infty & \text{otherwise.} \end{cases} \tag{3.1}$$

As mentioned before, existing literature on brittle fracture often deals with an energy similar to ours, but without pressure terms. We define these in the following. Let $\widetilde{F} \colon L^1((a,b)) \times L^1((a,b)) \to [0,+\infty]$ *and* $\widetilde{F}_\varepsilon \colon L^1((a,b)) \times L^1((a,b)) \to [0,+\infty]$ *be given by*

$$\widetilde{F}(u,\varphi) = \begin{cases} \int_a^b \gamma |u'|^2 \,\mathrm{dt} + G_c \mathcal{H}^0(J_u) & \text{if } u \in SBV^2((a,b)),\ \varphi = 1 \text{ a.e. in } (a,b), \\ +\infty & \text{otherwise,} \end{cases} \tag{3.2}$$

$$\widetilde{F}_\varepsilon(u,\varphi) = \begin{cases} \int_a^b \gamma\left(k_\varepsilon + \varphi^2\right)|u'|^2 \,\mathrm{dt} + \frac{G_c}{2}\int_a^b \varepsilon|\varphi'|^2 + \frac{1}{\varepsilon}(1-\varphi)^2 \,\mathrm{dt} & \\ \qquad \text{if } u \in H^1((a,b)),\ \varphi \in H^1((a,b)),\ 0 \le \varphi \le 1, & \\ +\infty \qquad \text{otherwise,} & \end{cases} \tag{3.3}$$

where γ is some material constant. For fixed $\alpha > 0$ and $p \in W^{1,\infty}((a,b))$ we define $\widetilde{D}\colon L^1((a,b)) \times L^1((a,b)) \to [0,+\infty]$ and $\widetilde{D}_\varepsilon\colon L^1((a,b)) \times L^1((a,b)) \to (-\infty,+\infty]$ including pressure terms by

$$\widetilde{D}(u,\varphi) = \widetilde{F}(u,\varphi) + \int_a^b (1-\alpha)\, pu' + p'u \,\mathrm{d}t, \tag{3.4}$$

$$\widetilde{D}_\varepsilon(u,\varphi) = \widetilde{F}_\varepsilon(u,\varphi) + \int_a^b (1-\alpha)\, \varphi_\varepsilon p u_\varepsilon' + \varphi_\varepsilon p' u_\varepsilon \,\mathrm{d}t\,. \tag{3.5}$$

By adding the boundary terms, we finally end up with the total energy functional $\widetilde{E}\colon L^1((a,b)) \times L^1((a,b)) \to (-\infty,+\infty]$ and its approximation $\widetilde{E}_\varepsilon\colon L^1((a,b)) \times L^1((a,b)) \to (-\infty,+\infty]$, given by

$$\widetilde{E}(u,\varphi) = \begin{cases} \widetilde{D}(u,\varphi) - (p(b)\,u_D(b) - p(a)\,u_D(a)) & \text{if } u(a) = u_D(a),\ u(b) = u_D(b), \\ +\infty & \text{otherwise,} \end{cases} \tag{3.6}$$

$$\widetilde{E}_\varepsilon(u,\varphi) = \begin{cases} \widetilde{D}_\varepsilon(u,\varphi) - (p(b)\,u_D(b) - p(a)\,u_D(a)) & \text{if } u \in H^1_D((a,b)), \\ +\infty & \text{otherwise.} \end{cases} \tag{3.7}$$

Here $u_D \in H^1(\mathbb{R})$ denotes some given boundary function and the equalities $u(a) = u_D(a)$ and $u(b) = u_D(b)$ are to be understood in the sense of traces. Moreover we need the localized versions of the preceding functionals. Thus whenever we consider an open interval $I \subset \mathbb{R}$ as integration domain instead of (a,b), we substitute $\widetilde{F}(u,\varphi)$ and $\widetilde{F}_\varepsilon(u,\varphi)$ with

$$\widetilde{F}(u,\varphi;I) = \begin{cases} \int_I \gamma |u'|^2 \,\mathrm{d}t + G_c \mathcal{H}^0(J_u) & \text{if } u \in SBV^2(I),\ \varphi = 1 \text{ a.e. in } I, \\ +\infty & \text{otherwise,} \end{cases}$$

$$\widetilde{F}_\varepsilon(u,\varphi;I) = \begin{cases} \int_I \gamma\left(k_\varepsilon + \varphi^2\right)|u'|^2 \,\mathrm{d}t + \frac{G_c}{2}\int_I \varepsilon|\varphi'|^2 + \frac{1}{\varepsilon}(1-\varphi)^2 \,\mathrm{d}t \\ \qquad\qquad \text{if } u \in H^1(I),\ \varphi \in H^1(I),\ 0 \le \varphi \le 1, \\ +\infty \qquad\qquad \text{otherwise,} \end{cases}$$

The localized functionals $\widetilde{G}_\varepsilon(\varphi;I)$, $\widetilde{D}(u,\varphi;I)$, $\widetilde{D}_\varepsilon(u,\varphi;I)$, $\widetilde{E}(u,\varphi;I)$ and $\widetilde{E}_\varepsilon(u,\varphi;I)$ are defined analogously.

Remark: In the literature the term $\mathcal{H}^{n-1}(S_\mathbf{u})$ often appears instead of $\mathcal{H}^{n-1}(J_\mathbf{u})$, see for example [Foc01]. As $\mathcal{H}^{n-1}(S_\mathbf{u} \setminus J_\mathbf{u}) = 0$ for BV functions, this makes no difference in the setting above. Nevertheless we decided to use $\mathcal{H}^{n-1}(J_\mathbf{u})$ to be consistent with the higher-dimensional setting in Section 3.2. Therein we consider functions in $GSBD(\Omega;\mathbb{R}^n)$, for which it is necessary to use the term $\mathcal{H}^{n-1}(J_\mathbf{u})$, since it is not clear whether $J_\mathbf{u}$ and $S_\mathbf{u}$ coincide $\mathcal{H}^{n-1}$-almost everywhere.

In the following we prove Γ-convergence in the one-dimensional setting, following the proof of Braides [Bra98, Theorem 3.15]. The main difficulties in our case are the pressure terms $(1-\alpha)\,p\varphi_\varepsilon u_\varepsilon'$ and $\varphi_\varepsilon p' u_\varepsilon$ in the bulk energy. These might become negative due to negative displacement gradients and displacements. While the main work is in Theorem 3.1.2, Corollary 3.1.8 adds Dirichlet boundary conditions.

Theorem 3.1.2:
Let $G_c > 0$, $p \in W^{1,\infty}((a,b))$, $0 \leq \alpha \leq 1$, $k_\varepsilon \in o(\varepsilon)$ and $c > 0$ be some material parameter. Then $\widetilde{D}_\varepsilon$ Γ-converges for $\varepsilon \to 0^+$ to $\widetilde{D}$ with respect to the strong convergence in $L^1((a,b)) \times L^1((a,b))$.

Before we start with the proof of Theorem 3.1.2 let us recall an auxiliary lemma proven in the course of the proof of [Bra98, Theorem 3.10].

Lemma 3.1.3:
Let $\varphi_\varepsilon \in H^1((a,b))$, $z^1, z^2 \in \mathbb{R}$ and let $\zeta_\varepsilon^1, \zeta_\varepsilon^2 \in (a,b)$ for all $\varepsilon > 0$ be such that

$$\lim_{\varepsilon\to 0} \varphi_\varepsilon\left(\zeta_\varepsilon^1\right) = z^1 \text{ and } \lim_{\varepsilon\to 0} \varphi_\varepsilon\left(\zeta_\varepsilon^2\right) = z^2.$$

Then it holds

$$\liminf_{\varepsilon\to 0} \left| \int_{\zeta_\varepsilon^1}^{\zeta_\varepsilon^2} \frac{1}{2\varepsilon}\left(1-\varphi_\varepsilon(t)\right)^2 + \frac{\varepsilon}{2}\left|\varphi_\varepsilon'(t)\right|^2 \mathrm{d}t \right| \geq \left| \int_{z^1}^{z^2} (1-s)\,\mathrm{d}s \right|.$$

Using Young's inequality we can show that a bound on $\widetilde{D}_\varepsilon(u,\varphi)$ is sufficient to bound $\widetilde{F}_\varepsilon(u,\varphi)$ as well.

Lemma 3.1.4:
We can find constants $c_1,\ c_2,\ c_3 > 0$ such that for all $(u,\varphi) \in L^1((a,b)) \times L^1((a,b))$ it holds

$$\widetilde{D}_\varepsilon(u,\varphi) \geq c_1 \widetilde{F}_\varepsilon(u,\varphi) - c_2\|u\|_{L^1((a,b))} - c_3. \tag{3.8}$$

In particular $\sup_{\varepsilon>0}\left(\widetilde{D}_\varepsilon(u_\varepsilon,\varphi_\varepsilon) + \|u_\varepsilon\|_{L^1((a,b))}\right) < +\infty$ implies $\sup_{\varepsilon>0} \widetilde{F}_\varepsilon(u_\varepsilon,\varphi_\varepsilon) < +\infty$.

Proof of Lemma 3.1.4. Without loss of generality we can restrict ourselves to the case $(u,\varphi) \in H^1((a,b)) \times \left\{v \in H^1((a,b)) : 0 \leq v \leq 1\right\}$. Then for arbitrary $\delta > 0$ Young's inequality in combination with $|\varphi| \leq 1$ yields

$$\begin{aligned}
&\int_a^b c\left(k_\varepsilon + \varphi^2\right)|u'|^2\,\mathrm{d}t + \int_a^b (1-\alpha)\,p\varphi u'\,\mathrm{d}t + \int_a^b \varphi p' u\,\mathrm{d}t \\
&\quad\geq \int_a^b c\left(k_\varepsilon + \varphi^2\right)|u'|^2\,\mathrm{d}t - \int_a^b \frac{1}{2\delta}\left|(1-\alpha)\,p\right|^2 + \frac{\delta}{2}\left|\varphi u'\right|^2\,\mathrm{d}t - \int_a^b |\varphi p' u|\,\mathrm{d}t \\
&\quad\geq \int_a^b \left(c - \frac{\delta}{2}\right)\left(k_\varepsilon + \varphi^2\right)|u'|^2\,\mathrm{d}t - \frac{(1-\alpha)^2}{2\delta}\|p\|^2_{L^2((a,b))} - \|p'\|_{L^\infty((a,b))}\|u\|_{L^1((a,b))}.
\end{aligned}$$

Hence choosing δ such that $c - \frac{\delta}{2} > 0$, $c_1 = \min\left(1, c - \frac{\delta}{2}\right)$, $c_2 = \|p'\|_{L^\infty((a,b))}$ and $c_3 = \frac{(1-\alpha)^2}{2\delta}\|p\|^2_{L^2((a,b))}$ implies equation (3.8). Obviously for $\sup_{\varepsilon>0}\left(\widetilde{D}_\varepsilon(u_\varepsilon,\varphi_\varepsilon) + \|u_\varepsilon\|_{L^1((a,b))}\right) < +\infty$

it holds

$$\sup_{\varepsilon>0} \widetilde{F}_\varepsilon(u_\varepsilon, \varphi_\varepsilon) \leq \frac{1}{c_1} \sup_{\varepsilon>0} \left(\widetilde{D}_\varepsilon(u_\varepsilon, \varphi_\varepsilon) + c_2 \|u_\varepsilon\|_{L^1((a,b))} + c_3 \right) < +\infty,$$

which completes the proof. □

The proof of Theorem 3.1.2 follows the proof of [Bra98, Theorem 3.15]. For the reader's convenience we give an outline of the proof and point out the adjustments dealing with the pressure terms. The proof is split into three parts. Starting with a lim inf inequality for the surface part in Lemma 3.1.5, we deduce the total lim inf inequality in Theorem 3.1.6. Finally in Theorem 3.1.7 we construct a recovery sequence to obtain the lim sup inequality.

Lemma 3.1.5:
Let $I \subset (a,b)$ be open and bounded. Consider a sequence $(u_\varepsilon, \varphi_\varepsilon)$ converging to (u, φ) with respect to the $L^1((a,b))$ topology and satisfying

$$\liminf_{\varepsilon\to 0} \widetilde{F}_\varepsilon(u_\varepsilon, \varphi_\varepsilon; I) < +\infty. \tag{3.9}$$

Then it holds $\mathcal{H}^0(I \cap J_u) < +\infty$ and

$$\liminf_{\varepsilon\to 0} \widetilde{G}_\varepsilon(\varphi; I) \geq G_c \mathcal{H}^0(I \cap J_u). \tag{3.10}$$

Proof of Lemma 3.1.5. Note that this statement is independent of the pressure terms in our energy formulation. Thus the proof goes exactly as in [Bra98, Theorem 3.15]. It goes back to the ideas of Ambrosio and Tortorelli in [AT90], see also [Foc01, Lemma 3.2]. For the reader's convenience we recall the main steps here. Let $\varphi_\varepsilon \to \varphi$ in $L^1(\Omega)$. Passing to a subsequence we can assume the convergence $\varphi_\varepsilon \to \varphi$ to hold almost everywhere and that $\lim_{\varepsilon\to 0} \widetilde{F}_\varepsilon(u_\varepsilon, \varphi_\varepsilon; I) < +\infty$ exists. In particular

$$\sup_{\varepsilon>0} \frac{G_c}{2\varepsilon} \int_I (1-\varphi_\varepsilon)^2 \,\mathrm{dt} < +\infty,$$

hence $\varphi = 1$ holds $\mathcal{L}^n$-almost everywhere in I. Even more so, $\|\varphi_\varepsilon - 1\|_{L^2(I)} \to 0$ for $\varepsilon \to 0$ and uniqueness of the limit implies $\varphi = 1$ almost everywhere. Consider an arbitrary jump point $t \in J_u$ of u. Then there exist sequences of real numbers $\left(t_\varepsilon^1\right), (s_\varepsilon)$ and $\left(t_\varepsilon^2\right)$ such that $t_\varepsilon^1 < s_\varepsilon < t_\varepsilon^2$ and

$$\lim_{\varepsilon\to 0} t_\varepsilon^1 = \lim_{\varepsilon\to 0} s_\varepsilon = \lim_{\varepsilon\to 0} t_\varepsilon^2 = t \tag{3.11}$$

$$\text{and } \lim_{\varepsilon\to 0} \varphi_\varepsilon\left(t_\varepsilon^1\right) = \lim_{\varepsilon\to 0} \varphi_\varepsilon\left(t_\varepsilon^2\right) = 1. \tag{3.12}$$

Moreover we can assure that $\lim_{\varepsilon\to 0} \varphi_\varepsilon(s_\varepsilon) = 0$. Indeed, if no such sequence s_ε would exist, we would find a neighborhood of t in which u' is bounded, which contradicts $t \in J_u$. The application

of Lemma 3.1.3 yields

$$\begin{aligned}
&\liminf_{\varepsilon\to 0} \int_{t_\varepsilon^1}^{t_\varepsilon^2} \frac{1}{2\varepsilon}(1-\varphi_\varepsilon)^2 + \frac{\varepsilon}{2}|\varphi_\varepsilon'|^2 \,\mathrm{dt} \\
&\quad = \liminf_{\varepsilon\to 0} \left(\left| \int_{s_\varepsilon}^{t_\varepsilon^2} \frac{1}{2\varepsilon}(1-\varphi_\varepsilon)^2 + \frac{\varepsilon}{2}|\varphi_\varepsilon'|^2 \,\mathrm{dt} \right| + \left| \int_{s_\varepsilon}^{t_\varepsilon^1} \frac{1}{2\varepsilon}(1-\varphi_\varepsilon)^2 + \frac{\varepsilon}{2}|\varphi_\varepsilon'|^2 \,\mathrm{dt} \right| \right) \\
&\quad \geq 2 \left| \int_0^1 (1-s)\,\mathrm{ds} \right| = 1.
\end{aligned}$$

Suppose now that $\{t_1, \dots, t_N\} \subset J_u$ for an arbitrary $N \in \mathbb{N}$. Repeating the above argument on disjoint intervals I_i with $t_i \in I_i$ we obtain

$$\begin{aligned}
G_c N = \sum_{i=1}^N G_c &\leq \sum_{i=1}^N \liminf_{\varepsilon\to 0} \frac{G_c}{2} \int_{(t_\varepsilon^1)_i}^{(t_\varepsilon^2)_i} \frac{1}{\varepsilon}(1-\varphi_\varepsilon)^2 + \varepsilon|\varphi_\varepsilon'|^2 \,\mathrm{dt} \\
&\leq \liminf_{\varepsilon\to 0} \frac{G_c}{2} \int_I \frac{1}{\varepsilon}(1-\varphi_\varepsilon)^2 + \varepsilon|\varphi_\varepsilon'|^2 \,\mathrm{dt},
\end{aligned}$$

where $\left(t_\varepsilon^1\right)_i \in I_i$ and $\left(t_\varepsilon^2\right)_i \in I_i$ are chosen as in equation (3.11) with t replaced by t_i. By the arbitrariness of $N \in \mathbb{N}$ we deduce the finiteness of $\mathcal{H}^0(J_u \cap I)$ as well as equation (3.10). □

Theorem 3.1.6 (lim inf inequality in the one-dimensional case)**:**
Consider a sequence $(u_\varepsilon, \varphi_\varepsilon) \in L^1((a,b)) \times L^1((a,b))$ *converging to* (u,φ) *in* $L^1((a,b)) \times L^1((a,b))$ *and satisfying*

$$\liminf_{\varepsilon\to 0} \widetilde{D}_\varepsilon(u_\varepsilon, \varphi_\varepsilon) < +\infty. \tag{3.13}$$

Then it holds $u \in SBV((a,b))$, $\varphi = 1$ $\mathcal{L}^n$*-almost everywhere in* (a,b) *and*

$$\widetilde{D}(u,\varphi) \leq \liminf_{\varepsilon\to 0} \widetilde{D}_\varepsilon(u_\varepsilon, \varphi_\varepsilon). \tag{3.14}$$

Proof of Theorem 3.1.6. As mentioned before we follow the proof of [Bra98, Theorem 3.15]. First we note that by extracting subsequences we can assume without loss of generality that $(u_\varepsilon, \varphi_\varepsilon) \to (u,\varphi)$ holds $\mathcal{L}^n$-almost everywhere. Indeed, assume that equation (3.14) was proven for all pointwise almost everywhere convergent sequences $(u_\varepsilon, \varphi_\varepsilon)$ but

$$\widetilde{D}(u,\varphi) > \liminf_{\varepsilon\to 0} \widetilde{D}_\varepsilon(u_\varepsilon, \varphi_\varepsilon).$$

Then we have a subsequence such that

$$\widetilde{D}(u,\varphi) > \lim_{\varepsilon\to 0} \widetilde{D}_\varepsilon(u_\varepsilon, \varphi_\varepsilon).$$

This is a contradiction as this sequence has an $\mathcal{L}^n$-almost-everywhere convergent subsequence that satisfies equation (3.14) by assumption. Thus it remains to show equation (3.14) for all pointwise almost-everywhere convergent sequences $(u_\varepsilon, \varphi_\varepsilon)$. Following the same argumentation it is sufficient to prove equation (3.14) for sequences satisfying

$$\lim_{\varepsilon\to 0} \widetilde{D}_\varepsilon(u_\varepsilon, \varphi_\varepsilon) = \liminf_{\varepsilon\to 0} \widetilde{D}_\varepsilon(u_\varepsilon, \varphi_\varepsilon) < +\infty.$$

According to Lemma 3.1.4 and since u_ε is uniformly bounded in L^1, this leads to a bound of $\limsup_{\varepsilon\to 0} \widetilde{F}_\varepsilon(u_\varepsilon, \varphi_\varepsilon)$ and thus $\limsup_{\varepsilon\to 0} \widetilde{G}_\varepsilon(\varphi_\varepsilon)$. Hence $\varphi_\varepsilon \to 1$ in $L^2((a,b))$ and $\varphi = 1$ holds $\mathcal{L}^n$-almost everywhere. Let now $I \subset (a,b)$ be any open set. Then by Lemma 3.1.4 we have $\widetilde{F}_\varepsilon(u_\varepsilon, \varphi_\varepsilon; I) \leq \widetilde{F}_\varepsilon(u_\varepsilon, \varphi_\varepsilon) < +\infty$ and thus Lemma 3.1.5 implies

$$\mathcal{H}^0(I \cap J_u) \leq \liminf_{\varepsilon\to 0} \widetilde{G}_\varepsilon(\varphi; I). \tag{3.15}$$

The next step is to prove weak convergence of u_ε in $H^1(I')$, where $I' \subset (a,b) \setminus J_u$ is some compactly embedded interval, away from the discontinuities of u. Further we want to prove the lim inf inequality for the bulk part of the energy functional. While keeping in mind the bounds of the occurring terms that we get from Lemma 3.1.4, this step goes through as in [Bra98, Theorem 3.15]. Therefore we only give a short summary below. Let the interval I be such that $I \cap J_u = \emptyset$ and divide I into N disjoint subintervals I_N^k of length $\frac{1}{N}$. When defining for every $N \in \mathbb{N}$ and every $0 < z < 1$ the set $J_N^z = \left\{k \in \{1,\dots,N\} : \lim_{\varepsilon\to 0} \inf_{t\in I_N^k} \varphi_\varepsilon(t) \leq z\right\}$, Lemma 3.1.5 implies

$$\begin{aligned}\mathcal{H}^0(J_N^z) \int_z^1 (1-s)\,\mathrm{d}s &\leq \frac{1}{G_c} \liminf_{\varepsilon\to 0} \sum_{k\in J_N^z} \widetilde{G}_\varepsilon\left(\varphi_\varepsilon; I_N^k\right) \\ &\leq \frac{1}{G_c} \liminf_{\varepsilon\to 0} \widetilde{G}_\varepsilon(\varphi_\varepsilon) < +\infty.\end{aligned}$$

Thus $L = \mathcal{H}^0(J_N^z)$ is finite and independent of the length of the intervals I_N^k, i. e. the number N of these intervals. Hence we can write $J_N^z = \left\{k_N^1, \dots, k_N^L\right\}$ and define the finite set $S = \left\{t_i : i = 1,\dots,L \text{ and } t_i = \lim_{N\to+\infty} \frac{k_N^i}{N}\right\}$. Note that for every $\eta > 0$, every $k \in J_N^z$ and N sufficiently large we have $I_N^k \subset S + [-\eta, \eta]$. This yields

$$\begin{aligned}\liminf_{\varepsilon\to 0} \quad z^2 \int_{I\setminus(S+[-\eta,\eta])} |u_\varepsilon'|^2\,\mathrm{d}t &\leq \liminf_{\varepsilon\to 0} \sum_{k\notin J_N^z} \int_{I_N^k} z^2 |u_\varepsilon'|^2\,\mathrm{d}t \\ &\leq \liminf_{\varepsilon\to 0} \sum_{k\notin J_N^z} \int_{I_N^k} \varphi_\varepsilon^2 |u_\varepsilon'|^2\,\mathrm{d}t \\ &\leq \liminf_{\varepsilon\to 0} \int_I \varphi_\varepsilon^2 |u_\varepsilon'|^2\,\mathrm{d}t.\end{aligned}$$

Thus, as u_ε is bounded in $L^1((a,b))$ and u_ε' is bounded in $L^2(I \setminus (S + [-\eta,\eta]))$ by the Poincaré-Wirtinger inequality, u_ε is also bounded in $H^1(I \setminus (S + [-\eta,\eta]))$. Consequently by the Urysohn property $\mathbf{u}_\varepsilon$ weakly converges in $H^1(I \setminus (S + [-\eta,\eta]))$ to $u \in H^1(I \setminus (S + [-\eta,\eta]))$. As $\eta > 0$ was

arbitrary and $I \cap J_u = \emptyset$ we conclude $u \in H^1(I)$, and by letting $z \to 1$ we obtain

$$\int_I c\,|u'|^2 \,\mathrm{d}t \leq \liminf_{\varepsilon \to 0} \int_I c\left(\varphi_\varepsilon^2 + k_\varepsilon\right) |u_\varepsilon'|^2 \,\mathrm{d}t\,. \tag{3.16}$$

In particular, since $\mathcal{H}^0(J_u) < +\infty$ we obtain $u \in SBV^2((a,b))$. As $(u_\varepsilon, \varphi_\varepsilon) \to (u, 1)$ in $L^1(I)$ and $|\varphi_\varepsilon| \leq 1$, Lebesgue's dominated convergence theorem implies $\varphi_\varepsilon u \to u$ in $L^1(I)$. Thus

$$\begin{aligned}\lim_{\varepsilon \to 0} \int_I p' \,|\varphi_\varepsilon u_\varepsilon - u| \,\mathrm{d}t &\leq \lim_{\varepsilon \to 0} \int_I p' \left(|\varphi_\varepsilon|\,|u_\varepsilon - u| + |\varphi_\varepsilon u - u|\right) \mathrm{d}t \\ &\leq \lim_{\varepsilon \to 0} \|p'\|_{L^\infty(I)} \left(\|u_\varepsilon - u\|_{L^1(I)} + \|\varphi_\varepsilon u - u\|_{L^1(I)}\right) \\ &= 0.\end{aligned} \tag{3.17}$$

Having $u_\varepsilon' \rightharpoonup u'$ in $H^1(I \setminus (S + [-\eta, \eta]))$ and $\varphi_\varepsilon \to 1$ in $L^2([a,b])$ we obtain $\varphi_\varepsilon u_\varepsilon' \rightharpoonup u'$ in $L^1(I \setminus (S + [-\eta, \eta]))$. Thus $p \in W^{1,\infty}([a,b])$ yields

$$\int_{I \setminus (S + [-\eta, \eta])} (1 - \alpha)\, p u' \,\mathrm{d}t = \lim_{\varepsilon \to 0} \int_{I \setminus (S + [-\eta, \eta])} (1 - \alpha)\, p \varphi_\varepsilon u_\varepsilon' \,\mathrm{d}t\,. \tag{3.18}$$

Finally we combine the results from equations (3.15) to (3.18) to get inequality (3.14). For $\eta > 0$ define $I_\eta^0 = (a,b) \setminus (J_u + [-\eta, \eta])$ and $I_\eta^1 = (a,b) \cap (J_u + (-\eta, \eta))$. Then for all $\eta > 0$ it holds

$$\begin{aligned}&\widetilde{D}(u, \varphi) \\ &\quad \leq G_c \mathcal{H}^0\left(I_\eta^0 \cap J_u\right) + G_c \mathcal{H}^0\left(I_\eta^1 \cap J_u\right) \\ &\qquad + \int_{I_\eta^0} c\,|u'|^2 + (1 - \alpha)\, p u' + p' u \,\mathrm{d}t + \int_{I_\eta^1} c\,|u'|^2 + (1 - \alpha)\, p u' + p' u \,\mathrm{d}t \\ &\quad \leq \liminf_{\varepsilon \to 0} \Bigg(\widetilde{G}_\varepsilon(\varphi_\varepsilon) + \int_{I_\eta^0} c\left(\varphi_\varepsilon^2 + k_\varepsilon\right) |u_\varepsilon'|^2 + (1 - \alpha)\, p \varphi_\varepsilon u_\varepsilon' + p' \varphi_\varepsilon u_\varepsilon \,\mathrm{d}t \\ &\qquad + \int_{I_\eta^1} c\,|u'|^2 + (1 - \alpha)\, p u' + p' u \,\mathrm{d}t \Bigg) \\ &\quad \leq \liminf_{\varepsilon \to 0} \left(\widetilde{D}_\varepsilon(u_\varepsilon, \varphi_\varepsilon) - \int_{I_\eta^1} (1 - \alpha)\, p \varphi_\varepsilon u_\varepsilon' + p' \varphi_\varepsilon u_\varepsilon \,\mathrm{d}t + \int_{I_\eta^1} c\,|u'|^2 + (1 - \alpha)\, p u' + p' u \,\mathrm{d}t \right).\end{aligned}$$

It remains to show that the last two integrals vanish for $\eta \to 0$. As

$$\begin{aligned}\sup_{\varepsilon > 0} \|\varphi_\varepsilon u_\varepsilon'\|_{L^2((a,b))} &\leq \sup_{\varepsilon > 0} \widetilde{F}_\varepsilon(u_\varepsilon, \varphi_\varepsilon) < +\infty \\ \text{and } \sup_{\varepsilon > 0} \|\varphi_\varepsilon u_\varepsilon\|_{L^1((a,b))} &\leq \sup_{\varepsilon > 0} \|u_\varepsilon\|_{L^1((a,b))} < +\infty\end{aligned}$$

the aforementioned vanishing follows from Hölder's inequality and the absolute continuity of the Lebesgue integral together with the fact that $\mathcal{L}^n\left(I_\eta^1\right) \to 0$ for $\eta \to 0$. Hence equation (3.14) is proven. □

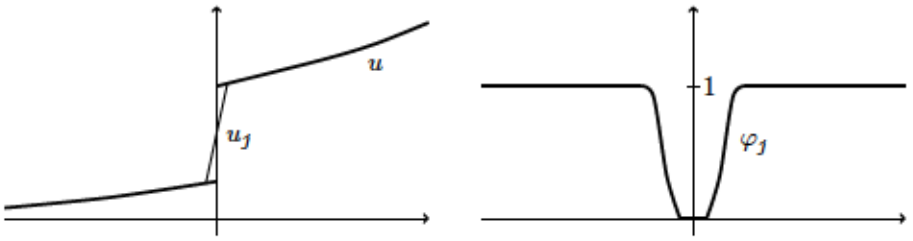

Figure 3.1: Recovery sequences for the proof of the lim sup-inequality in one dimension.

Theorem 3.1.7 (lim sup inequality in the one-dimensional case)**:**
For every $(u,\varphi) \in SBV((a,b)) \times \{v : v = 1 \text{ holds } \mathcal{L}^n\text{-a. e. in } (a,b)\}$ *we can find a sequence* $(u_\varepsilon,\varphi_\varepsilon) \in L^1((a,b)) \times L^1((a,b))$ *such that* $(u_\varepsilon,\varphi_\varepsilon) \to (u,\varphi)$ *in* $L^1((a,b)) \times L^1((a,b))$ *and*

$$\widetilde{D}(u,\varphi) \geq \liminf_{\varepsilon\to 0} \widetilde{D}_\varepsilon(u_\varepsilon,\varphi_\varepsilon). \tag{3.19}$$

Proof of Theorem 3.1.7. We need to construct a recovery sequence $(u_\varepsilon,\varphi_\varepsilon) \in H^1((a,b)) \times \left\{v \in H^1((a,b)) : 0 \leq v \leq 1\right\}$ such that $\limsup_{\varepsilon\to 0} \widetilde{D}_\varepsilon(u_\varepsilon,\varphi_\varepsilon) \leq \widetilde{D}(u,\varphi)$. Without loss of generality we restrict ourselves to the case $(a,b) = (-1,1)$, $u' \in L^2((-1,1))$ and $J_u = \{0\}$. The case of an arbitrary interval (a,b) with one jump discontinuity can be dealt with by rescaling. The case of finitely many jump discontinuities is handled with a similar approximation for each jump point.

Note that the reconstruction sequence is exactly the same as in [Bra98, Theorem 3.15]. We recall its definition here for convenience, see Figure 3.1 for the general idea. Let $\xi_\varepsilon = \sqrt{k_\varepsilon \varepsilon}$ and $u_\varepsilon \in H^1((-1,1))$ such that for all $t \in (-1,1)$ with $|t| > \xi_\varepsilon$ it holds $u_\varepsilon(t) = u(t)$. For $|t| \leq \xi_\jmath$ we interpolate linearly, setting

$$u_\varepsilon(t) = \frac{(u(\xi_\varepsilon) - u(-\xi_\varepsilon))\,t}{2\xi_\varepsilon} + \frac{u(\xi_\varepsilon) + u(-\xi_\varepsilon)}{2},$$

having obviously $u_\varepsilon \to u$ in $L^1((-1,1))$. For every fixed $\eta > 0$ we can find $T > 0$ and $\widetilde{\varphi} \in H^1((0,T))$ satisfying $\widetilde{\varphi}(0) = 0$, $\widetilde{\varphi}(T) = 1$ and $0 \leq \widetilde{\varphi} \leq 1$ as well as

$$\int_0^T \left((\widetilde{\varphi} - 1)^2 + |\widetilde{\varphi}'|^2\right) \mathrm{dt} \leq 1 + \eta. \tag{3.20}$$

We define

$$\varphi_\varepsilon(t) := \begin{cases} 0 & \text{if } |t| \leq \xi_\varepsilon, \\ \widetilde{\varphi}\left(\frac{|t| - \xi_\varepsilon}{\varepsilon}\right) & \text{if } \xi_\varepsilon < |t| < \xi_\varepsilon + \varepsilon T, \\ 1 & \text{if } \xi_\varepsilon + \varepsilon T \leq |t|. \end{cases}$$

Notice that this definition satisfies $0 \leq \varphi_\varepsilon \leq 1$ and $\varphi_\varepsilon \to \varphi$ in $L^1((-1,1))$. We only give the proof of the lim sup inequality for the pressure terms here. For the linear elasticity and the surface energy term the reader is referred to [Bra98]. In a first step we show that $\varphi_\varepsilon \to 1$ in

$L^2((-\xi_\varepsilon - \varepsilon T, \xi_\varepsilon + \varepsilon T))$. The substitution $s = \frac{|t|-\xi_\varepsilon}{\varepsilon}$ and equation (3.20) yield

$$\begin{aligned}
\|\varphi_\varepsilon - 1\|^2_{L^2((-\xi_\varepsilon-\varepsilon T,\xi_\varepsilon+\varepsilon T))} &= \int_{-\xi_\varepsilon-\varepsilon T}^{-\xi_\varepsilon} \left(\widetilde{\varphi}\left(\frac{-t-\xi_\varepsilon}{\varepsilon}\right) - 1\right)^2 \mathrm{d}t + \int_{-\xi_\varepsilon}^{\xi_\varepsilon} (0-1)^2 \,\mathrm{d}t \\
&\quad + \int_{\xi_\varepsilon}^{\xi_\varepsilon+\varepsilon T} \left(\widetilde{\varphi}\left(\frac{t-\xi_\varepsilon}{\varepsilon}\right) - 1\right)^2 \mathrm{d}t \\
&= 2\int_0^T \varepsilon \left(\widetilde{\varphi}(s) - 1\right)^2 \mathrm{d}s + \int_{-\xi_\varepsilon}^{\xi_\varepsilon} 1 \,\mathrm{d}t \\
&\leq 2\left(\varepsilon + \varepsilon\eta + \xi_\varepsilon\right),
\end{aligned}$$

which tends to 0 for $\varepsilon \to 0$. By Lebesgue's dominated convergence theorem $\varphi_\varepsilon u \to u$ in $L^1((-1,1))$, hence Hölder's inequality leads to

$$\begin{aligned}
&\lim_{\varepsilon\to 0} \int_{-\xi_\varepsilon-\varepsilon T}^{\xi_\varepsilon+\varepsilon T} (1-\alpha)\left|p\varphi_\varepsilon u' - pu'\right| + \left|p'\varphi_\varepsilon u - p'u\right| \mathrm{d}t \\
&\qquad \leq \lim_{\varepsilon\to 0} \Big((1-\alpha)\|p\|_{L^\infty((-1,1))}\|u'\|_{L^2((-1,1))}\|\varphi_\varepsilon - 1\|_{L^2((-\xi_\varepsilon-\varepsilon T,\xi_\varepsilon+\varepsilon T))} \\
&\qquad\quad + \|p'\|_{L^\infty((-1,1))}\|\varphi_\varepsilon u - u\|_{L^1((-1,1))}\Big) \\
&\qquad = 0.
\end{aligned} \tag{3.21}$$

The definition of φ_ε and u_ε yields

$$\begin{aligned}
&\int_{-1}^{1} (1-\alpha)\, p\varphi_\varepsilon u_\varepsilon' + p'\varphi_\varepsilon u_\varepsilon \,\mathrm{d}t \\
&\quad = \int_{-1}^{1} (1-\alpha)\, p\varphi_\varepsilon u' + p'\varphi_\varepsilon u \,\mathrm{d}t \\
&\quad = \int_{-1}^{-\xi_\varepsilon-\varepsilon T} (1-\alpha)\, pu' + p'u \,\mathrm{d}t + \int_{-\xi_\varepsilon-\varepsilon T}^{\xi_\varepsilon+\varepsilon T} (1-\alpha)\, p\varphi_\varepsilon u' + p'\varphi_\varepsilon u \,\mathrm{d}t + \int_{\xi_\varepsilon+\varepsilon T}^{1} (1-\alpha)\, pu' + p'u \,\mathrm{d}t\,.
\end{aligned}$$

Together with equation (3.21) we finally have the desired lim sup inequality

$$\limsup_{\varepsilon\to 0} \int_{-1}^{1} (1-\alpha)\, p\varphi_\varepsilon u_\varepsilon' + p'\varphi_\varepsilon u_\varepsilon \,\mathrm{d}t \leq \int_{-1}^{1} (1-\alpha)\, pu' + p'u \,\mathrm{d}t\,. \qquad \square$$

Proof of Theorem 3.1.2. The Γ-convergence result follows immediately from Theorems 3.1.6 and 3.1.7. $\square$

Corollary 3.1.8:

Let c, G_c, p, α and k_ε be as in Theorem 3.1.2. Then the functionals $\widetilde{E}_\varepsilon$ including Dirichlet boundary conditions Γ-converge for $\varepsilon \to 0^+$ to $\widetilde{E}$ with respect to convergence in $L^1((a,b)) \times L^1((a,b))$.

Proof of Corollary 3.1.8. Observe that adding the term $-(p(b)u_D(b) - p(a)u_D(a))$ is a continuous perturbation of the energy functional and that $H^1_D((a,b)) \subset H^1((a,b))$ as well as $\{u \in SBV((a,b)) : u(a) = u_D(a),\ u(b) = u_D(b)\} \subset SBV((a,b))$. Hence the lim inf inequality is a direct consequence of Theorem 3.1.6 and Lemma 2.3.3.
The important part in the proof of the lim sup inequality is to show that for any given function $u \in \{u \in SBV((a,b)) : u(a) = u_D(a),\ u(b) = u_D(b)\}$ we can construct a recovery sequence satisfying the same boundary conditions, namely $u_\varepsilon \in H^1_D((a,b))$. This is obviously satisfied by the sequence constructed in the proof of Theorem 3.1.7, as therein $u_\varepsilon = u$ away from J_u. □

3.2 Higher dimensions

In this section we give a proof of Γ-convergence for $n > 1$. Originally we hoped to carry over the results from the preceding section using the "slicing" method as described for example in [Bra02, Chapter 15]. Unfortunately this is *not* possible, since in general slices of the pressure terms *can not* be bound by their one-dimensional counterparts. Indeed, following the standard procedure, at some point we would need the estimate $e(\mathbf{u})\xi \cdot \xi \leq \operatorname{tr}(e(\mathbf{u}))$ for all $\xi \in \mathbb{S}^{n-1}$ or at least a dense subset of $\mathbb{S}^{n-1}$. However, this is not satisfied in general. Hence in this section we follow a different approach. We prove the lim inf inequality following the ideas of [Foc01], taking advantage of the work of Dal Maso on the space $GSBD(\Omega;\mathbb{R}^n)$ [DM13]. The proof of the lim sup inequality relies on standard techniques to construct a recovery sequence and takes advantage of the recently proven density result for functions in $GSBD(\Omega;\mathbb{R}^n)$ by Chambolle and Crismale [CC19]. The results in this section are joint work with Annika Bach and were previously published in [BS19]. We start by defining the functionals which play a role in this section. They are the n-dimensional equivalents of the functionals in Definition 3.1.1.

Definition 3.2.1:
The first functional $G_\varepsilon : L^1(\Omega) \to [0,+\infty]$ defined by

$$G_\varepsilon(\varphi) = \begin{cases} \frac{G_c}{2}\int_\Omega \varepsilon|\nabla\varphi|^2 + \frac{1}{\varepsilon}(1-\varphi)^2\,\mathrm{d}x & \text{if } \varphi \in H^1(\Omega), \\ +\infty & \text{otherwise,} \end{cases} \tag{3.22}$$

considers only the surface part of the energy. In analogy to the one-dimensional case, we first define the functionals only considering the elasticity part of the bulk energy and subsequently add the pressure terms. Thus let $\mathcal{V} = \{\varphi : \varphi = 1 \text{ holds } \mathcal{L}^n\text{-a. e. in } \Omega\}$ and $\mathcal{V}_\varepsilon = \{\varphi \in H^1(\Omega) : 0 \leq \varphi \leq 1\}$. Further let $F : L^1(\Omega;\mathbb{R}^n) \times L^1(\Omega) \to [0,+\infty]$ and its approximation $F_\varepsilon : L^1(\Omega;\mathbb{R}^n) \times L^1(\Omega) \to [0,+\infty]$ be given by

$$F(\mathbf{u},\varphi) = \begin{cases} \int_\Omega \frac{1}{2}(e(\mathbf{u}) : \mathbb{C}e(\mathbf{u}))\,\mathrm{d}x + G_c\mathcal{H}^{n-1}(J_\mathbf{u}) & \text{if } \mathbf{u} \in GSBD^2(\Omega;\mathbb{R}^n),\ \varphi \in \mathcal{V}, \\ +\infty & \text{otherwise,} \end{cases} \tag{3.23}$$

$$F_\varepsilon(\mathbf{u},\varphi)=\begin{cases}\int_\Omega \frac{1}{2}\left(k_\varepsilon+\varphi^2\right)e(\mathbf{u}):\mathbb{C}e(\mathbf{u})\,\mathrm{d}x+\frac{G_c}{2}\int_\Omega \varepsilon|\nabla\varphi|^2+\frac{1}{\varepsilon}(1-\varphi)^2\,\mathrm{d}x \\ \qquad\qquad \text{if } \mathbf{u}\in H^1(\Omega;\mathbb{R}^n),\ \varphi\in\mathcal{V}_\varepsilon, \\ +\infty \qquad\qquad \text{otherwise.}\end{cases} \tag{3.24}$$

Moreover let $D\colon L^1(\Omega;\mathbb{R}^n)\times L^1(\Omega)\to[-\infty,+\infty]$ *and* $D_\varepsilon\colon L^1(\Omega;\mathbb{R}^n)\times L^1(\Omega)\to[-\infty,+\infty]$ *be defined as*

$$D(\mathbf{u},\varphi)=F(\mathbf{u},\varphi)+\int_\Omega(1-\alpha)p\nabla\cdot\mathbf{u}+\nabla p\mathbf{u}\,\mathrm{d}x, \tag{3.25}$$

$$D_\varepsilon(\mathbf{u},\varphi)=F_\varepsilon(\mathbf{u},\varphi)+\int_\Omega(1-\alpha)\varphi p\nabla\cdot\mathbf{u}+\varphi\nabla p\mathbf{u}\,\mathrm{d}x. \tag{3.26}$$

Finally we obtain the total energy formulation by adding Dirichlet boundary conditions, see also equation (2.9)*. Thus* $E\colon L^1(\Omega;\mathbb{R}^n)\times L^1(\Omega)\to(-\infty,+\infty]$ *and its approximation* $E_\varepsilon\colon L^1(\Omega;\mathbb{R}^n)\times L^1(\Omega)\to(-\infty,+\infty]$ *are given by*

$$E(\mathbf{u},\varphi)=D(\mathbf{u},\varphi)+G_c\mathcal{H}^{n-1}(\Gamma_D\cap\{\operatorname{tr}\mathbf{u}\neq\operatorname{tr}\mathbf{u}_D\}), \tag{3.27}$$

$$E_\varepsilon(\mathbf{u},\varphi)=\begin{cases}D_\varepsilon(\mathbf{u},\varphi) & \text{if } \operatorname{tr}\mathbf{u}=\operatorname{tr}\mathbf{u}_D \text{ on } \Gamma_D,\ \operatorname{tr}\varphi=1 \text{ on } \Gamma_D,\\ +\infty & \text{otherwise.}\end{cases} \tag{3.28}$$

Here $\mathbf{u}_D\in H^1(\mathbb{R}^n;\mathbb{R}^n)$ *denotes some given boundary function. As before, we consider localized versions of the preceding functionals. Thus whenever we consider an open set* $A\in\mathcal{A}(\Omega)$ *instead of* Ω *as integration domain, we replace* $G(\varphi)$ *and* $G_\varepsilon(\varphi)$ *by*

$$F(\mathbf{u},\varphi;A)=\begin{cases}\int_A \frac{1}{2}(e(\mathbf{u}):\mathbb{C}e(\mathbf{u}))\,\mathrm{d}x+G_c\mathcal{H}^{n-1}(J_{\mathbf{u}}) & \text{if } \mathbf{u}\in GSBD^2(\Omega;\mathbb{R}^n),\ \varphi\in\mathcal{V},\\ +\infty & \text{otherwise,}\end{cases} \tag{3.29}$$

$$F_\varepsilon(\mathbf{u},\varphi;A)=\begin{cases}\int_A \frac{1}{2}\left(k_\varepsilon+\varphi^2\right)e(\mathbf{u}):\mathbb{C}e(\mathbf{u})\,\mathrm{d}x+\frac{G_c}{2}\int_A \varepsilon|\nabla\varphi|^2+\frac{1}{\varepsilon}(1-\varphi)^2\,\mathrm{d}x \\ \qquad\qquad \text{if } \mathbf{u}\in H^1(\Omega;\mathbb{R}^n),\ \varphi\in\mathcal{V}_\varepsilon, \\ +\infty \qquad\qquad \text{otherwise.}\end{cases} \tag{3.30}$$

The localized functionals $G_\varepsilon(\varphi;A)$*,* $D(\mathbf{u},\varphi;A)$*,* $D_\varepsilon(\mathbf{u},\varphi;A)$*,* $E(\mathbf{u},\varphi;A)$ *and* $E_\varepsilon(\mathbf{u},\varphi;A)$ *are defined analogously.*

Keeping these definitions in mind we can state the main result of this section. Note that we first treat the situation without boundary conditions and subsequently deal with them in Theorem 3.2.7.

Theorem 3.2.2:
Let $G_c>0$*,* $p\in W^{1,\infty}(\Omega)$*,* $0\le\alpha\le1$ *and* $k_\varepsilon\in o(\varepsilon)$*, as well as* $\mathbb{C}$ *be the linear elasticity tensor as in* (2.1) *with* $\mu,\lambda>0$*. Then* D_ε Γ*-converges for* $\varepsilon\to0^+$ *to* D *with respect to the strong convergence in* $L^1(\Omega;\mathbb{R}^n)\times L^1(\Omega)$*.*

Before starting the proof of Theorem 3.2.2 we formulate the n-dimensional version of Lemma 3.1.4, stating that $F_\varepsilon(\mathbf{u},\varphi)$ can be bounded by $D_\varepsilon(\mathbf{u},\varphi)$.

Lemma 3.2.3:
We can find constants $c_1,\ c_2,\ c_3 > 0$ such that for all $(\mathbf{u},\varphi) \in L^1(\Omega;\mathbb{R}^n) \times L^1(\Omega)$ it holds

$$D_\varepsilon(\mathbf{u},\varphi) \geq c_1 F_\varepsilon(\mathbf{u},\varphi) - c_2\|\mathbf{u}\|_{L^1(\Omega;\mathbb{R}^n)} - c_3. \tag{3.31}$$

In particular if $\sup_{\varepsilon>0}\left(D_\varepsilon(\mathbf{u}_\varepsilon,\varphi_\varepsilon) + \|\mathbf{u}_\varepsilon\|_{L^1(\Omega;\mathbb{R}^n)}\right) < +\infty$ for $(\mathbf{u}_\varepsilon,\varphi_\varepsilon) \in L^1(\Omega;\mathbb{R}^n) \times L^1(\Omega)$ then $\sup_{\varepsilon>0} F_\varepsilon(\mathbf{u},\varphi) < +\infty$ and $\sup_{\varepsilon>0} G_\varepsilon(\varphi) < +\infty$.

Proof of Lemma 3.2.3. The proof goes exactly as in the one-dimensional case. Without loss of generality we can restrict ourselves to the case $(\mathbf{u},\varphi) \in H^1(\Omega;\mathbb{R}^n) \times \mathcal{V}_\varepsilon$. Then choose $\delta > 0$ such that $\mu - \frac{n\delta}{2} > 0$ and define $c_1 = \min\left(1, \mu - \frac{n\delta}{2}\right)$, $c_2 = \|\nabla p\|_{L^\infty(\Omega)}$ and $c_3 = \frac{(1-\alpha)^2}{2\delta}\|p\|^2_{L^2(\Omega)}$. Thus Young's inequality in combination with $|\varphi| < 1$ and the positive definiteness of $\mathbb{C}$ yield equation (3.31). Obviously for $\sup_{\varepsilon>0}\left(D_\varepsilon(\mathbf{u}_\varepsilon,\varphi_\varepsilon) + \|\mathbf{u}_\varepsilon\|_{L^1(\Omega;\mathbb{R}^n)}\right) < +\infty$ it holds

$$\sup_{\varepsilon>0} G_\varepsilon(\varphi_\varepsilon) \leq \sup_{\varepsilon>0} F_\varepsilon(\mathbf{u}_\varepsilon,\varphi_\varepsilon) \leq \frac{1}{c_1}\sup_{\varepsilon>0}\left(D_\varepsilon(\mathbf{u}_\varepsilon,\varphi_\varepsilon) + c_2\|\mathbf{u}_\varepsilon\|_{L^1(\Omega;\mathbb{R}^n)} + c_3\right) < +\infty, \tag{3.32}$$

which completes the proof of Lemma 3.2.3. □

As in the one-dimensional case we deal with the lim inf and the lim sup inequality separately and immediately obtain Theorem 3.2.2 from Theorems 3.2.4 and 3.2.5.

Theorem 3.2.4:
For every sequence $(\mathbf{u}_\varepsilon,\varphi_\varepsilon) \subseteq L^1(\Omega;\mathbb{R}^n) \times L^1(\Omega)$ that converges to $(\mathbf{u},\varphi) \in GSBD^2(\Omega;\mathbb{R}^n) \times \mathcal{V}$ in $L^1(\Omega;\mathbb{R}^n) \times L^1(\Omega)$ it holds

$$D(\mathbf{u},\varphi) \leq \liminf_{\varepsilon\to 0} D_\varepsilon(\mathbf{u}_\varepsilon,\varphi_\varepsilon).$$

Proof. The proof follows the ideas of Focardi [Foc01]. As usual we can assume that the sequence $(\mathbf{u}_\varepsilon,\varphi_\varepsilon)$ satisfies

$$\lim_{\varepsilon\to 0} D_\varepsilon(\mathbf{u}_\varepsilon,\varphi_\varepsilon) = \liminf_{\varepsilon\to 0} D_\varepsilon(\mathbf{u}_\varepsilon,\varphi_\varepsilon) < +\infty.$$

Further we can extract a subsequence, still denoted by $(\mathbf{u}_\varepsilon,\varphi_\varepsilon)$, that converges $\mathcal{L}^n$-a. e. to $(\mathbf{u},\varphi)$. Using equation (3.32) we get $\limsup_{\varepsilon\to 0}\int_\Omega \frac{(1-\varphi_\varepsilon)^2}{\varepsilon}\,\mathrm{d}x < +\infty$ and thus $\varphi = 1$ holds $\mathcal{L}^n$-a. e. in Ω and $\varphi_\varepsilon \to \varphi$ in $L^2(\Omega)$. The proof is now divided into two steps. First we consider the bulk part of the energy in a similar fashion as Focardi. Second the surface part is proven using slicing arguments.

Step 1: (*Bulk energy inequality*) By extracting a further subsequence we may assume

$$\liminf_{\varepsilon\to 0}\int_\Omega \left(\varphi_\varepsilon^2+k_\varepsilon\right)e\left(\mathbf{u}_\varepsilon\right):\mathbb{C}e\left(\mathbf{u}_\varepsilon\right)\mathrm{d}x=\lim_{\varepsilon\to 0}\int_\Omega \left(\varphi_\varepsilon^2+k_\varepsilon\right)e\left(\mathbf{u}_\varepsilon\right):\mathbb{C}e\left(\mathbf{u}_\varepsilon\right)\mathrm{d}x.$$

Define now $\Phi\colon [0,1]\to\left[0,\frac{1}{2}\right]$ as $\Phi(t)=\int_0^t (1-s)\,\mathrm{d}s$ and note $\Phi(0)=0$ and $\Phi(1)=\frac{1}{2}$. Note further that Φ and Φ^{-1} are positive and increasing. Then the classical Modica-Mortola trick yields

$$\left|D\Phi\left(\varphi_\varepsilon\right)\right|=\int_\Omega \left|\nabla\varphi_\varepsilon\right|\left|\varphi_\varepsilon-1\right|\mathrm{d}x\le\int_\Omega \frac{\left(\varphi_\varepsilon-1\right)^2}{2\varepsilon}+\frac{\varepsilon}{2}\left|\nabla\varphi_\varepsilon\right|^2\mathrm{d}x.$$

Thus equation (3.32) yields $\sup_{\varepsilon>0}\left|D\Phi\left(\varphi_\varepsilon\right)\right|<+\infty$. Next, let us define the superlevel sets $U_{\varepsilon,t}=\{x\in\Omega:\Phi\left(\varphi_\varepsilon(x)\right)>t\}$ and their perimeter $p_\varepsilon(t)=\mathrm{Per}\left(U_{\varepsilon,t}\right)$. By the Fleming-Rishel coarea formula (Proposition 2.4.6) we have

$$\int_{-\infty}^{+\infty}\left|p_\varepsilon(t)\right|(\Omega)\,\mathrm{d}t=\left|D\Phi\left(\varphi_\varepsilon\right)\right|(\Omega)<+\infty$$

and thus $U_{\varepsilon,t}$ has finite perimeter for all $t\in\mathbb{R}$. Choosing $0<\gamma<\gamma'<\frac{1}{2}=\Phi(1)$ arbitrarily, by the mean value theorem for integrals we find some $t_\varepsilon\in(\gamma,\gamma')$ such that

$$\sup_{\varepsilon>0}\left(\gamma'-\gamma\right)p_\varepsilon\left(t_\varepsilon\right)\le\sup_{\varepsilon>0}\int_0^{\Phi(1)}p_\varepsilon(t)\,\mathrm{d}t\le\sup_{\varepsilon>0}\left|D\Phi\left(\varphi_\varepsilon\right)\right|<+\infty.$$

Fixing this choice of $t=t_\varepsilon$ and setting $U_\varepsilon=U_{\varepsilon,t_\varepsilon}$ we define the functions $\mathbf{w}_\varepsilon=\mathbf{u}_\varepsilon\mathcal{X}_{U_\varepsilon}$. An easy calculation shows $\nabla\mathbf{w}_\varepsilon=\nabla\mathbf{u}_\varepsilon\mathcal{X}_{U_\varepsilon}$ and $e\left(\mathbf{w}_\varepsilon\right)=e\left(\mathbf{u}_\varepsilon\right)\mathcal{X}_{U_\varepsilon}$. To show that $\mathbf{u}\in GSBD^2\left(\Omega;\mathbb{R}^n\right)$ we want to apply Theorem 2.4.25 to the sequence $\mathbf{w}_\varepsilon$. As $\mathbf{u}_\varepsilon\in H^1\left(\Omega;\mathbb{R}^n\right)$, we obviously have $\mathbf{w}_\varepsilon\in GSBV^2\left(\Omega;\mathbb{R}^n\right)\subset GSBD^2\left(\Omega;\mathbb{R}^n\right)$. As $\mathbf{u}_\varepsilon\to\mathbf{u}$ in $L^1\left(\Omega;\mathbb{R}^n\right)$, we have $\sup_{\varepsilon>0}\|\mathbf{w}_\varepsilon\|_{L^1(\Omega;\mathbb{R}^n)}\le\sup_{\varepsilon>0}\|\mathbf{u}_\varepsilon\|_{L^1(\Omega;\mathbb{R}^n)}<+\infty$. Thus Lemma 3.2.3 yields

$$\begin{aligned}
&\sup_{\varepsilon>0}\left(\int_\Omega\left|\mathbf{w}_\varepsilon\right|\mathrm{d}x+\int_\Omega\left|e\left(\mathbf{w}_\varepsilon\right)\right|^2\mathrm{d}x+\mathcal{H}^{n-1}\left(J_{\mathbf{w}_\varepsilon}\right)\right)\\
&\quad\le\sup_{\varepsilon>0}\left(\int_\Omega\left|\mathbf{w}_\varepsilon\right|\mathrm{d}x+\int_{U_\varepsilon}\frac{\left(\Phi^{-1}\left(t_\varepsilon\right)\right)^2}{\left(\Phi^{-1}(\gamma)\right)^2}\left|e\left(\mathbf{u}_\varepsilon\right)\right|^2\mathrm{d}x+p_\varepsilon\left(t_\varepsilon\right)\right)\\
&\quad\le\sup_{\varepsilon>0}\left(\int_\Omega\left|\mathbf{w}_\varepsilon\right|\mathrm{d}x+\int_{U_\varepsilon}\frac{\left(\varphi_\varepsilon\right)^2}{\left(\Phi^{-1}(\gamma)\right)^2}\left|e\left(\mathbf{u}_\varepsilon\right)\right|^2\mathrm{d}x+p_\varepsilon\left(t_\varepsilon\right)\right)\\
&\quad\le c\sup_{\varepsilon>0}\left(\int_\Omega\left|\mathbf{w}_\varepsilon\right|\mathrm{d}x+\int_{U_\varepsilon}\left(\varphi_\varepsilon^2+k_\varepsilon\right)e\left(\mathbf{u}_\varepsilon\right):\mathbb{C}e\left(\mathbf{u}_\varepsilon\right)\mathrm{d}x+p_\varepsilon\left(t_\varepsilon\right)\right)\\
&\quad<+\infty.
\end{aligned}\tag{3.33}$$

Thus Theorem 2.4.25 yields a subsequence of $\left(\mathbf{w}_\varepsilon\right)$, still denoted $\mathbf{w}_\varepsilon$, that converges $\mathcal{L}^n$-a.e. to

some $\mathbf{w} \in GSBD^2(\Omega;\mathbb{R}^n)$. In addition we have

$$\begin{aligned} e(\mathbf{w}_\varepsilon) &\rightharpoonup e(\mathbf{w}) \qquad \text{weakly in } L^1\left(\Omega;\mathbb{R}^{n\times n}_{\mathrm{sym}}\right) \\ \text{and } \mathcal{H}^{n-1}(J_{\mathbf{w}}) &\leq \liminf_{\varepsilon\to 0} \mathcal{H}^{n-1}(J_{\mathbf{w}_\varepsilon}). \end{aligned}$$

From $\mathbf{u}_\varepsilon \to \mathbf{u}$ and $\chi_{U_\varepsilon} \leq 1$ and since $\chi_{U_\varepsilon} \to \chi_\Omega$ holds $\mathcal{L}^n$-almost everywhere we may deduce that $\mathbf{w}_\varepsilon \to \mathbf{u}$ holds $\mathcal{L}^n$-almost everywhere. Thus $\mathbf{u} = \mathbf{w} \in GSBD^2(\Omega;\mathbb{R}^n)$ by the uniqueness of the limit. Furthermore, as equation (3.33) yields $\sup_{\varepsilon>0}\|e(\mathbf{w}_\varepsilon)\|_{L^2(\Omega;\mathbb{R}^{n\times n}_{\mathrm{sym}})} < +\infty$, the weak convergence $e(\mathbf{w}_\varepsilon) \rightharpoonup e(\mathbf{u})$ is in $L^2\left(\Omega;\mathbb{R}^{n\times n}_{\mathrm{sym}}\right)$. Hence

$$\begin{aligned} &\lim_{\varepsilon\to 0}\int_\Omega e(\mathbf{w}_\varepsilon) : \mathbb{C}e(\mathbf{w}_\varepsilon)\,\mathrm{d}x \\ &\quad= \lim_{\varepsilon\to 0}\int_\Omega e(\mathbf{w}_\varepsilon - \mathbf{u}_\varepsilon) : \mathbb{C}e(\mathbf{w}_\varepsilon - \mathbf{u}_\varepsilon)\,\mathrm{d}x + 2\int_\Omega e(\mathbf{w}_\varepsilon) : \mathbb{C}e(\mathbf{u})\,\mathrm{d}x - \int_\Omega e(\mathbf{u}) : \mathbb{C}e(\mathbf{u})\,\mathrm{d}x \\ &\quad\geq 0 + 2\int_\Omega e(\mathbf{u}) : \mathbb{C}e(\mathbf{u})\,\mathrm{d}x - \int_\Omega e(\mathbf{u}) : \mathbb{C}e(\mathbf{u})\,\mathrm{d}x \\ &\quad= \int_\Omega e(\mathbf{u}) : \mathbb{C}e(\mathbf{u})\,\mathrm{d}x, \end{aligned}$$

leading to

$$\begin{aligned} &\liminf_{\varepsilon\to 0}\int_\Omega \frac{1}{2}\left(\varphi_\varepsilon^2 + k_\varepsilon\right) e(\mathbf{u}_\varepsilon) : \mathbb{C}e(\mathbf{u}_\varepsilon)\,\mathrm{d}x \\ &\quad\geq \liminf_{\varepsilon\to 0}\frac{1}{2}\left(\Phi^{-1}(\gamma)\right)^2\int_{U_\varepsilon} e(\mathbf{u}_\varepsilon) : \mathbb{C}e(\mathbf{u}_\varepsilon)\,\mathrm{d}x \\ &\quad= \liminf_{\varepsilon\to 0}\frac{1}{2}\left(\Phi^{-1}(\gamma)\right)^2\int_{U_\varepsilon} e(\mathbf{w}_\varepsilon) : \mathbb{C}e(\mathbf{w}_\varepsilon)\,\mathrm{d}x \\ &\quad= \liminf_{\varepsilon\to 0}\frac{1}{2}\left(\Phi^{-1}(\gamma)\right)^2\int_{\Omega} e(\mathbf{w}_\varepsilon) : \mathbb{C}e(\mathbf{w}_\varepsilon)\,\mathrm{d}x \\ &\quad\geq \liminf_{\varepsilon\to 0}\frac{1}{2}\left(\Phi^{-1}(\gamma)\right)^2\int_{\Omega} e(\mathbf{u}) : \mathbb{C}e(\mathbf{u})\,\mathrm{d}x. \end{aligned}$$

Letting $\gamma \to \Phi(1)$ we obtain for the elasticity part of the bulk energy

$$\liminf_{\varepsilon\to 0}\int_\Omega \frac{1}{2}\left(\varphi_\varepsilon^2 + k_\varepsilon\right) e(\mathbf{u}_\varepsilon) : \mathbb{C}e(\mathbf{u}_\varepsilon)\,\mathrm{d}x \geq \frac{1}{2}\int_\Omega e(\mathbf{u}) : \mathbb{C}e(\mathbf{u})\,\mathrm{d}x. \tag{3.34}$$

Let us now consider the pressure-dependent terms. As $e(\mathbf{w}_\varepsilon) \rightharpoonup e(\mathbf{u})$ in $L^2\left(\Omega;\mathbb{R}^{n\times n}_{\mathrm{sym}}\right)$ and $\varphi_\varepsilon \to 1$ in $L^2(\Omega)$ we have $\varphi_\varepsilon e(\mathbf{w}_\varepsilon) \rightharpoonup e(\mathbf{u})$ in $L^1\left(\Omega;\mathbb{R}^{n\times n}_{\mathrm{sym}}\right)$. This convergence holds componentwise, thus $\varphi_\varepsilon \partial_{x_i}(\mathbf{w}_\varepsilon)_i \rightharpoonup \partial_{x_i}\mathbf{u}_i$ in $L^1(\Omega)$. Since $(1-\alpha)\,p \in L^\infty(\Omega)$ it holds

$$\lim_{\varepsilon\to 0}\int_\Omega (1-\alpha)\,\varphi_\varepsilon p\nabla\cdot\mathbf{w}_\varepsilon\,\mathrm{d}x = \int_\Omega (1-\alpha)\,p\nabla\cdot\mathbf{u}\,\mathrm{d}x.$$

Using that $\sup_\varepsilon \|\varphi_\varepsilon e(\mathbf{u}_\varepsilon)\|_{L^2(\Omega;\mathbb{R}^{n\times n}_{\mathrm{sym}})} < +\infty$ as well as $|\varphi_\varepsilon| \leq 1$ and $\lim_{\varepsilon\to 0} \mathcal{L}^n(\Omega \setminus U_\varepsilon) = 0$ we can conclude

$$\begin{aligned}
&\liminf_{\varepsilon\to 0} \int_\Omega (1-\alpha)\,\varphi_\varepsilon p \nabla\cdot \mathbf{u}_\varepsilon \,\mathrm{d}x \\
&= \liminf_{\varepsilon\to 0} \left(\int_{U_\varepsilon} (1-\alpha)\,\varphi_\varepsilon p \nabla\cdot \mathbf{w}_\varepsilon \,\mathrm{d}x + \int_{\Omega\setminus U_\varepsilon} (1-\alpha)\,\varphi_\varepsilon p \nabla\cdot \mathbf{u}_\varepsilon \,\mathrm{d}x \right) \\
&\geq \liminf_{\varepsilon\to 0} \left(\int_\Omega (1-\alpha)\,\varphi_\varepsilon p \nabla\cdot \mathbf{w}_\varepsilon \,\mathrm{d}x - c\|p\|_{L^\infty(\Omega)} \|\varphi_\varepsilon e(\mathbf{u}_\varepsilon)\|_{L^2(\Omega;\mathbb{R}^{n\times n}_{\mathrm{sym}})} \left(\mathcal{L}^n(\Omega\setminus U_\varepsilon)\right)^{\frac{1}{2}} \right) \\
&\geq \int_\Omega (1-\alpha)\, p \nabla\cdot \mathbf{u}\,\mathrm{d}x\,.
\end{aligned} \tag{3.35}$$

As $(\mathbf{u}_\varepsilon, \varphi_\varepsilon) \to (\mathbf{u}, 1)$ in $L^1(\Omega;\mathbb{R}^n) \times L^1(\Omega)$ and $|\varphi_\varepsilon| \leq 1$, Lebesgue's dominated convergence theorem yields $\varphi_\varepsilon \mathbf{u} \to \mathbf{u}$ in $L^1(\Omega;\mathbb{R}^n)$ and thus

$$\begin{aligned}
&\lim_{\varepsilon\to 0} \left| \int_\Omega \nabla p\,(\varphi_\varepsilon \mathbf{u}_\varepsilon - \mathbf{u})\,\mathrm{d}x \right| \\
&\quad \leq \lim_{\varepsilon\to 0} \|\nabla p\|_{L^\infty(\Omega)} \left(\int_\Omega |\varphi_\varepsilon|\,|\mathbf{u}_\varepsilon - \mathbf{u}|\,\mathrm{d}x + \int_\Omega |\varphi_\varepsilon \mathbf{u} - \mathbf{u}|\,\mathrm{d}x \right) \\
&\quad \leq \lim_{\varepsilon\to 0} \|\nabla p\|_{L^\infty(\Omega)} \left(\|\mathbf{u}_\varepsilon - \mathbf{u}\|_{L^1(\Omega;\mathbb{R}^n)} + \|\varphi_\varepsilon \mathbf{u} - \mathbf{u}\|_{L^1(\Omega;\mathbb{R}^n)} \right) \\
&\quad = 0.
\end{aligned}$$

This implies

$$\liminf_{\varepsilon\to 0} \int_\Omega \nabla p \varphi_\varepsilon \mathbf{u}_\varepsilon \,\mathrm{d}x \geq \int_\Omega \nabla p \mathbf{u}\,\mathrm{d}x\,. \tag{3.36}$$

Combining equations (3.34) to (3.36) finally yields the lim inf inequality for the bulk part.

Step 2: (*Surface energy inequality*) The lim inf inequality for the surface part of the energy is standard nowadays and can be proven for example as in [Foc01]. It uses the slicing technique as introduced by Ambrosio [AFP00], see also [Bra02, Chapter 15]. Let us give a short overview of the proof for the reader's convenience. We want to prove

$$\liminf_{\varepsilon\to 0} G_\varepsilon(\varphi_\varepsilon) \geq G_c \mathcal{H}^{n-1}(J_{\mathbf{u}})\,.$$

To this end, we use the notation from Theorem 2.4.13 and start from the one-dimensional result Lemma 3.1.5. Considering the localized versions of the functionals we define for every $A \in \mathcal{A}(\Omega)$

and every $\xi \in \mathbb{S}^{n-1}$ the integrals over the one-dimensional functionals as

$$F_\varepsilon^\xi(\mathbf{u}_\varepsilon, \varphi_\varepsilon; A) = \int_{\Pi^\xi} \widetilde{F}_\varepsilon\left((\hat{\mathbf{u}}_\varepsilon)_y^\xi, (\varphi_\varepsilon)_y^\xi; A_y^\xi\right) \mathrm{d}\mathcal{H}^{n-1}(y)$$
$$\text{and } G_\varepsilon^\xi(\varphi_\varepsilon; A) = \int_{\Pi^\xi} \widetilde{G}_\varepsilon\left((\varphi_\varepsilon)_y^\xi; A_y^\xi\right) \mathrm{d}\mathcal{H}^{n-1}(y).$$

Fubini's Theorem yields $G_\varepsilon^\xi(\varphi_\varepsilon; A) \leq G_\varepsilon(\varphi_\varepsilon; A)$ and $F_\varepsilon^\xi((\mathbf{u}_\varepsilon), \varphi_\varepsilon; A) \leq F_\varepsilon(\mathbf{u}_\varepsilon, \varphi_\varepsilon; A)$. Thus Lemma 3.2.3 leads to $F_\varepsilon^\xi((\mathbf{u}_\varepsilon), \varphi_\varepsilon; A) \leq F_\varepsilon(\mathbf{u}_\varepsilon, \varphi_\varepsilon) < +\infty$. Hence we obtain boundedness of $\liminf_{\varepsilon\to 0} \widetilde{F}_\varepsilon\left((\hat{\mathbf{u}}_\varepsilon)_y^\xi, (\varphi_\varepsilon)_y^\xi; A_y^\xi\right)$ and can apply Lemma 3.1.5 to get

$$\liminf_{\varepsilon\to 0} \widetilde{G}_\varepsilon\left((\varphi_\varepsilon)_y^\xi; A_y^\xi\right) \geq \mathcal{H}^0\left(A_y^\xi \cap J_{\hat{\mathbf{u}}_y^\xi}\right). \tag{3.37}$$

Hence Fatou's lemma yields

$$\begin{aligned}\liminf_{\varepsilon\to 0} G_\varepsilon(\varphi_\varepsilon; A) &\geq \liminf_{\varepsilon\to 0} G_\varepsilon^\xi(\varphi_\varepsilon; A)\\ &\geq \int_{\Pi^\xi} \liminf_{\varepsilon\to 0} \widetilde{G}_\varepsilon\left((\varphi_\varepsilon)_y^\xi; A_y^\xi\right) \mathrm{d}\mathcal{H}^{n-1}(y)\\ &\geq \int_{\Pi^\xi} G_c \mathcal{H}^0\left(A_y^\xi \cap J_{\hat{\mathbf{u}}_y^\xi}\right) \mathrm{d}\mathcal{H}^{n-1}(y).\end{aligned}$$

Thus by Theorem 2.4.13 we get

$$\liminf_{\varepsilon\to 0} G(\varphi_\varepsilon; A) \geq G_c \int_{A\cap J_{\mathbf{u}_y^\xi}} |\nu_{\mathbf{u}}(y)\cdot\xi| \,\mathrm{d}\mathcal{H}^{n-1}(y) \quad \forall\, \xi \in \mathbb{S}^{n-1}.$$

Taking the supremum over a countable dense family $(\xi_i) \subset \left\{\xi \in \mathbb{S}^{n-1} : \mathcal{H}^{n-1}\left(J_{\mathbf{u}} \setminus J_{\mathbf{u}}^\xi\right) = 0\right\}$, Proposition 2.4.2 finally yields

$$\begin{aligned}\liminf_{\varepsilon\to 0} G(\varphi_\varepsilon) &\geq G_c \int_{J_{\mathbf{u}}} \sup_i |\nu_{\mathbf{u}}(y)\cdot\xi_i| \,\mathrm{d}\mathcal{H}^{n-1}(y)\\ &= G_c \mathcal{H}^{n-1}(J_{\mathbf{u}}).\end{aligned} \tag{3.38}$$

In combination with Step 1, equation (3.38) concludes the proof of Theorem 3.2.4. □

Let us now prove the following lim sup inequality.

Theorem 3.2.5:
For all $(\mathbf{u}, \varphi) \in GSBD^2(\Omega; \mathbb{R}^n) \times \mathcal{V}$ there exists a sequence $(\mathbf{u}_\varepsilon, \varphi_\varepsilon) \in L^1(\Omega; \mathbb{R}^n) \times L^1(\Omega)$ that converges to $(\mathbf{u}, \varphi)$ in $L^1(\Omega; \mathbb{R}^n) \times L^1(\Omega)$ and satisfies

$$D(\mathbf{u}, \varphi) \geq \limsup_{\varepsilon\to 0} D_\varepsilon(\mathbf{u}_\varepsilon, \varphi_\varepsilon). \tag{3.39}$$

Proof. For the proof of the lim sup inequality we use the standard technique of proof by density (Lemma 2.3.3) as described in [Bra98, Section 4.2] and as applied for example by [Iur14, CC19]. It remains to find a suitable dense set $\mathcal{D} \subset GSBD^2(\Omega;\mathbb{R}^n)$ and to construct a recovery sequence for all $(\mathbf{u},\varphi) \in \mathcal{D} \times \mathcal{V}$.

Step 1: (*Construction of the dense set* $\mathcal{D}$)
In this step we combine the density results of Theorems 2.4.15 and 2.4.26. For every $\mathbf{u} \in GSBD^2(\Omega;\mathbb{R}^n) \cap L^1(\Omega;\mathbb{R}^n)$ Theorem 2.4.26 yields a sequence $\mathbf{u}_j \in SBV^2(\Omega;\mathbb{R}^n) \cap L^\infty(\Omega;\mathbb{R}^n)$ such that $J_{\mathbf{u}_j} \subset \Omega$ is closed and included in a finite union of closed connected pieces of $\mathcal{C}^1(\Omega)$ curves and $\mathbf{u}_j \in W^{1,\infty}\left(\Omega \setminus J_{\mathbf{u}_j};\mathbb{R}^n\right)$. In addition it holds

$$\begin{aligned}\lim_{j\to+\infty} \|\mathbf{u}_j - \mathbf{u}\|_{L^1(\Omega;\mathbb{R}^n)} &= 0,\\ \lim_{j\to+\infty} \|e(\mathbf{u}_j) - e(\mathbf{u})\|_{L^2(\Omega;\mathbb{R}^{n\times n}_{\mathrm{sym}})} &= 0,\\ \text{and } \lim_{j\to+\infty} \mathcal{H}^{n-1}\left(J_{\mathbf{u}_j} \Delta J_{\mathbf{u}}\right) &= 0.\end{aligned}$$

Since every $\mathbf{u}_j$ as given above is in $GSBV^2(\Omega)$, Theorem 2.4.15 yields a further sequence $\mathbf{u}_{j_k} \in SBV^2(\Omega;\mathbb{R}^n)$ for every $j \in \mathbb{N}$, which satisfies $\mathbf{u}_{j_k} \in \mathcal{W}(\Omega;\mathbb{R}^n)$ as well as

$$\begin{aligned}\lim_{k\to+\infty} \|\mathbf{u}_{j_k} - \mathbf{u}_j\|_{L^2(\Omega;\mathbb{R}^n)} &= 0,\\ \lim_{k\to+\infty} \|\nabla \mathbf{u}_{j_k} - \nabla \mathbf{u}_j\|_{L^2(\Omega;\mathbb{R}^{n\times n})} &= 0,\\ \lim_{k\to+\infty} \left|\mathcal{H}^{n-1}\left(J_{\mathbf{u}_{j_k}}\right) - \mathcal{H}^{n-1}\left(J_{\mathbf{u}_j}\right)\right| &= 0.\end{aligned}$$

Combining the two results we can choose $\mathcal{D} = \mathcal{W}(\Omega;\mathbb{R}^n)$. By a diagonalization argument we obtain a sequence $\mathbf{u}_j \in \mathcal{W}(\Omega;\mathbb{R}^n)$ such that

$$\lim_{j\to+\infty} \|\mathbf{u}_j - \mathbf{u}\|_{L^1(\Omega;\mathbb{R}^n)} = 0, \tag{3.40}$$

$$\lim_{j\to+\infty} \|e(\mathbf{u}_j) - e(\mathbf{u})\|_{L^2(\Omega;\mathbb{R}^{n\times n}_{\mathrm{sym}})} = 0, \tag{3.41}$$

$$\lim_{j\to+\infty} \left|\mathcal{H}^{n-1}\left(J_{\mathbf{u}_j}\right) - \mathcal{H}^{n-1}\left(J_{\mathbf{u}}\right)\right| = 0. \tag{3.42}$$

Here we used $\|\cdot\|_{L^1(\Omega;\mathbb{R}^n)} \leq C\|\cdot\|_{L^2(\Omega;\mathbb{R}^n)}$ and $\|e(\cdot)\|_{L^2(\Omega;\mathbb{R}^{n\times n}_{\mathrm{sym}})} \leq \|\nabla(\cdot)\|_{L^2(\Omega;\mathbb{R}^{n\times n})}$. It remains to show $\lim_{j\to+\infty} D(\mathbf{u}_j,1) = D(\mathbf{u},1)$. By equation (3.42) it suffices to show convergence for the bulk energy. For its linear elasticity part we have convergence since

$$\begin{aligned}\lim_{j\to+\infty} \left|\int_\Omega \frac{1}{2}\left(e(\mathbf{u}_j) - e(\mathbf{u})\right) : \mathbb{C}\left(e(\mathbf{u}_j) - e(\mathbf{u})\right) \mathrm{d}x\right| &\leq c \lim_{j\to+\infty} \int_\Omega \left|\left(e(\mathbf{u}_j) - e(\mathbf{u})\right)\right|^2 \mathrm{d}x\\ &= c \lim_{j\to+\infty} \|e(\mathbf{u}_j) - e(\mathbf{u})\|^2_{L^2(\Omega;\mathbb{R}^n)}\\ &= 0.\end{aligned}$$

For the pressure terms Hölder's inequality yields

$$\begin{aligned}\lim_{j\to+\infty}\left|\int_\Omega |1-\alpha|\, p\,(\nabla\cdot\mathbf{u}_j-\nabla\cdot\mathbf{u})\,\mathrm{dx}\right| &\le c\lim_{j\to+\infty}(1-\alpha)\,\|p\|_{L^\infty(\Omega)}\|e(\mathbf{u}_j)-e(\mathbf{u})\|_{L^1(\Omega;\mathbb{R}^n)}\\ &\le c\lim_{j\to+\infty}|1-\alpha|\,\|p\|_{L^\infty(\Omega)}\|e(\mathbf{u}_j)-e(\mathbf{u})\|_{L^2(\Omega;\mathbb{R}^n)}\\ &= 0\end{aligned}$$

and

$$\lim_{j\to+\infty}\left|\int_\Omega \nabla p\cdot(\mathbf{u}_j-\mathbf{u})\,\mathrm{dx}\right| \le \lim_{j\to+\infty}\|\nabla p\|_{L^\infty(\Omega)}\|\mathbf{u}_j-\mathbf{u}\|_{L^1(\Omega;\mathbb{R}^n)} = 0.$$

Hence the total energy satisfies $\lim_{j\to+\infty}|D(\mathbf{u}_j,1)-D(\mathbf{u},1)|=0$.

Step 2: (*Construction of a recovery sequence*)

The construction of a recovery sequence in the case $(\mathbf{u},\varphi)\in\mathcal{W}(\Omega;\mathbb{R}^n)\times\mathcal{V}$ is standard nowadays. We follow the approach of [Foc01], see also [Iur14, Cha04, Cha05], and prove the lim sup inequality for the additional, pressure dependent, terms in our energy functional.

As $\mathbf{u}\in\mathcal{W}(\Omega;\mathbb{R}^n)$, without loss of generality we assume that $\overline{J_\mathbf{u}} = K\cap\Omega$ for some polyhedral set K contained in the $(n-1)$-dimensional hyperplane Π. Let ν be the normal to Π, let $\pi\colon\mathbb{R}^n\to\Pi$ be the orthogonal projection onto Π and let $d(x)=\operatorname{dist}(x,\Pi)$ be the distance from Π. Set $K^\delta=\{y\in\Pi:\operatorname{dist}(y,K)<\delta\}$. For $\varepsilon,\ \xi_\varepsilon>0$ with $\xi_\varepsilon=\sqrt{k_\varepsilon\varepsilon}\ll\varepsilon$ consider the sets illustrated by Figure 3.2 and defined via

$$\begin{aligned}A_\varepsilon &= \{x\in\Omega:\pi(x)\in K^\varepsilon,\ d(x)\le\xi_\varepsilon\},\\ B_\varepsilon &= \left\{x\in\Omega:\pi(x)\in K^{2\varepsilon},\ d(x)\le\xi_\varepsilon+\varepsilon T\right\},\\ C_\varepsilon &= \left\{x\in\Omega:\pi(x)\in K^{\varepsilon/2},\ d(x)\le\xi_\varepsilon/2\right\}.\end{aligned}$$

Defining ρ_ε as cut-off function between C_ε and A_ε, that is $\rho_\varepsilon\in C_c^\infty(A_\varepsilon)$, $0\le\rho_\varepsilon\le1$ and $\rho_\varepsilon\equiv1$ on C_ε, we set $\mathbf{u}_\varepsilon=\mathbf{u}(1-\rho_\varepsilon)$ and have $\mathbf{u}_\varepsilon\equiv0$ on C_ε and hence $\mathbf{u}_\varepsilon\in H^1(\Omega;\mathbb{R}^n)$.

For all $\eta>0$ we can find $T>0$ and $f_\eta\in H^1((0,T))$ with $0\le f_\eta\le1$, $f_\eta(0)=0$ and $f_\eta(T)=1$ such that

$$\int_0^T (f_\eta-1)^2+\left(f_\eta'\right)^2\,\mathrm{dt}\le1+\eta. \tag{3.43}$$

Further let $\gamma_\varepsilon\in C_c^\infty\left(K^{2\varepsilon}\right)$ be a cut-off function between K^ε and $K^{2\varepsilon}$ satisfying $0\le\gamma_\eta\le1$, $\gamma_\varepsilon\equiv1$ on K^ε and $\|\nabla\gamma_\varepsilon\|_{L^\infty(\Pi)}\le c/\varepsilon$ for some constant c. Finally we construct the recovery sequence φ_ε

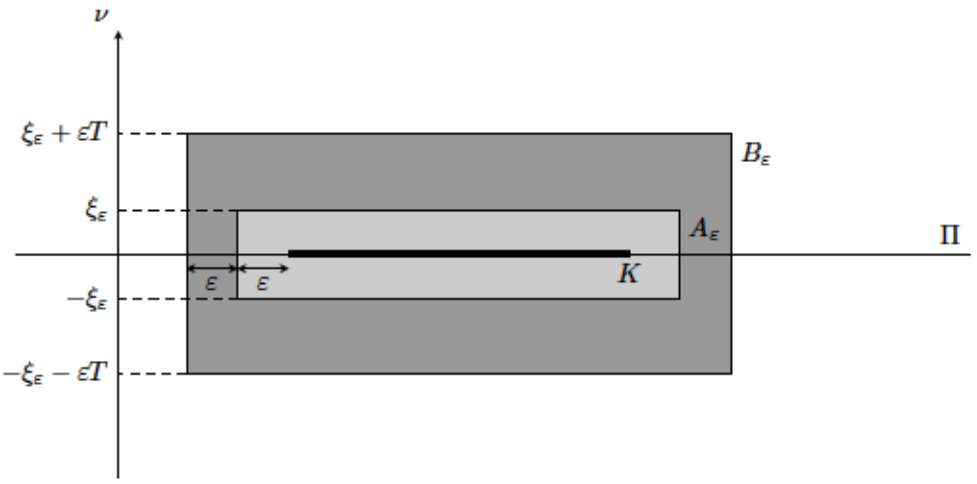

Figure 3.2: Construction of the recovery sequences: Sets A_ε and B_ε.

for the phase field φ by setting

$$h_\varepsilon(t) = \begin{cases} 0 & \text{if } |t| \le \xi_\varepsilon, \\ f_\eta\left(\frac{|t|-\xi_\varepsilon}{\varepsilon}\right) & \text{if } \xi_\varepsilon \le |t| \le \xi_\varepsilon + \varepsilon T, \\ 1 & \text{if } \xi_\varepsilon + \varepsilon T \le |t| \end{cases}$$

$$\text{and } \varphi_\varepsilon(x) = \gamma_\varepsilon(\pi(x))\, h_\varepsilon(d(x)) + 1 - \gamma_\varepsilon(p(x)).$$

It remains to show that this choice of $(\mathbf{u}_\varepsilon, \varphi_\varepsilon)$ satisfies $\mathbf{u}_\varepsilon \to \mathbf{u}$ and $\varphi_\varepsilon \to 1$ in $L^1(\Omega;\mathbb{R}^n) \times L^1(\Omega)$ as well as $D(\mathbf{u},\varphi) \ge \limsup_{\varepsilon\to 0} D_\varepsilon(\mathbf{u}_\varepsilon, \varphi_\varepsilon)$. Let us first show the convergence of the sequences $(\mathbf{u}_\varepsilon, \varphi_\varepsilon)$. As $\mathcal{L}^n(A_\varepsilon) \le c\xi_\varepsilon$ for ε small, $\mathbf{u}_\varepsilon \le \mathbf{u}$ in Ω and $\mathbf{u}_\varepsilon = \mathbf{u}$ in $\Omega \setminus A_\varepsilon$ we obviously have

$$\lim_{\varepsilon\to 0} \int_\Omega |\mathbf{u}_\varepsilon - \mathbf{u}|\,\mathrm{d}x = \lim_{\varepsilon\to 0} \left(\int_{\Omega\setminus A_\varepsilon} |\mathbf{u}_\varepsilon - \mathbf{u}|\,\mathrm{d}x + \int_{A_\varepsilon} |\mathbf{u}_\varepsilon - \mathbf{u}|\,\mathrm{d}x \right) \le \lim_{\varepsilon\to 0} \left(\int_{\Omega\setminus A_\varepsilon} 0\,\mathrm{d}x + \int_{A_\varepsilon} 2\,|\mathbf{u}|\,\mathrm{d}x \right) = 0.$$

Further $\varphi_\varepsilon - 1 = \gamma_\varepsilon(\pi(x))\,(h_\varepsilon(d(x)) - 1) \le 1$ and $d(x) = 1$ in $\Omega \setminus B_\varepsilon$ and thus $\varphi_\varepsilon - 1 = 0$ in $\Omega \setminus B_\varepsilon$. Hence the convergence $\varphi_\varepsilon \to 1$ in $L^1(\Omega)$ follows from $\mathcal{L}^n(B_\varepsilon) \le c(\xi_\varepsilon + \varepsilon T)$.
Consider now the different parts of the energy. Having $\varphi_\varepsilon \equiv 0$ in A_ε and $\mathbf{u}_\varepsilon = \mathbf{u}$ in $\Omega \setminus A_\varepsilon$ yields

$$\begin{aligned} &\limsup_{\varepsilon\to 0} \int_\Omega \frac{1}{2}(\varphi_\varepsilon + k_\varepsilon)^2\, e(\mathbf{u}_\varepsilon) : \mathbb{C}e(\mathbf{u}_\varepsilon)\,\mathrm{d}x \\ &= \limsup_{\varepsilon\to 0} \left(\int_{\Omega\setminus A_\varepsilon} \frac{1}{2}(\varphi_\varepsilon + k_\varepsilon)^2\, e(\mathbf{u}_\varepsilon) : \mathbb{C}e(\mathbf{u}_\varepsilon)\,\mathrm{d}x + \int_{A_\varepsilon} \frac{1}{2}(\varphi_\varepsilon + k_\varepsilon)^2\, e(\mathbf{u}_\varepsilon) : \mathbb{C}e(\mathbf{u}_\varepsilon)\,\mathrm{d}x \right) \\ &\le \limsup_{\varepsilon\to 0} \left(\int_{\Omega\setminus A_\varepsilon} \frac{1}{2}(1 + k_\varepsilon)^2\, e(\mathbf{u}) : \mathbb{C}e(\mathbf{u})\,\mathrm{d}x + \int_{A_\varepsilon} \frac{1}{2} k_\varepsilon^2 e(\mathbf{u}_\varepsilon) : \mathbb{C}e(\mathbf{u}_\varepsilon)\,\mathrm{d}x \right) \\ &\le \int_\Omega \frac{1}{2}(e(\mathbf{u}) : \mathbb{C}e(\mathbf{u}))\,\mathrm{d}x, \end{aligned} \tag{3.44}$$

using $\mathcal{L}^n(A_\varepsilon) \to 0$ for $\varepsilon \to 0$ in the last inequality. It holds $\mathcal{L}^n(B_\varepsilon) \to 0$ for $\varepsilon \to 0$, $\mathbf{u} \in L^1(\Omega;\mathbb{R}^n)$ and $e(\mathbf{u}) \in L^2(\Omega;\mathbb{R}^{n\times n})$, hence by the absolute continuity of the Lebesgue integral

$$\lim_{\varepsilon\to 0}\left|\int_{B_\varepsilon}(1-\alpha)\,p\nabla\cdot\mathbf{u}\,\mathrm{d}x\right| \le \sqrt{n}\lim_{\varepsilon\to 0}\left(\mathcal{L}^n(B_\varepsilon)\right)^{\frac{1}{2}}(1-\alpha)\,\|p\|_{L^\infty(B_\varepsilon)}\|\|e(\mathbf{u})\|\|_{L^2(B_\varepsilon)}\,\mathrm{d}x = 0$$

$$\text{and } \lim_{\varepsilon\to 0}\left|\int_{B_\varepsilon}\nabla p\cdot\mathbf{u}\,\mathrm{d}x\right| \le \lim_{\varepsilon\to 0}\|\nabla p\|_{L^\infty(B_\varepsilon)}\int_{B_\varepsilon}|\mathbf{u}|\,\mathrm{d}x = 0.$$

Furthermore, since $\varphi_\varepsilon = 0$ in A_ε, $\varphi_\varepsilon \le 1$ and $\mathbf{u}_\varepsilon = \mathbf{u}$ in $\Omega\setminus A_\varepsilon$,

$$\lim_{\varepsilon\to 0}\left|\int_{B_\varepsilon}(1-\alpha)\,\varphi_\varepsilon p\nabla\cdot\mathbf{u}_\varepsilon\,\mathrm{d}x\right| \le \sqrt{n}\lim_{\varepsilon\to 0}\left(\mathcal{L}^n(B_\varepsilon)\right)^{\frac{1}{2}}(1-\alpha)\,\|p\|_{L^\infty(B_\varepsilon)}\|\|e(\mathbf{u})\|\|_{B_\varepsilon\setminus A_\varepsilon}\,\mathrm{d}x = 0$$

$$\text{and } \lim_{\varepsilon\to 0}\left|\int_{B_\varepsilon}\varphi_\varepsilon\,\nabla p\cdot\mathbf{u}_\varepsilon\right|\mathrm{d}x \le \lim_{\varepsilon\to 0}\|\nabla p\|_{L^\infty(B_\varepsilon)}\int_{B_\varepsilon\setminus A_\varepsilon}|\mathbf{u}|\,\mathrm{d}x = 0.$$

Recalling that $\varphi_\varepsilon = 1$ in $\Omega\setminus B_\varepsilon$ we finally obtain the following results for the pressure terms,

$$\begin{aligned}
\lim_{\varepsilon\to 0}\int_\Omega(1-\alpha)\,\varphi_\varepsilon p\nabla\cdot\mathbf{u}_\varepsilon\,\mathrm{d}x &= \lim_{\varepsilon\to 0}\left(\int_{B_\varepsilon}(1-\alpha)\,\varphi_\varepsilon p\nabla\cdot\mathbf{u}_\varepsilon\,\mathrm{d}x + \int_{\Omega\setminus B_\varepsilon}(1-\alpha)\,p\nabla\cdot\mathbf{u}\,\mathrm{d}x\right)\\
&= \lim_{\varepsilon\to 0}\left(\int_{B_\varepsilon}(1-\alpha)\,p\,(\varphi_\varepsilon\nabla\cdot\mathbf{u}_\varepsilon - \nabla\cdot\mathbf{u})\,\mathrm{d}x + \int_\Omega(1-\alpha)\,p\nabla\cdot\mathbf{u}\,\mathrm{d}x\right)\\
&= \int_\Omega(1-\alpha)\,p\nabla\cdot\mathbf{u}\,\mathrm{d}x\\
\text{and } \lim_{\varepsilon\to 0}\int_\Omega\varphi_\varepsilon\,\nabla p\cdot\mathbf{u}_\varepsilon\,\mathrm{d}x &= \lim_{\varepsilon\to 0}\left(\int_{B_\varepsilon}\varphi_\varepsilon\,\nabla p\cdot\mathbf{u}_\varepsilon\,\mathrm{d}x + \int_{\Omega\setminus B_\varepsilon}\nabla p\cdot\mathbf{u}\,\mathrm{d}x\right)\\
&= \lim_{\varepsilon\to 0}\left(\int_{B_\varepsilon}\nabla p\cdot(\varphi_\varepsilon\mathbf{u}_\varepsilon - \mathbf{u})\,\mathrm{d}x + \int_\Omega\nabla p\cdot\mathbf{u}\,\mathrm{d}x\right)\\
&= 0.
\end{aligned}$$

For the surface term we can estimate in a first step

$$\begin{aligned}
G_c\int_\Omega\frac{1}{2\varepsilon}(\varphi_\varepsilon-1)^2 + \frac{\varepsilon}{2}|\nabla\varphi_\varepsilon|^2\,\mathrm{d}x &= G_c\int_{\Omega\setminus B_\varepsilon}\frac{1}{2\varepsilon}(\varphi_\varepsilon-1)^2 + \frac{\varepsilon}{2}|\nabla\varphi_\varepsilon|^2\,\mathrm{d}x\\
&\quad + G_c\int_{B_\varepsilon\setminus A_\varepsilon}\frac{1}{2\varepsilon}(\varphi_\varepsilon-1)^2 + \frac{\varepsilon}{2}|\nabla\varphi_\varepsilon|^2\,\mathrm{d}x\\
&\quad + G_c\int_{A_\varepsilon}\frac{1}{2\varepsilon}(\varphi_\varepsilon-1)^2 + \frac{\varepsilon}{2}|\nabla\varphi_\varepsilon|^2\,\mathrm{d}x\\
&= I_1 + I_2 + I_3.
\end{aligned}$$

In $\Omega \setminus B_\varepsilon$ it holds $\varphi_\varepsilon = 1$ and $\nabla \varphi_\varepsilon = 0$, hence

$$I_1 = G_c \int\limits_{\Omega \setminus B_\varepsilon} \frac{1}{2\varepsilon} (1-1)^2 + \frac{\varepsilon}{2} |0|^2 \,\mathrm{dx} = G_c \int\limits_{\Omega \setminus B_\varepsilon} 0 \,\mathrm{dx} = 0.$$

In A_ε it holds $\varphi_\varepsilon = \nabla \varphi_\varepsilon = 0$ and thus $\xi_\varepsilon \in o(\varepsilon)$ implies

$$\lim_{\varepsilon \to 0} I_3 = \lim_{\varepsilon \to 0} G_c \int\limits_{A_\varepsilon} \frac{1}{2\varepsilon} \,\mathrm{dx} = \lim_{\varepsilon \to 0} G_c \frac{\mathcal{L}^n(A_\varepsilon)}{2\varepsilon} \leq \lim_{\varepsilon \to 0} c \frac{\xi_\varepsilon}{\varepsilon} = 0.$$

To estimate I_2, the set $B_\varepsilon \setminus A_\varepsilon$ is further divided into three parts, see also Figure 3.3,

$$\begin{aligned}
D_\varepsilon &= \{x \in \Omega : \pi(x) \in K^\varepsilon, \xi_\varepsilon \leq d(x) \leq \xi_\varepsilon + \varepsilon T\}, \\
E_\varepsilon^1 &= \left\{x \in \Omega : \pi(x) \in K^{2\varepsilon} \setminus K^\varepsilon, d(x) \leq \xi_\varepsilon\right\}, \\
E_\varepsilon^2 &= \left\{x \in \Omega : \pi(x) \in K^{2\varepsilon} \setminus K^\varepsilon, \xi_\varepsilon \leq d(x) \leq \xi_\varepsilon + \varepsilon T\right\}.
\end{aligned}$$

In D_ε we have $\gamma_\varepsilon(\pi(x)) \equiv 1$, hence $\varphi_\varepsilon(x) = f_\eta\left(\frac{|d(x)| - \xi_\varepsilon}{\varepsilon}\right)$. By equation (3.43) and the relation $\nabla d(x) = \pm\nu$ it holds

$$\begin{aligned}
&\lim_{\varepsilon \to 0} \int\limits_{D_\varepsilon} \frac{1}{2\varepsilon} (\varphi_\varepsilon - 1)^2 + \frac{\varepsilon}{2} |\nabla \varphi_\varepsilon|^2 \,\mathrm{dx} \\
&= \lim_{\varepsilon \to 0} 2 \int\limits_{K^\varepsilon} \int\limits_{\xi_\varepsilon}^{\xi_\varepsilon + \varepsilon T} \frac{1}{2\varepsilon} \left(f_\eta\left(\frac{|t| - \xi_\varepsilon}{\varepsilon}\right) - 1\right)^2 + \frac{\varepsilon}{2} \left|f_\eta'\left(\frac{|t| - \xi_\varepsilon}{\varepsilon}\right) \frac{\nu}{\varepsilon}\right|^2 \mathrm{dt}\, \mathrm{d}\mathcal{H}^{n-1}(y) \\
&= \lim_{\varepsilon \to 0} \frac{1}{\varepsilon} \int\limits_{K^\varepsilon} \int\limits_0^T \left((f_\eta(s) - 1)^2 + \left|f_\eta'(s)\right|^2\right) \varepsilon \,\mathrm{ds}\, \mathrm{d}\mathcal{H}^{n-1}(y) \\
&\leq \lim_{\varepsilon \to 0} \mathcal{H}^{n-1}(K^\varepsilon)(1+\eta) \\
&= \mathcal{H}^{n-1}(K)(1+\eta) \\
&= \mathcal{H}^{n-1}\left(\overline{J_{\mathbf{u}}}\right)(1+\eta).
\end{aligned} \tag{3.45}$$

Now let D_π denote the Jacobian of π. It satisfies $\|D_\pi\|_{L^\infty(\Omega;\mathbb{R}^{n\times n})} \leq 1$ with respect to the matrix norm $\|\cdot\|_\infty$. As $\varphi_\varepsilon(x) = 1 - \gamma_\varepsilon(\pi(x))$ in E_ε^1 we can estimate

$$\begin{aligned}
&\lim_{\varepsilon \to 0} \int\limits_{E_\varepsilon^1} \frac{1}{2\varepsilon} (\varphi_\varepsilon - 1)^2 + \frac{\varepsilon}{2} |\nabla \varphi_\varepsilon|^2 \,\mathrm{dx} \\
&= \lim_{\varepsilon \to 0} \int\limits_{E_\varepsilon^1} \frac{(\gamma_\varepsilon(\pi(x)))^2}{2\varepsilon} \frac{\varepsilon}{2} |\nabla \gamma_\varepsilon(\pi(x)) D_\pi(x)|^2 \,\mathrm{dx} \\
&\leq \lim_{\varepsilon \to 0} \int\limits_{K^{2\varepsilon} \setminus K^\varepsilon} \int\limits_{-\xi_\varepsilon}^{\xi_\varepsilon} \frac{(\gamma_\varepsilon(y))^2}{2\varepsilon} + \frac{\varepsilon}{2} |\nabla \gamma_\varepsilon(y)|^2 \,\mathrm{dt}\, \mathrm{d}\mathcal{H}^{n-1}(y) \\
&\leq \lim_{\varepsilon \to 0} \frac{c}{\varepsilon} \xi_\varepsilon \mathcal{H}^{n-1}\left(K^{2\varepsilon} \setminus K^\varepsilon\right) \\
&= 0,
\end{aligned} \tag{3.46}$$

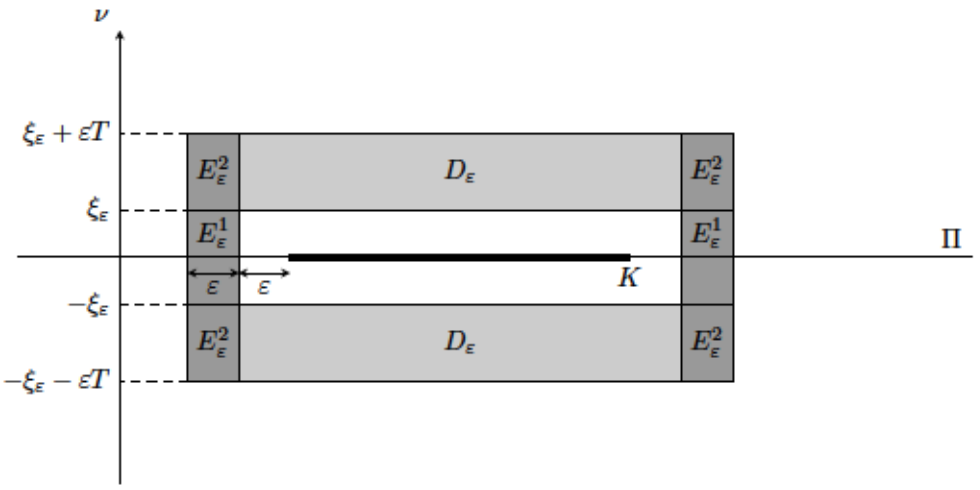

Figure 3.3: Construction of the recovery sequences: Decomposition of $B_\varepsilon \setminus A_\varepsilon$ into the sets D_ε, E_ε^1 and E_ε^2.

where we used $0 \leq \gamma_\varepsilon \leq 1$ and $0 \leq \|\nabla \gamma_\varepsilon\|_{L^\infty(\Pi)} \leq c/\varepsilon$ in the last inequality. These properties of γ_ε together with $h_\varepsilon(d(x)) = f_\eta\left(\frac{|d(x)|-\xi_\varepsilon}{\varepsilon}\right)$ in E_ε^2 yield the following for every $\eta > 0$ for the remaining term.

$$
\begin{aligned}
&\lim_{\varepsilon\to 0} \int_{E_\varepsilon^2} \frac{1}{2\varepsilon}(\varphi_\varepsilon - 1)^2 + \frac{\varepsilon}{2}|\nabla \varphi_\varepsilon|^2 \,\mathrm{dx} \\
&\quad = \lim_{\varepsilon\to 0} \int_{E_\varepsilon^2} \frac{1}{2\varepsilon}(\gamma_\varepsilon(\pi(x)))^2 \left(f_\eta\left(\frac{|d(x)|-\xi_\varepsilon}{\varepsilon}\right) - 1\right)^2 \mathrm{dx} \\
&\qquad + \lim_{\varepsilon\to 0} \frac{\varepsilon}{2} \int_{E_\varepsilon^2} \left|\nabla \gamma_\varepsilon(\pi(x)) D_\pi(x) \left(f_\eta\left(\frac{|d(x)|-\xi_\varepsilon}{\varepsilon}\right) - 1\right) + \frac{\nu}{\varepsilon} f_\eta'\left(\frac{|d(x)|-\xi_\varepsilon}{\varepsilon}\right)\right|^2 \mathrm{dx} \\
&\quad \leq \lim_{\varepsilon\to 0} \int_{K^{2\varepsilon}\setminus K^\varepsilon} \int_{\xi_\varepsilon}^{\xi_\varepsilon+\varepsilon T} \frac{1}{\varepsilon}\left(f_\eta\left(\frac{t-\xi_\varepsilon}{\varepsilon}\right) - 1\right)^2 \mathrm{dt}\,\mathrm{d}\mathcal{H}^{n-1}(y) \\
&\qquad + \lim_{\varepsilon\to 0} \frac{c}{\varepsilon} \int_{K^{2\varepsilon}\setminus K^\varepsilon} \int_{\xi_\varepsilon}^{\xi_\varepsilon+\varepsilon T} \left|\left(f_\eta\left(\frac{t-\xi_\varepsilon}{\varepsilon}\right) - 1\right) + f_\eta'\left(\frac{t-\xi_\varepsilon}{\varepsilon}\right)\right|^2 \mathrm{dt}\,\mathrm{d}\mathcal{H}^{n-1}(y) \\
&\quad \leq \lim_{\varepsilon\to 0} \int_{K^{2\varepsilon}\setminus K^\varepsilon} \int_0^T \left(\frac{1}{\varepsilon}(f_\eta(s) - 1)^2 + \frac{c}{\varepsilon}\left|(f_\eta(s) - 1) + f_\eta'(s)\right|^2\right) \varepsilon \,\mathrm{ds}\,\mathrm{d}\mathcal{H}^{n-1}(y) \\
&\quad \leq \lim_{\varepsilon\to 0} c \int_{K^{2\varepsilon}\setminus K^\varepsilon} (1+\eta)\,\mathrm{d}\mathcal{H}^{n-1}(y) \\
&\quad \leq \lim_{\varepsilon\to 0} c(1+\eta)\mathcal{H}^{n-1}\left(K^{2\varepsilon}\setminus K^\varepsilon\right) \\
&\quad = 0.
\end{aligned}
\tag{3.47}
$$

Finally equations (3.45) to (3.47) yield $\lim_{\varepsilon\to 0} I_2 = G_c \mathcal{H}^{n-1}\left(\overline{J_{\mathbf{u}}}\right)(1+\eta)$. Since $\eta > 0$ was arbitrary, equation (3.39) is proven. □

As in the one-dimensional situation, from a numerical point of view we are interested in the situation including boundary conditions. Following the approach of [CC19, Theorem 5.5] we prove a Γ-convergence result in the case of the prescription of Dirichlet boundary conditions on a subset Γ_D of $\partial\Omega$, where the Dirichlet part Γ_D of $\partial\Omega$ satisfies the same geometric condition as in [CC19, Theorem 5.5]. More precisely, we assume that $\Omega \subset \mathbb{R}^n$ is open, bounded, connected and with Lipschitz-boundary $\partial\Omega$. Furthermore, Γ_D and Γ_N are such that

$$\partial\Omega = \Gamma_D \cup \Gamma_N \cup N$$

with Γ_D, Γ_N relatively open, $\Gamma_D \cap \Gamma_N = \emptyset$, $\mathcal{H}^{n-1}(N) = 0$, $\Gamma_D \neq \emptyset$ and $\Sigma = \partial\Gamma_D = \partial\Gamma_N$ has finite $\mathcal{H}^{n-2}$-measure. Moreover, we assume that there exists $\bar{\delta} > 0$ and $x_0 \in \mathbb{R}^n$ such that for all $0 < \delta < \bar{\delta}$ it holds

$$f_{\delta,x_0}(\Gamma_D) \subset \Omega, \tag{3.48}$$

where $f_{\delta,x_0}(x) = x_0 + (1-\delta)(x - x_0)$. The main difficulty in proving Γ-convergence in the presence of Dirichlet boundary conditions consists in proving the lim sup inequality. Following the strategy in [CC19, Theorem 5.5], for a given $\mathbf{u} \in GSBD^2(\Omega;\mathbb{R}^n)$ and for every $\eta > 0$ we find $\mathbf{u}^\eta \in SBV^2(\Omega;\mathbb{R}^n) \cap L^\infty(\Omega;\mathbb{R}^n)$ such that $\mathbf{u}^\eta = \mathbf{u}_D$ in the intersection of $\overline{\Omega}$ with an n-dimensional neighborhood of Γ_D and such that

$$E(\mathbf{u}^\eta, 1) < E(\mathbf{u}, 1) + \eta.$$

To obtain the required function $\mathbf{u}^\eta$, according to [CC19, Theorem 5.5] the first step consists in suitably extending $\mathbf{u}$ outside of Ω. Indeed, the main idea is to extend $\mathbf{u}$ by $\mathbf{u}_D$ in the intersection of $\mathbb{R}^n \setminus \Omega$ with an n-dimensional neighborhood of Γ_D, while across the Neumann part Γ_N of the boundary $\partial\Omega$ a suitable reflection argument is used. The key ingredient to control the energy of the reflection is [CC19, Lemma 2.8], that we recall here for the reader's convenience.

Lemma 3.2.6:
For any open rectangle $R \subset \mathbb{R}^n$ let R' be its reflection with respect to one face F of R and let $\widehat{R} = R \cup F \cup R'$. Suppose that $\mathbf{v} \in GSBD^2(R;\mathbb{R}^n)$. Then we can extend $\mathbf{v}$ to a function $\widehat{\mathbf{v}} \in GSBD^2\left(\widehat{R};\mathbb{R}^n\right)$ such that

$$\mathcal{H}^{n-1}(J_{\widehat{\mathbf{v}}} \cap F) = 0, \tag{3.49}$$

$$\mathcal{H}^{n-1}(J_{\widehat{\mathbf{v}}}) \leq c\,\mathcal{H}^{n-1}(J_{\mathbf{v}}) \quad \text{and} \tag{3.50}$$

$$\int_{\widehat{R}} |e(\widehat{\mathbf{v}})|^2 \,\mathrm{dx} \leq c \int_R |e(\mathbf{v})|^2 \,\mathrm{dx}, \tag{3.51}$$

where $c > 0$ is a suitable constant independent of R and $\mathbf{v}$.

Remark: Suppose that in Lemma 3.2.6 the function $\mathbf{v}$ belongs to $GSBD^2(R;\mathbb{R}^n) \cap L^1(R;\mathbb{R}^n)$. Then, recalling the construction of $\widehat{\mathbf{v}}$ in the proof of [CC19, Lemma 2.8] it can easily be shown

that $\hat{\mathbf{v}} \in GSBD^2\left(\widehat{R};\mathbb{R}^n\right) \cap L^1\left(\widehat{R};\mathbb{R}^n\right)$ and that in addition to equation (3.49) it holds

$$\int_{\widehat{R}} |\hat{\mathbf{v}}| \,\mathrm{dx} \leq c \int_{R} |\mathbf{v}| \,\mathrm{dx}\,. \tag{3.52}$$

We are now in the position to prove the following result.

Theorem 3.2.7:
Let E_ε and E be as in equations (3.27) and (3.28). Then the functionals E_ε Γ-converge with respect to convergence in $L^1(\Omega;\mathbb{R}^n) \times L^1(\Omega)$ to the functional E.

Proof. The proof follows the lines of [CC19, Theorem 5.5]. The main work in proving Theorem 3.2.7 lies in the restriction of the energy functionals to spaces satisfying the boundary conditions.

The first step consists in proving the lim inf inequality. To this end, let $(\mathbf{u}_\varepsilon, \varphi_\varepsilon) \subset L^1(\Omega;\mathbb{R}^n) \times L^1(\Omega)$ be a sequence converging in $L^1(\Omega;\mathbb{R}^n) \times L^1(\Omega)$ to a pair $(\mathbf{u}, \varphi)$ such that

$$\sup_{\varepsilon>0} E_\varepsilon(\mathbf{u}_\varepsilon, \varphi_\varepsilon) < +\infty. \tag{3.53}$$

Thanks to Lemma 3.2.3, equation (3.53) immediately implies that $\varphi = 1$ holds $\mathcal{L}^n$-a. e. in Ω and as in the proof of Theorem 3.2.4 we deduce $\mathbf{u} \in GSBD^2(\Omega;\mathbb{R}^n)$. Moreover, equation (3.53) implies that $\operatorname{tr}\mathbf{u}_\varepsilon = \operatorname{tr}\mathbf{u}_D$ and $\operatorname{tr}\varphi_\varepsilon = 1$ on Γ_D. Let us now choose $\widetilde{\Omega} \subset \mathbb{R}^n$ open, bounded and with Lipschitz-boundary such that $\Omega \subset \widetilde{\Omega}$ and $\widetilde{\Omega} \cap \partial\Omega = \Gamma_D$. Then, thanks to the boundary conditions satisfied by $\mathbf{u}_\varepsilon$ and φ_ε, the functions $\widetilde{\mathbf{u}}_\varepsilon$, $\widetilde{\varphi}_\varepsilon$ defined as

$$\widetilde{\mathbf{u}}_\varepsilon := \begin{cases} \mathbf{u}_\varepsilon & \text{in } \Omega, \\ \mathbf{u}_D & \text{in } \widetilde{\Omega}\setminus\Omega \end{cases} \quad \text{and} \quad \widetilde{\varphi}_\varepsilon := \begin{cases} \varphi_\varepsilon & \text{in } \Omega, \\ 1 & \text{in } \widetilde{\Omega}\setminus\Omega, \end{cases}$$

belong to $H^1\left(\widetilde{\Omega};\mathbb{R}^n\right)$ and $H^1\left(\widetilde{\Omega}\right)$, respectively. Moreover, as $\varepsilon \to 0$ the sequence $(\widetilde{\mathbf{u}}_\varepsilon, \widetilde{\varphi}_\varepsilon)$ converges in $L^1\left(\widetilde{\Omega};\mathbb{R}^n\right) \times L^1\left(\widetilde{\Omega}\right)$ to the pair $(\widetilde{\mathbf{u}}, 1)$, where

$$\widetilde{\mathbf{u}} := \begin{cases} \mathbf{u} & \text{in } \Omega, \\ \mathbf{u}_D & \text{in } \widetilde{\Omega}\setminus\Omega. \end{cases}$$

Since $\mathbf{u} \in GSBD^2(\Omega;\mathbb{R}^n)$ and $\mathbf{u}_D \in H^1(\mathbb{R}^n;\mathbb{R}^n)$, we have $\widetilde{\mathbf{u}} \in GSBD^2\left(\widetilde{\Omega};\mathbb{R}^n\right)$. Thus, from Theorem 3.2.4 we deduce that

$$\liminf_{\varepsilon\to 0} D_\varepsilon\left(\widetilde{\mathbf{u}}_\varepsilon, \widetilde{\varphi}_\varepsilon; \widetilde{\Omega}\right) \geq D\left(\widetilde{\mathbf{u}}, 1; \widetilde{\Omega}\right).$$

Recalling $\lim_{\varepsilon\to 0} k_\varepsilon = 0$ we can prove the lim inf inequality as follows,

$$\begin{aligned}
&\liminf_{\varepsilon\to 0} E_\varepsilon(\mathbf{u}_\varepsilon, \varphi_\varepsilon)\\
&\quad\geq \liminf_{\varepsilon\to 0} D_\varepsilon(\mathbf{u}_\varepsilon, \varphi_\varepsilon)\\
&\quad= \liminf_{\varepsilon\to 0} D_\varepsilon\left(\widetilde{\mathbf{u}}_\varepsilon, \widetilde{\varphi}_\varepsilon; \widetilde{\Omega}\right) - \int_{\overline{\Omega}\setminus\Omega} \frac{1}{2} e(\mathbf{u}_D) : \mathbb{C}e(\mathbf{u}_D) + (1-\alpha)\, p\nabla\cdot\mathbf{u}_D + \nabla p\cdot\mathbf{u}_D \,\mathrm{dx}\\
&\quad\geq D\left(\widetilde{\mathbf{u}}, 1; \widetilde{\Omega}\right) - \int_{\overline{\Omega}\setminus\Omega} \frac{1}{2} e(\mathbf{u}_D) : \mathbb{C}e(\mathbf{u}_D) + (1-\alpha)\, p\nabla\cdot\mathbf{u}_D + \nabla p\cdot\mathbf{u}_D \,\mathrm{dx}\\
&\quad= D(\mathbf{u}, 1) + G_c\mathcal{H}^{n-1}\left(\Gamma_D \cap \{\operatorname{tr}\mathbf{u} \neq \operatorname{tr}\mathbf{u}_D\}\right)\\
&\quad= E(\mathbf{u}, 1).
\end{aligned}$$

It remains to prove the Γ-lim sup inequality. To this end, let $\mathbf{u} \in GSBD^2(\Omega;\mathbb{R}^n) \cap L^1(\Omega;\mathbb{R}^n)$ and let $\eta > 0$ be arbitrary. Suppose we can construct a function $\mathbf{u}^\eta \in SBV^2(\Omega;\mathbb{R}^n) \cap L^\infty(\Omega;\mathbb{R}^n)$ such that $\mathbf{u}^\eta = \mathbf{u}_D$ in the intersection of $\overline{\Omega}$ with an n-dimensional neighborhood of Γ_D and it holds

$$\lim_{\eta\to 0} \|\mathbf{u}^\eta - \mathbf{u}\|_{L^1(\Omega;\mathbb{R}^n)} = 0 \tag{3.54}$$

$$\text{and } E(\mathbf{u}, 1) + \eta > E(\mathbf{u}^\eta, 1). \tag{3.55}$$

Then for every fixed $\eta > 0$ we could apply the construction in the proof of Theorem 3.2.5 to $\mathbf{u}^\eta$ and obtain sequences $(\mathbf{u}_\varepsilon^\eta, \varphi_\varepsilon^\eta) \in L^1(\Omega;\mathbb{R}^n) \times L^1(\Omega)$ such that

$$\limsup_{\varepsilon\to 0} E_\varepsilon(\mathbf{u}_\varepsilon^\eta, \varphi_\varepsilon^\eta) \leq E(\mathbf{u}^\eta, 1) < E(\mathbf{u}, 1) + \eta.$$

Thus by a diagonal argument and the arbitrariness of η we could find an applicable recovery sequence.

What remains is to find a suitable function $\mathbf{u}^\eta$. To this end we employ the construction described in the proof of [CC19, Theorem 5.5]. We describe the main ideas how $\mathbf{u}^\eta$ is constructed and prove that it satisfies equation (3.55). For more details and the explicit construction we refer the interested reader to the original paper.

As mentioned before we want to extend $\mathbf{u}$ to the outside of Ω, more precisely to $\Omega_t = \Omega + B_t(0)$ with $t > 0$ small. Recall the notation $\Sigma = \partial\Gamma_N = \partial\Gamma_D$. As $\mathcal{H}^{n-2}(\Sigma) < +\infty$ for any $\varepsilon > 0$ we can find a neighborhood $\widetilde{\Sigma}$ of Σ, such that $\mathcal{H}^{n-1}\left(\widetilde{\Sigma} \cap \partial\Omega\right) < \varepsilon$ and $\mathcal{L}^n(\Sigma) < \varepsilon$. Subsequently we cover $\Gamma_N \setminus \widetilde{\Sigma}$ with finitely many cubes $(Q_h)_{h=1}^{\bar{h}}$ with side length ρ_h, center x_h and pairwise disjoint closure. For arbitrary $\varepsilon > 0$ the cubes Q_h can be constructed such that the following estimates

hold.

$$\begin{aligned}
&\mathcal{H}^{n-1}\left(\left(\Gamma_N \setminus \widetilde{\Sigma}\right) \setminus \bigcup_{h=1}^{\hbar} Q_h\right) < \varepsilon,\\
&\mathcal{H}^{n-1}\left(\left(\Gamma_N \setminus \widetilde{\Sigma}\right) \cap \overline{Q}_h\right) > (1-\varepsilon)\,(2\rho_h)^{n-1},\\
&\left(\Gamma_N \setminus \widetilde{\Sigma}\right) \cap \overline{Q}_h \subset \left\{x_h + \sum_{i=1}^{n-1} y_i b_{h,i} + y_n \nu_h : y_i \in (-\rho_h, \rho_h),\ y_n \in (-\varepsilon\rho_h, \varepsilon\rho_h)\right\}.
\end{aligned} \tag{3.56}$$

Here, ν_h denotes the generalized outer normal to Ω at x_h and $(b_{h,i})$ denotes an orthonormal basis of $(\nu_h)^{\perp}$. For details and the proofs of equation (3.56) we refer to the construction carried out in the proof of [CC19, Theroem 1.1]. As in the construction realized by Chambolle and Crismale we continue by defining the rectangles

$$\begin{aligned}
R_h &= \left\{x_h + \sum_{i=1}^{n-1} y_i b_{h,i} + y_n \nu_h : y_i \in (-\rho_h, \rho_h),\ y_n \in (-3\varepsilon\rho_h - t, -\varepsilon\rho_h)\right\},\\
R'_h &= \left\{x_h + \sum_{i=1}^{n-1} y_i b_{h,i} + y_n \nu_h : y_i \in (-\rho_h, \rho_h),\ y_n \in (-\varepsilon\rho_h, \varepsilon\rho_h + t)\right\}\\
\text{and } \widehat{R}_h &= \left\{x_h + \sum_{i=1}^{n-1} y_i b_{h,i} + y_n \nu_h : y_i \in (-\rho_h, \rho_h),\ y_n \in (-3\varepsilon\rho_h - t, \varepsilon\rho_h + t)\right\}.
\end{aligned}$$

Note that R_h, R'_h and $\widehat{R}_h$ satisfy the requirements of Lemma 3.2.6. Hence we obtain a function $\widehat{\mathbf{u}}_h$ satisfying

$$\int_{\widehat{R}_h} |e(\widehat{\mathbf{u}}_h)|^2 \,\mathrm{d}x \le c \int_{R_h} |e(\mathbf{u})|^2 \,\mathrm{d}x, \tag{3.57}$$

$$\mathcal{H}^{n-1}\left(J_{\widehat{\mathbf{u}}_h} \cap \widehat{R}_h\right) \le c\mathcal{H}^{n-1}\left(J_{\mathbf{u}} \cap R_h\right) \tag{3.58}$$

$$\text{and } \int_{\widehat{R}_h} |\widehat{\mathbf{u}}_h| \,\mathrm{d}x \le c \int_{R_h} |\mathbf{u}| \,\mathrm{d}x\,. \tag{3.59}$$

This procedure yields an extension of $\mathbf{u}$ across the Neumann boundary. We extend $\mathbf{u}$ by $\mathbf{u}_D$ across the Dirichlet boundary, thus defining

$$\widetilde{\mathbf{u}} = \begin{cases} \mathbf{u} & \text{in } \Omega \setminus \bigcup_{h=1}^{\hbar} R'_h \\ \widehat{\mathbf{u}}_h & \text{in } \widehat{R}_h \\ \mathbf{u}_D & \text{elsewhere in } \Omega_t. \end{cases}$$

Collecting the preceding estimates for $\widetilde{\mathbf{u}}$, Chambolle and Crismale [CC19] prove

$$F(\widetilde{\mathbf{u}}, 1; \Omega_t) < F(\mathbf{u}, 1) + G_c \mathcal{H}^{n-1}\left(\Gamma_D \cap \{\operatorname{tr}\mathbf{u} \neq \operatorname{tr}\mathbf{u}_D\}\right) + \eta. \tag{3.60}$$

Thus, for our purpose it suffices to notice that the same function $\widetilde{\mathbf{u}}$ also satisfies

$$\int_{\Omega_t} p\nabla\cdot\widetilde{\mathbf{u}}\,\mathrm{d}x < \int_{\Omega} p\nabla\cdot\mathbf{u}\,\mathrm{d}x+\eta \qquad \text{and} \qquad \int_{\Omega_t} \nabla p\cdot\widetilde{\mathbf{u}}\,\mathrm{d}x < \int_{\Omega} \nabla p\cdot\mathbf{u}\,\mathrm{d}x+\eta. \tag{3.61}$$

Indeed, it can easily be seen that the first inequality in (3.61) follows as in [CC19] from equation (3.57) together with Hölder's inequality, namely for t sufficiently small

$$\begin{aligned}\int_{\Omega_t\setminus\Omega} p\nabla\cdot\mathbf{u}_D\,\mathrm{d}x &\leq \sqrt{n}\|p\|_{L^\infty(\Omega_t\setminus\Omega)}\left(\mathcal{L}^n\left(\Omega_t\setminus\Omega\right)\right)^{\frac{1}{2}}\|e\left(\mathbf{u}_D\right)\|_{L^2(\Omega_t\setminus\Omega;\mathbb{R}^{n\times n})}\\ &< \eta\end{aligned}$$

and

$$\begin{aligned}\int_{\widehat{R_h}} p\nabla\cdot\widehat{\mathbf{u}}_h &\leq \sqrt{n}\|p\|_{L^\infty\left(\widehat{R}_h\right)}\left(\mathcal{L}^n\left(\widehat{R}_h\right)\right)^{\frac{1}{2}}\|e\left(\widehat{\mathbf{u}}_h\right)\|_{L^2\left(\widehat{R}_h;\mathbb{R}^{n\times n}\right)}\\ &\leq c\sqrt{n}\|p\|_{L^\infty\left(\widehat{R}_h\right)}\left(\mathcal{L}^n\left(R_h\right)\right)^{\frac{1}{2}}\|e\left(\mathbf{u}\right)\|_{L^2\left(R_h;\mathbb{R}^{n\times n}\right)}\\ &< \eta.\end{aligned}$$

The second inequality in (3.61) follows from equation (3.59) together with the absolute continuity of the Lebesgue integral, keeping in mind that in our case $\mathbf{u}\in L^1\left(\Omega;\mathbb{R}^n\right)$ and hence $\widetilde{\mathbf{u}}\in L^1\left(\Omega_t;\mathbb{R}^n\right)$. Thus $\widetilde{\mathbf{u}}$ fulfills

$$E\left(\widetilde{\mathbf{u}},1;\Omega_t\right) < E\left(\mathbf{u},1\right)+\eta. \tag{3.62}$$

Moreover, we observe that $\|\widetilde{\mathbf{u}}-\mathbf{u}\|_{L^1(\Omega;\mathbb{R}^n)}<\eta$ for t sufficiently small.

As in [CC19] we shift the constructed $\widetilde{\mathbf{u}}$ slightly, thus ensuring that it satisfies the Dirichlet boundary condition. Namely we define

$$\widetilde{\mathbf{u}}^\delta = \widetilde{\mathbf{u}}\circ\left(f_{\delta,x_0}\right)^{-1}+\mathbf{u}_D-\mathbf{u}_D\circ\left(f_{\delta,x_0}\right)^{-1},$$

which for δ sufficiently small coincides with $\mathbf{u}_D$ in a neighborhood of Γ_D thanks to assumption (3.48). Note that for δ sufficiently small we have

$$\begin{aligned}\int_{\Omega}\left|\widetilde{\mathbf{u}}-\widetilde{\mathbf{u}}^\delta\right|\mathrm{d}x &\leq \int_{\Omega}\left|\widetilde{\mathbf{u}}-\widetilde{\mathbf{u}}\circ\left(f_{\delta,x_0}\right)^{-1}\right|\mathrm{d}x+\int_{\Omega}\left|\mathbf{u}_D-\mathbf{u}_D\circ\left(f_{\delta,x_0}\right)^{-1}\right|\mathrm{d}x\\ &= \int_{\Omega}\left|\widetilde{\mathbf{u}}\right|(x)-\widetilde{\mathbf{u}}\left(\frac{x-\delta x_0}{1-\delta}\right)\mathrm{d}x+\int_{\Omega}\left|\mathbf{u}_D(x)-\mathbf{u}_D\left(\frac{x-\delta x_0}{1-\delta}\right)\right|\mathrm{d}x<\eta.\end{aligned} \tag{3.63}$$

In fact, since $\widetilde{\mathbf{u}},\mathbf{u}_D\in L^1\left(\Omega_t;\mathbb{R}^n\right)$ and $\left(f_{\delta,x_0}\right)^{-1}(\Omega)\subset\Omega_t$ for δ sufficiently small, we obtain equation (3.63) by approximating $\widetilde{\mathbf{u}}$ and $\mathbf{u}_D$ by $\mathcal{C}_c\left(\Omega_t;\mathbb{R}^n\right)$-functions, exploiting their continuity. Anal-

ogously, we get

$$\begin{aligned}
&\int_\Omega \left|e\left(\widetilde{\mathbf{u}}\right)-e\left(\widetilde{\mathbf{u}}^\delta\right)\right|^2 \mathrm{d}x \\
&\quad\leq 2\int_\Omega \left|e\left(\widetilde{\mathbf{u}}\right)-e\left(\widetilde{\mathbf{u}}\circ\left(f_{\delta,x_0}\right)^{-1}\right)\right|^2 \mathrm{d}x+2\int_\Omega \left|e\left(\mathbf{u}_D\right)-e\left(\mathbf{u}_D\circ\left(f_{\delta,x_0}\right)^{-1}\right)\right|^2 \mathrm{d}x \\
&\quad= 2\int_\Omega \left|e\left(\widetilde{\mathbf{u}}(x)\right)-e\left(\widetilde{\mathbf{u}}\left(\frac{x-\delta x_0}{1-\delta}\right)\right)\right|^2 \mathrm{d}x+2\int_\Omega \left|e\left(\mathbf{u}_D(x)\right)-e\left(\mathbf{u}_D\left(\frac{x-\delta x_0}{1-\delta}\right)\right)\right|^2 \mathrm{d}x \\
&\quad<\eta,
\end{aligned} \tag{3.64}$$

for δ sufficiently small (see also [CC19, Theorem 5.5]). As in [CC19], from equation (3.64) we deduce that

$$F\left(\widetilde{\mathbf{u}}^\delta,1\right)<F\left(\widetilde{\mathbf{u}},1;\Omega_t\right)+\eta.$$

Then, thanks to equation (3.63) we also obtain $E\left(\widetilde{\mathbf{u}}^\delta,1\right)<E\left(\widetilde{\mathbf{u}},1;\Omega_t\right)+\eta$, which together with equation (3.62) yields

$$E\left(\widetilde{\mathbf{u}}^\delta,1\right)<E\left(\mathbf{u},1\right)+\eta. \tag{3.65}$$

Finally, the required function $\mathbf{u}^\eta$ is obtained by suitably regularizing $\widetilde{\mathbf{u}}^\delta$ using the construction of the proof of [CC19, Theorem 1.1]. As $\widetilde{\mathbf{u}}^\delta=\mathbf{u}_D$ in a neighborhood U of Γ_D, its approximating functions $\widetilde{\mathbf{u}}_k^\delta$ constructed as in [CC19, Theorem 1.1] satisfy $\widetilde{\mathbf{u}}_k^\delta=\mathbf{u}_D*\rho_k$ in U. Thus we define the final approximating functions as $\mathbf{u}^\eta=\widetilde{\mathbf{u}}_k^\delta+\mathbf{u}_D-\mathbf{u}_D*\rho_k$, where k depends on η. These functions obviously fulfill the Dirichlet boundary condition in U. Further, as $\lim_{k\to+\infty}\|\mathbf{u}_D-\mathbf{u}_D*\rho_k\|_{H^1(\mathbb{R}^n;\mathbb{R}^n)}=0$ we can ensure that $\|\mathbf{u}^\eta-\mathbf{u}\|_{L^1(\Omega;\mathbb{R}^n)}$ and $E\left(\mathbf{u}^\eta,1\right)<E\left(\widetilde{\mathbf{u}}^\delta,1\right)+\eta$ by exploiting the approximation properties of [CC19, Theorem 1.1] and proceeding as in the proof of Theorem 3.2.5. Thus, together with equation (3.65), we obtain equation (3.55). □

3.3 Convergence of minimizers

As mentioned in the preliminaries, the main application of Γ-convergence is the study of the asymptotic behavior of minimizers for energy minimizing problems. In fact, assume we can show that a sequence of minimizers $(\mathbf{u}_\varepsilon,\varphi_\varepsilon)$ for E_ε converges in $L^1\left(\Omega;\mathbb{R}^n\right)\times L^1\left(\Omega\right)$ to $(\mathbf{u},1)$, with $\mathbf{u}\in GSBD^2\left(\Omega;\mathbb{R}^n\right)$ a minimizer of E. This would imply that by solving the numerically well-posed problem $\min E_\varepsilon$ for a small $\varepsilon>0$, we obtain a good approximation of the desired minimizer for E. According to Theorem 2.3.6 we need to prove equi-coercivity of E_ε with respect to the strong $L^1\left(\Omega;\mathbb{R}^n\right)\times L^1\left(\Omega\right)$ topology, in addition to Theorem 3.2.7, to obtain convergence of minimizers. Recalling Definition 2.3.5, to this end it suffices to show compactness of sequences $(\mathbf{u}_\varepsilon,\varphi_\varepsilon)\subset L^1\left(\Omega;\mathbb{R}^n\right)\times L^1\left(\Omega\right)$ satisfying $\sup_{\varepsilon>0}E_\varepsilon\left(\mathbf{u}_\varepsilon,\varphi_\varepsilon\right)<+\infty$. Unfortunately, to our knowledge the equi-coercivity in the strong $L^1\left(\Omega;\mathbb{R}^n\right)\times L^1\left(\Omega\right)$ topology for the functionals that we considered in

this paper cannot be proven without additional assumptions. See for example the introduction of [CC19] for a discussion of the simpler case of F_ε without pressure terms. The aim of the present section is to discuss under which assumptions one gains compactness.

In the case without pressure terms a frequently chosen approach is described for example in the aforementioned paper and also in [Iur14]. It consists of perturbing the functionals F_ε by adding what is known as a fidelity term, namely $\int_\Omega |\mathbf{u}-\mathbf{g}|^2 \,\mathrm{dx}$ with $\mathbf{g} \in L^2(\Omega;\mathbb{R}^n)$. This term is also present in the Mumford-Shah functional and its approximation according to Ambrosio and Tortorelli, see equations (2.11) and (2.12). In the context of image segmentation, the fidelity term forces the reconstruction u of an input image g to take values close to g. At the same time it guarantees the equi-coercivity of AT_ε. Also the functionals $F_\varepsilon^{\mathbf{g}}$ defined as

$$F_\varepsilon^{\mathbf{g}}(\mathbf{u},\varphi) = F_\varepsilon(\mathbf{u},\varphi) + \int_\Omega |\mathbf{u}-\mathbf{g}|^2 \,\mathrm{dx},$$

with $\mathbf{g} \in L^2(\Omega;\mathbb{R}^n)$ are equi-coercive in the strong $L^1(\Omega;\mathbb{R}^n) \times L^1(\Omega)$ topology, for a proof of this fact see [Iur14, Proposition 1]. This leads us to consider the perturbed functionals $D_\varepsilon^{\mathbf{g}}$ defined as

$$D_\varepsilon^{\mathbf{g}}(\mathbf{u},\varphi) = D_\varepsilon(\mathbf{u},\varphi) + \int_\Omega |\mathbf{u}-\mathbf{g}|^2 \,\mathrm{dx},$$

with Γ-limit $D^{\mathbf{g}}(\mathbf{u},\varphi) = D(\mathbf{u},\varphi) + \int_\Omega |\mathbf{u}-\mathbf{g}|^2 \,\mathrm{dt}$. Note that while this approach is customary, the fidelity term and the function $\mathbf{g}$ have no physical meaning in the context of fracture propagation, thus rendering it somewhat artificial. The main result of this section is the following theorem.

Theorem 3.3.1:
Let $\mathbf{g} \in L^2(\Omega;\mathbb{R}^n)$ and let $D_\varepsilon^{\mathbf{g}}$ and $D^{\mathbf{g}}$ be given as above. Further for any given $\varepsilon > 0$ let $(\mathbf{u}_\varepsilon, \varphi_\varepsilon)$ be a solution of the minimization problem

$$m_\varepsilon = \min\left\{ D_\varepsilon^{\mathbf{g}}(\mathbf{u},\varphi) : (\mathbf{u},\varphi) \in L^1(\Omega;\mathbb{R}^n) \times L^1(\Omega) \right\}.$$

Then, up to subsequences, the sequence $(\mathbf{u}_\varepsilon, \varphi_\varepsilon)$ converges in $L^1(\Omega;\mathbb{R}^n) \times L^1(\Omega)$ to a pair $(\widetilde{\mathbf{u}}, \widetilde{\varphi})$ with $\widetilde{\mathbf{u}} \in GSBD^2(\Omega;\mathbb{R}^n) \cap L^2(\Omega;\mathbb{R}^n)$ being a solution to the problem

$$m = \min\left\{ D^{\mathbf{g}}(\mathbf{u},1) : \mathbf{u} \in GSBD^2(\Omega;\mathbb{R}^n) \right\}.$$

Finally, $m_\varepsilon \to m$ as $\varepsilon \to 0$.

In order to prove Theorem 3.3.1 we show some intermediate results in Propositions 3.3.2 to 3.3.4. In a first step we prove Γ-convergence of the functionals $D_\varepsilon^{\mathbf{g}}$ to $D^{\mathbf{g}}$.

Proposition 3.3.2:
Let $G_c > 0$, $p \in W^{1,\infty}(\Omega)$, $0 \le \alpha \le 1$ and $k_\varepsilon \in o(\varepsilon)$. Further let $\mathbb{C}$ be the linear elasticity tensor as in (2.1) with $\mu, \lambda > 0$ and let $\mathbf{g} \in L^2(\Omega;\mathbb{R}^n)$. Then $D_\varepsilon^{\mathbf{g}}$ Γ-converges for $\varepsilon \to 0^+$ to $D^{\mathbf{g}}$ with respect to strong convergence in $L^1(\Omega;\mathbb{R}^n) \times L^1(\Omega)$.

Proof. We begin by proving the Γ-liminf inequality. Let $(\mathbf{u}_\varepsilon, \varphi_\varepsilon) \in L^1(\Omega;\mathbb{R}^n) \times L^1(\Omega)$ be a sequence converging to $(\mathbf{u}, \varphi) \in GSBD^2(\Omega;\mathbb{R}^n) \times \mathcal{V}$. Then Theorem 3.2.2 and Fatou's lemma imply

$$\begin{aligned}\liminf_{\varepsilon\to 0} D_\varepsilon^{\mathbf{g}}(\mathbf{u}_\varepsilon, \varphi_\varepsilon) &\geq \liminf_{\varepsilon\to 0} E_\varepsilon(\mathbf{u}_\varepsilon, \varphi_\varepsilon) + \liminf_{\varepsilon\to 0} \int_\Omega |\mathbf{u}_\varepsilon - \mathbf{g}|^2 \,\mathrm{d}x \\ &\geq E(\mathbf{u}, \varphi) + \int_\Omega \liminf_{\varepsilon\to 0} |\mathbf{u}_\varepsilon - \mathbf{g}|^2 \,\mathrm{d}x \\ &\geq D^{\mathbf{g}}(\mathbf{u}, \varphi).\end{aligned}$$

For the Γ-limsup inequality suppose without loss of generality that $(\mathbf{u}, \varphi)$ satisfies $D^{\mathbf{g}}(\mathbf{u}, \varphi) < +\infty$. Recalling Lemma 3.2.3 we obtain the bounds $D(\mathbf{u}, \varphi) < +\infty$ and $\int_\Omega |\mathbf{u} - \mathbf{g}|^2 \,\mathrm{d}x < +\infty$. In particular the domain of the Γ-limit reduces to the space $\mathbf{u} \in GSBD^2(\Omega;\mathbb{R}^n) \cap L^2(\Omega;\mathbb{R}^n)$. Applying the density results 2.4.26 and 2.4.15 hence yields a sequence $\mathbf{u}_\jmath \in \mathcal{W}(\Omega;\mathbb{R}^n)$ satisfying $\lim_{\jmath\to+\infty} D(\mathbf{u}_\jmath, \varphi) = D(\mathbf{u}, \varphi)$ as in Step 1 of the proof of Theorem 3.2.5. In addition $\lim_{\jmath\to+\infty} \|\mathbf{u}_\jmath - \mathbf{u}\|_{L^2(\Omega;\mathbb{R}^n)} = 0$ is guaranteed. The obtained convergence with respect to $L^2(\Omega;\mathbb{R}^n)$ finally implies convergence of the fidelity term and thus

$$\lim_{\jmath\to+\infty} D^{\mathbf{g}}(\mathbf{u}_\jmath, \varphi) = D^{\mathbf{g}}(\mathbf{u}, \varphi).$$

Hence it suffices to construct a recovery sequence for any given $(\mathbf{u}_\jmath, \varphi) \in \mathcal{W}(\Omega;\mathbb{R}^n) \times \mathcal{V}$. Taking the sequence $\mathbf{u}_\varepsilon$ as in Step 2 of the proof of Theorem 3.2.5 we notice that $\lim_{\varepsilon\to 0} \|\mathbf{u}_\varepsilon - \mathbf{u}_\jmath\|_{L^2(\Omega;\mathbb{R}^n)} = 0$. This implies $\lim_{\varepsilon\to 0} \int_\Omega |\mathbf{u}_\varepsilon - \mathbf{g}|^2 \,\mathrm{d}x = \int_\Omega |\mathbf{u}_\jmath - \mathbf{g}|^2 \,\mathrm{d}x$ and thus the Γ-limsup inequality is proven. □

Next, we show equi-coercivity of the functionals $D_\varepsilon^{\mathbf{g}}$.

Proposition 3.3.3:
Let $\mathbf{g} \in L^2(\Omega;\mathbb{R}^n)$. Further suppose that $(\mathbf{u}_\varepsilon, \varphi_\varepsilon) \in L^1(\Omega;\mathbb{R}^n) \times L^1(\Omega)$ is a sequence satisfying $\sup_{\varepsilon>0} D_\varepsilon^{\mathbf{g}}(\mathbf{u}_\varepsilon, \varphi_\varepsilon) < +\infty$. Then there exists $\mathbf{u} \in GSBD^2(\Omega;\mathbb{R}^n) \cap L^2(\Omega;\mathbb{R}^n)$ such that $\varphi_\varepsilon \to 1$ in $L^1(\Omega)$ and, up to subsequences, $\mathbf{u}_\varepsilon \to \mathbf{u}$ in $L^1(\Omega;\mathbb{R}^n)$.

Proof. Suppose $(\mathbf{u}_\varepsilon, \varphi_\varepsilon) \in L^1(\Omega;\mathbb{R}^n) \times L^1(\Omega)$ satisfies $\sup_{\varepsilon>0} D_\varepsilon^{\mathbf{g}}(\mathbf{u}_\varepsilon, \varphi_\varepsilon) < +\infty$. Then Lemma 3.2.3 and an additional application of Young's inequality imply

$$\begin{aligned}D_\varepsilon^{\mathbf{g}}(\mathbf{u}_\varepsilon, \varphi_\varepsilon) &\geq c_1 F_\varepsilon^{\mathbf{g}}(\mathbf{u}_\varepsilon, \varphi_\varepsilon) - c_2\|\mathbf{u}_\varepsilon\|_{L^1(\Omega;\mathbb{R}^n)} - c_3 + \int_\Omega |\mathbf{u}_\varepsilon - \mathbf{g}|^2 \,\mathrm{d}x \\ &\geq c_1 F_\varepsilon^{\mathbf{g}}(\mathbf{u}_\varepsilon, \varphi_\varepsilon) - \frac{c_2^2}{2} - \frac{1}{2}\|\mathbf{u}_\varepsilon - g\|_{L^2(\Omega;\mathbb{R}^n)}^2 - c + \int_\Omega |\mathbf{u}_\varepsilon - \mathbf{g}|^2 \,\mathrm{d}x \\ &\geq c_1 F_\varepsilon^{\mathbf{g}}(\mathbf{u}_\varepsilon, \varphi_\varepsilon) + \frac{1}{2}\int_\Omega |\mathbf{u}_\varepsilon - \mathbf{g}|^2 \,\mathrm{d}x - c.\end{aligned} \tag{3.66}$$

Thus $\sup_{\varepsilon>0} F_\varepsilon^{\mathbf{g}}(\mathbf{u}_\varepsilon, \varphi_\varepsilon) < +\infty$ and the result follows directly from [Iur14, Proposition 1]. □

Finally, let us show the existence of minimizers for the approximative energy $D_\varepsilon^{\mathbf{g}}$ for fixed $\varepsilon > 0$.

Proposition 3.3.4:
Let $\varepsilon > 0$ be fixed and $\mathbf{g} \in L^2(\Omega;\mathbb{R}^n)$. Then the minimizing problem

$$m_\varepsilon = \min\left\{D_\varepsilon^{\mathbf{g}}(\mathbf{u},\varphi) : (\mathbf{u},\varphi) \in L^1(\Omega;\mathbb{R}^n) \times L^1(\Omega)\right\} \tag{3.67}$$

admits a solution $(\mathbf{u}_\varepsilon, \varphi_\varepsilon)$.

Proof. We prove the theorem applying the direct method of the calculus of variations. Let $(\mathbf{u}_\jmath, \varphi_\jmath) \in L^1(\Omega;\mathbb{R}^n) \times L^1(\Omega)$ be a minimizing sequence for equation (3.67). Proceeding as in estimate (3.66) we obtain

$$\sup_\jmath \left(\int_\Omega (\varphi_\jmath + k_\varepsilon)^2 e(\mathbf{u}_\jmath) : \mathbb{C}e(\mathbf{u}_\jmath)\,\mathrm{dx} + \int_\Omega \frac{(1-\varphi_\jmath)^2}{\varepsilon} + \varepsilon |\nabla \varphi_\jmath|^2\,\mathrm{dx} + \int_\Omega |\mathbf{u}_\jmath - \mathbf{g}|^2\,\mathrm{dx} \right) < +\infty.$$

Thus $\|e(\mathbf{u}_\jmath)\|_{L^2(\Omega;\mathbb{R}^{n\times n}_{sym})}$ and $\|\mathbf{u}_\jmath\|_{L^2(\Omega;\mathbb{R}^n)}$ are bounded uniformly. Hence by Korn's inequality $\mathbf{u}_\jmath$ is bounded in $H^1(\Omega;\mathbb{R}^n)$ and there exists a subsequence, not relabeled for convenience, weakly converging to some $\mathbf{u}_\varepsilon \in H^1(\Omega;\mathbb{R}^n)$. Moreover the subsequence can be chosen such that the convergence holds pointwise $\mathcal{L}^n$-a. e. in Ω. Further we obtain boundedness of $\varphi_\jmath$ in $H^1(\Omega)$. Taking another subsequence, not relabeled, provides us with some $\varphi_\varepsilon \in H^1(\Omega)$ such that $\varphi_\jmath \rightharpoonup \varphi_\varepsilon$ weakly in $H^1(\Omega)$ and $\varphi_\jmath \to \varphi_\varepsilon$ strongly in $L^2(\Omega)$. It remains to show

$$D_\varepsilon^{\mathbf{g}}(\mathbf{u}_\varepsilon, \varphi_\varepsilon) \le \liminf_{\jmath\to+\infty} D_\varepsilon^{\mathbf{g}}(\mathbf{u}_\jmath, \varphi_\jmath)\,. \tag{3.68}$$

Ioffe's theorem [AFP00, Theorem 5.8] implies

$$\int_\Omega (\varphi_\varepsilon + k_\varepsilon)^2 e(\mathbf{u}_\varepsilon) : \mathbb{C}e(\mathbf{u}_\varepsilon)\,\mathrm{dx} \le \liminf_{\jmath\to+\infty} \int_\Omega (\varphi_\jmath + k_\varepsilon)^2 e(\mathbf{u}_\jmath) : \mathbb{C}e(\mathbf{u}_\jmath)\,\mathrm{dx}\,. \tag{3.69}$$

Since the weak convergence of $\nabla\,\mathbf{u}_\jmath$ in $L^2(\Omega;\mathbb{R}^{n\times n})$ holds componentwise, we obtain $\nabla\cdot\mathbf{u}_\jmath \rightharpoonup \nabla\cdot\mathbf{u}_\varepsilon$ in $L^2(\Omega)$ and thus $\varphi_\jmath\mathbf{u}_\jmath \to \varphi_\varepsilon\mathbf{u}_\varepsilon$ strongly in $L^1(\Omega)$. Additionally it holds $\varphi_\jmath\mathbf{u}_\jmath \to \varphi_\varepsilon\mathbf{u}_\varepsilon$ strongly in $L^2(\Omega;\mathbb{R}^n)$. Thus we obtain convergence of the pressure terms, namely

$$\int_\Omega (1-\alpha)\varphi_\varepsilon p\nabla\cdot\mathbf{u}_\varepsilon + \varphi_\varepsilon \nabla p\mathbf{u}_\varepsilon\,\mathrm{dx} = \lim_{\jmath\to+\infty} \int_\Omega (1-\alpha)\varphi_\jmath p\nabla\cdot\mathbf{u}_\jmath + \varphi_\jmath \nabla p\mathbf{u}_\jmath\,\mathrm{dx}\,. \tag{3.70}$$

Further the convergence of $\varphi_\jmath$ implies

$$\int_\Omega \frac{(1-\varphi_\varepsilon)^2}{\varepsilon} + \varepsilon|\nabla\varphi_\varepsilon|^2\,\mathrm{dx} \le \liminf_{\jmath\to+\infty} \int_\Omega \frac{(1-\varphi_\jmath)^2}{\varepsilon} + \varepsilon|\nabla\varphi_\jmath|^2\,\mathrm{dx}\,. \tag{3.71}$$

Finally an application of Fatou's lemma for the fidelity term yields

$$\int_\Omega |\mathbf{u}_\varepsilon - \mathbf{g}|^2 \, \mathrm{dx} \leq \liminf_{j \to +\infty} \int_\Omega |\mathbf{u}_j - \mathbf{g}|^2 \, \mathrm{dx} \,. \tag{3.72}$$

Collecting equations (3.69) to (3.72) we obtain equation (3.68). □

Proof of Theorem 3.3.1. Thanks to Theorem 2.3.6, the result follows immediately from Propositions 3.3.2 to 3.3.4. □

Remark: Assuming that the pressure p is constant in space, in other words $\nabla p = 0$ holds $\mathcal{L}^n$-almost everywhere in Ω, it should be possible to prove the Γ-convergence results Theorems 3.2.2 and 3.2.7 with respect to the metric induced by the convergence in measure. As a consequence, it would be sufficient to prove compactness of a sequence of minimizers for E_ε with respect to this metric. In this case we could benefit from some recent development concerning the existence of minimizers in the context of the Dirichlet problem. Namely, in dimension 2 we could use the general compactness result of Friedrich and Solombrino [FS18, Theorem 6.1] and follow their strategy in [FS18, Theorem 6.2] to prove the existence of minimizers. Moreover there exists a very recent compactness result in arbitrary dimensions by Chambolle and Crismale [CC18, Theorem 1.1], based on which the authors also prove that minimizers of the Dirichlet problem related to F_ε converge in measure to a minimizer of the Dirichlet problem related to F. Following their argument it should then be possible to prove an analogous result for E_ε in the case where $\nabla p = 0$ holds $\mathcal{L}^n$-almost everywhere in Ω.

4 Numerical methods

4.1 Discretization

In this section we discuss how to discretize equation (2.13). Parts of it were already published in [ES17]. We start by including the constraints for the phase field into the equation. As we are interested in the quasi-static simulation, we can assume that we have the phase field and the solution given at a previous time step, namely $\varphi_{\text{previous}}$ and $\mathbf{u}_{\text{previous}}$. Assuming further that $0 \leq \varphi_{\text{previous}} \leq 1$ the constraints $0 \leq \varphi \leq 1$ and $\frac{\partial}{\partial t}\varphi \leq 0$ for the phase field translate to $0 \leq \varphi \leq \varphi_{\text{previous}}$. Thus by defining the obstacle function

$$\Phi(\varphi) = \begin{cases} 0 & 0 \leq \varphi \leq \varphi_{\text{previous}} \\ +\infty & \text{otherwise,} \end{cases}$$

equation (2.13) transforms to

Definition 4.1.1 (Approximative energy minimization problem)**:**
Find $\mathbf{u} \in H_D^1(\Omega; \mathbb{R}^n)$ *and* $\varphi \in H^1(\Omega)$ *such that*

$$\begin{aligned} E_\varepsilon(\mathbf{u}, \varphi) &= \min_{\mathbf{v},\psi} E_\varepsilon(\mathbf{v}, \psi) \\ &= \min_{\mathbf{v},\psi} \int_\Omega \frac{1}{2}\left(\psi^2 + k_\varepsilon\right) e(\mathbf{v}) : \mathbb{C}e(\mathbf{v}) + (1-\alpha)\,\psi p \nabla \cdot \mathbf{v} + \psi \nabla p \cdot \mathbf{v}\,\mathrm{dx} \\ &\quad - \int_{\Gamma_N} (\tau + p\nu) \cdot \mathbf{v}\,\mathrm{ds} - \int_{\Gamma_D} p\nu \cdot \mathbf{u}_D\,\mathrm{ds} + G_c \int_\Omega \frac{1}{2\varepsilon}(1-\psi)^2 + \frac{\varepsilon}{2}|\nabla\psi|^2\,\mathrm{dx} + \Phi(\psi). \end{aligned} \tag{4.1}$$

We solve the minimization problem using a fixed-point iteration scheme, similar to [MWW15b]. Therefore we first fix φ and minimize (4.1) with respect to $\mathbf{u}$ and then fix $\mathbf{u}$ and minimize (4.1) with respect to φ. This alternation is repeated until convergence is achieved. More precisely we stop the iteration if $|||\varphi - \varphi_{\text{previous}}||| \leq \rho$, where ρ is some threshold and $|||\cdot|||$ denotes the energy norm with respect to φ. In what follows we derive the discretizations for the two subproblems.

4.1.1 DG discretization of the displacement equation

Assume now that the phase field is fixed and we want to determine the minimum of equation (4.1) only with respect to the displacement. Taking free variations yields the following Euler-Lagrange equation.
Find $\mathbf{u} \in H_D^1(\Omega; \mathbb{R}^n)$ such that

$$0 = \int_\Omega \left(\varphi^2 + k_\varepsilon\right) e(\mathbf{u}) : \mathbb{C}e(\mathbf{v}) + (1-\alpha)\,\varphi p \nabla \cdot \mathbf{v} + \varphi \nabla p \cdot \mathbf{v}\,\mathrm{dx} - \int_{\Gamma_N} (\tau + p\nu) \cdot \mathbf{v}\,\mathrm{ds} \tag{4.2}$$

for all $\mathbf{v} \in V = H_0^1(\Omega; \mathbb{R}^n)$.

An existence and regularity result for an equation of this type is stated in [MWW15b]. The only difference lies in the slightly modified factor $\left((1-k)\,\varphi^2 + k\right)$ instead of $\left(\varphi^2 + k_\varepsilon\right)$. From the well-known regularity results in the absence of pressure, see [Cia88], they conclude $W^{2,r}$-regularity for some $r > 3$ away from the contact regions of Γ_D and Γ_N, provided the data p, τ, and φ are sufficiently smooth.

To solve equation (4.2) we use the unfitted discontinuous Galerkin method presented in Section 2.5.3. As the major terms in equation (4.2) stem from linear elasticity, the present section relies heavily on the SIPG discretization for the linear elasticity equation as given in [Riv08], see also [LNSO04]. The novelty lies in the treatment of the additional pressure terms. We first derive the fitted SIPG discretization here and then discuss the modifications to include unfitted elements in Section 4.1.3.

Separating the bilinear terms in equation (4.2) from the linear terms, equation (4.2) becomes

$$\int_\Omega \left(\varphi^2 + k_\varepsilon\right) e(\mathbf{u}) : \mathbb{C}e(\mathbf{v})\,\mathrm{dx} = -\int_\Omega (1-\alpha)\,\varphi p \nabla \cdot \mathbf{v} + \varphi \nabla p \cdot \mathbf{v}\,\mathrm{dx} \quad + \int_{\Gamma_N} (\tau + p\nu) \cdot \mathbf{v}\,\mathrm{ds}\,.$$

With the definitions and notation from Section 2.5, taking $V_h = \mathcal{P}_k(\mathcal{T})$ as in Section 2.5.2, the SIPG discretization of the bilinear form is given for all $(\mathbf{u}_h, \mathbf{v}_h) \in V_h \times V_h$ by

$$\begin{aligned} a_h^{DG}(\mathbf{u}_h, \mathbf{v}_h) = &\sum_{T \in \mathcal{T}} \left(\int_T \left(\varphi_h^2 + k_\varepsilon\right) e(\mathbf{u}_h) : \mathbb{C}e(\mathbf{v}_h)\,\mathrm{dx} \right) \\ &- \sum_{F \in \mathcal{F} \setminus \Gamma_N} \left(\int_F \left(\varphi_h^2 + k_\varepsilon\right) \left([\![\mathbf{u}_h]\!] \{\!\{\mathbb{C}e(\mathbf{v}_h) \cdot \nu\}\!\} + \{\!\{\mathbb{C}e(\mathbf{u}_h) \cdot \nu\}\!\} [\![\mathbf{v}_h]\!] \right) \mathrm{ds} \right) \\ &+ \sum_{F \in \mathcal{F} \setminus \Gamma_N} \frac{\eta}{h_F} \int_F \left(\varphi_h^2 + k_\varepsilon\right) \left([\![\mathbf{u}_h]\!] \cdot \nu \right) : \mathbb{C}\left([\![\mathbf{v}_h]\!] \cdot \nu \right) \mathrm{ds}\,. \end{aligned} \tag{4.3}$$

The SIPG discretization of the linear form is given for all $\mathbf{v}_h \in V_h$ by

$$\begin{aligned} F_h^{DG}(\mathbf{v}_h) = &- \sum_{T\in\mathcal{T}} \int_T (1-\alpha)\,\varphi_h p \nabla\cdot\mathbf{v}_h + \varphi_h \nabla p\cdot\mathbf{v}_h \,\mathrm{dx} \\ &+ \sum_{F\in\mathcal{F}_{ext}\cap\Gamma_N} \int_F (\tau + p\nu)\cdot\mathbf{v}_h \,\mathrm{ds} \\ &- \sum_{F\in\mathcal{F}_{ext}\cap\Gamma_D} \int_F \left(\varphi_h^2 + k_\varepsilon\right)\mathbf{u}_D \left\{\!\!\left\{\mathbb{C}e(\mathbf{v}_h)\cdot\nu\right\}\!\!\right\} \mathrm{ds} \\ &+ \sum_{F\in\mathcal{F}_{ext}\cap\Gamma_D} \frac{\eta}{h_F} \int_F \left(\varphi_h^2 + k_\varepsilon\right)(\mathbf{u}_D\cdot\nu) : \mathbb{C}\left(\left[\!\left[\mathbf{v}_h\right]\!\right]\cdot\nu\right) \mathrm{ds} \\ &+ \sum_{F\in\mathcal{F}_{int}} \int_F (1-\alpha)\,\varphi_h p \left[\!\left[\mathbf{v}_h\right]\!\right]\cdot\nu \,\mathrm{ds}\,. \end{aligned} \tag{4.4}$$

Note that, as we discuss in Section 4.1.2, φ_h is continuous, hence φ_h is well defined on any $F \in \mathcal{F}$. As in Definition 2.5.4 the normal ν is defined for the face, thus continuous as well. Hence the discrete elasticity problem can then be formulated as follows. Find $\mathbf{u}_h \in V_h$ such that

$$a_h^{DG}(\mathbf{u}_h, \mathbf{v}_h) = F_h^{DG}(\mathbf{v}_h) \qquad \forall\, \mathbf{v}_h \in V_h. \tag{4.5}$$

Note in particular the occurrence of the factor $\left(\varphi_h^2 + k_\varepsilon\right)$ in the stabilization term. Including this dependency on φ_h results in less penalty for discontinuous solutions along the crack. Thereby the connectivity assumptions are weakened.

In the remainder of this chapter we prove convergence of the discrete solution $\mathbf{u}_h$ of equation (4.5) to the corresponding weak solution $\mathbf{u}$, namely the solution of equation (4.2). For the analysis of the approximation error we assume additional regularity of the weak solution. Writing $V_* = H_D^1(\Omega;\mathbb{R}^n) \cap H^2(\Omega;\mathbb{R}^n)$ and $V_{h,*} = V_* + V_h$ we demand $\mathbf{u} \in V_*$, which is guaranteed for sufficiently nicely given data and boundary as for example in the setting of [MWW15b, Proposition 3]. Before stating the main result in Theorem 4.1.3 let us define some norms.

Definition 4.1.2 (Jump semi-norm, energy norms)**:**
Let $\mathbf{v}_h \in V_h$ and $\mathbf{v} \in V_{h,*}$, we define

$$\begin{aligned} |\mathbf{v}_h|_J^2 &= \sum_{F\in\mathcal{F}} \frac{1}{h_F} \|\left[\!\left[\mathbf{v}_h\right]\!\right]\|_{L^2(F)}^2, \\ |||\mathbf{v}_h|||^2 &= \|e(\mathbf{v}_h)\|_{L^2(\mathcal{T})}^2 + |\mathbf{v}_h|_J^2 \quad \textit{and} \\ |||\mathbf{v}|||_*^2 &= |||\mathbf{v}|||^2 + \sum_{T\in\mathcal{T}} h_T \|e\left(\mathbf{v}_{|T}\right)\cdot\mathbf{n}_T\|_{L^2(\partial T)}^2. \end{aligned}$$

Remark: Obviously the energy norm $|||\cdot|||$ satisfies the triangle inequality and absolute homogeneity. It also is positive definite:
$|||\mathbf{v}_h||| = 0$ implies $\|e(\mathbf{v}_h)\|_{L^2(\mathcal{T})} = 0$, hence using Korn's second inequality [Nit81] we get $\|\nabla\mathbf{v}_h\|_{L^2(\mathcal{T})} = 0$ and thus $\mathbf{v}_h$ is piecewise constant. In addition we have $\left[\!\left[\mathbf{v}_h\right]\!\right] = 0$ on all faces including the boundaries and thus $\mathbf{v}_h \equiv 0$ on Ω. This induces that $|||\cdot|||_*$ is a norm as well.

Theorem 4.1.3 (Approximation error for the displacement)**:**
Let $\mathbf{u} \in V_*$ be the solution of equation (4.2) and let $\mathbf{u}_h \in V_h$ be the solution of equation (4.5). Furthermore, let η be sufficiently large. Then we can find a constant $c > 0$ independent of the mesh size h such that

$$|||\mathbf{u} - \mathbf{u}_h||| \leq c \inf_{\mathbf{v}_h \in V_h} |||\mathbf{u} - \mathbf{v}_h|||_* .$$

In order to prove Theorem 4.1.3 we follow the usual path showing discrete coercivity, boundedness and consistency of the bilinear form a_h^{DG} in the subsequent lemmata.

Lemma 4.1.4 (Discrete coercivity of a_h^{DG})**:**
Let a_h^{DG} be as in equation (4.3) and let the Lamé coefficients satisfy $\mu > 0$ and $2\mu + n\lambda > 0$. Further let $\eta > 0$ be sufficiently large. Then there exists a constant $c > 0$ such that

$$a_h^{DG}(\mathbf{v}_h, \mathbf{v}_h) \geq \left(\varphi^2 + k\right)^{1/2} c |||\mathbf{v}_h||| \tag{4.6}$$

for all $\mathbf{v}_h \in V_h$.

Proof. As the bilinear form a_h^{DG} is independent of the pressure p, it only differs from the classical SIPG formulation for linear elasticity as in [Riv08] by the factor $\left(\varphi^2 + k\right)$. Thus, carrying out the standard proof in [Riv08, Lemma 5.2] for $\widetilde{\mathbf{v}}_h = \left(\varphi^2 + k\right)^{1/2} \mathbf{v}_h$ we obtain

$$a_h^{DG}(\mathbf{v}_h, \mathbf{v}_h) \geq c |||\widetilde{\mathbf{v}}_h|||$$

for some $c > 0$ and sufficiently large penalty parameter η. Linearity of the norm yields equation (4.6). □

Lemma 4.1.5 (Boundedness of a_h^{DG})**:**
Let a_h^{DG} be as in equation (4.3). Then there exists a constant $c > 0$, independent of h, such that for all $(\mathbf{v}, \mathbf{w}_h) \in V_{h,*} \times V_h$ it holds

$$\left|a_h^{DG}(\mathbf{v}, \mathbf{w}_h)\right| \leq c \|\left(\varphi^2 + k\right)\|_{L^\infty(\partial\Omega)} |||\mathbf{v}|||_* |||\mathbf{w}_h||| .$$

Proof. Boundedness of the bilinear form can be shown similarly to the proof in the case of the Poisson model equation [DPE12, Lemma 4.16]. We first note that analogous to [DPE12, Lemma 4.11] the consistency term satisfies the following bound:

$$\left|\sum_{F \in \mathcal{F}} \int_F \{\!\{\mathbb{C}e(\mathbf{v}) \cdot \nu_F\}\!\} [\![\mathbf{w}_h]\!] \, \mathrm{ds}\right| \leq \left(\sum_{T \in \mathcal{T}} \sum_{F \in \partial T} h_F \|\mathbb{C}e\left(\mathbf{v}_{|T}\right) \cdot \nu_F\|_{L^2(F)}^2\right)^{\frac{1}{2}} |\mathbf{w}_h|_J \tag{4.7}$$

$\forall (\mathbf{v}, \mathbf{w}_h) \in V_{h,*} \times V_{h,*}$.

Next, let $(\mathbf{v}, \mathbf{w}_h) \in V_{h,*} \times V_h$ be arbitrary and consider the following four terms separately

$$\begin{aligned}
\left|a_h^{DG}(\mathbf{v}, \mathbf{w}_h)\right| \leq & \left| \sum_{T \in \mathcal{T}} \int_T \left(\varphi^2 + k\right) e(\mathbf{v}) : \mathbb{C}e(\mathbf{w}_h) \, \mathrm{dx} \right| \\
& + \left| \sum_{F \in \mathcal{F} \setminus \Gamma_N} \int_F \left(\varphi^2 + k\right) [\![\mathbf{v}]\!] \, \{\!\{\mathbb{C}e(\mathbf{w}_h) \cdot \nu\}\!\} \, \mathrm{ds} \right| \\
& + \left| \sum_{F \in \mathcal{F} \setminus \Gamma_N} \int_F \left(\varphi^2 + k\right) \{\!\{\mathbb{C}e(\mathbf{v}) \cdot \nu\}\!\} \, [\![\mathbf{w}_h]\!] \, \mathrm{ds} \right| \\
& + \left| \sum_{F \in \mathcal{F} \setminus \Gamma_N} \frac{\eta}{h_F} \int_F \left(\varphi^2 + k\right) ([\![\mathbf{v}]\!] \nu \cdot) : \mathbb{C}\left([\![\mathbf{w}_h]\!] \cdot \nu\right) \mathrm{ds} \right| \\
= & \, I + \, II + \, III + \, IV \\
\forall (\mathbf{v}, \mathbf{w}_h) \in & \, V_* \times V_h.
\end{aligned}$$

The Cauchy-Schwarz inequality immediately implies

$$I + \, IV \leq (2\mu + n\lambda)(1 + \eta)(1 + k) \, |||\mathbf{v}|||_* \, \, |||\mathbf{w}_h||| \, ,$$

where we used $\varphi \leq 1$ and equation (2.2). For the third term we apply equation (4.7) to obtain

$$\begin{aligned}
III \leq & (1 + k) \left(\sum_{T \in \mathcal{T}} \sum_{F \in \partial T} h_F \|\mathbb{C}e\left(\mathbf{v}_{|T}\right) \cdot \nu_F\|_{L^2(F)}^2 \right)^{1/2} |\mathbf{w}_h|_J \\
\leq & (1 + k)(2\mu + n\lambda) \, |||\mathbf{v}|||_* \, |||\mathbf{w}_h||| \, .
\end{aligned}$$

To obtain a bound on the second term we apply equation (4.7) once again. Further we make use of the discrete trace inequality [DPE12, Lemma 1.46] which yields $h_T^{1/2} \|e(\mathbf{w}_h)\|_{L^2(F)} \leq c\|e(\mathbf{w}_h)\|_{L^2(T)}$. Thus

$$II \leq c(1 + k)(2\mu + n\lambda) \, \|e(\mathbf{w}_h)\|_{L^2(\Omega)} \, |\mathbf{v}|_J$$

and summation of all the terms finally yields

$$\left|a_h^{DG}(\mathbf{v}, \mathbf{w}_h)\right| \leq (2 + \eta + c)(1 + k)(2\mu + n\lambda) \, |||\mathbf{v}|||_* \, |||\mathbf{w}_h||| \, . \qquad \square$$

Let us now discuss consistency of the bilinear form. Usually consistency is considered with respect to the strong solution, showing that

$$a_h^{DG}(\mathbf{u}, \mathbf{v}_h) = F_h^{DG}(\mathbf{v}_h)$$

holds for all $\mathbf{v}_h \in V_h$ and for the strong solution $\mathbf{u}$ solving equation (2.4). Unfortunately due to the Γ-convergence we cannot hope to find such a conclusion. After all we are no longer solving

the same problem but merely an approximation of it. What we can hope for is consistency with a weak solution, namely the solution of equation (4.2). This turns out to be true and guarantees the following Galerkin orthogonality.

Lemma 4.1.6 (Galerkin orthogonality for a_h^{DG})**:**
Let $\mathbf{u}$ *be the solution of equation* (4.2) *and assume* $\mathbf{u} \in V_*$*. Then it holds*

$$a_h^{DG}(\mathbf{u}, \mathbf{v}_h) = F_h^{DG}(\mathbf{v}_h)$$

for all $\mathbf{v}_h \in V_h$*. In other words* $a_h^{DG}(\mathbf{u} - \mathbf{u}_h, \mathbf{v}_h) = 0$ *for all* $\mathbf{v}_h \in V_h$*.*

Proof. The main idea for proving consistency of the discrete formulation with the weak equation is integration by parts. More precisely we integrate the weak formulation by parts on the domain Ω and then reverse this integration, but this time on the individual elements $T \in \mathcal{T}$. Therefore let us consider the bilinear term.

$$\begin{aligned}
&\int_\Omega \left(\varphi^2 + k_\varepsilon\right) e(\mathbf{u}) : e(\mathbf{v}_h)\,\mathrm{dx} \\
&\quad= \int_{\partial\Omega} \left(\varphi^2 + k_\varepsilon\right) (\mathbb{C}e(\mathbf{u}) \cdot \nu) \cdot \mathbf{v}_h\,\mathrm{ds} - \int_\Omega \nabla \cdot \left(\left(\varphi^2 + k_\varepsilon\right) \mathbb{C}e(\mathbf{u})\right) \cdot \mathbf{v}_h\,\mathrm{dx} \\
&\quad= \int_{\partial\Omega} \left(\varphi^2 + k_\varepsilon\right) (\mathbb{C}e(\mathbf{u}) \cdot \nu) \cdot \mathbf{v}_h\,\mathrm{ds} \\
&\qquad+ \sum_{T\in\mathcal{T}} \int_T \left(\varphi^2 + k_\varepsilon\right) e(\mathbf{u}) : \mathbb{C}e(\mathbf{v}_h)\,\mathrm{dx} \\
&\qquad- \sum_{T\in\mathcal{T}} \int_{\partial T} \left(\varphi^2 + k_\varepsilon\right) (\mathbb{C}e(\mathbf{u}) \cdot \nu) \cdot \mathbf{v}_h\,\mathrm{ds}
\end{aligned}$$

Reordering the second sum to run over faces we get

$$\begin{aligned}
&\int_\Omega \left(\varphi^2 + k_\varepsilon\right) e(\mathbf{u}) : \mathbb{C}e(\mathbf{v}_h)\,\mathrm{dx} \\
&\quad= \sum_{T\in\mathcal{T}} \int_T \left(\varphi^2 + k_\varepsilon\right) e(\mathbf{u}) : e(\mathbf{v}_h)\,\mathrm{dx} - \sum_{F\in\mathcal{F}_{int}} \int_F \left(\varphi^2 + k_\varepsilon\right) [\![\mathbb{C}e(\mathbf{u}) \cdot \nu \cdot \mathbf{v}_h]\!]\,\mathrm{ds},
\end{aligned}$$

where we consider the face normal $\nu = \nu_F$ as in Section 2.5.2. As $\mathbf{u} \in H^2(\Omega; \mathbb{R}^n)$ by assumption and thus $\mathbb{C}e(\mathbf{u}) \in H^1(\Omega; \mathbb{R}^n)$, their jumps across interfaces vanish. In other words for any interface $F \in \mathcal{F}_{int}$ one has

$$[\![\mathbf{u}]\!] = 0 \text{ and } [\![\mathbb{C}e(\mathbf{u}) \cdot \nu]\!] = 0, \tag{4.8}$$

see [DPE12, Lemmata 1.23, 1.24]. Recalling that for inner faces the product rule

$$[\![(\mathbb{C}e(\mathbf{u}) \cdot \nu) \cdot \mathbf{v}_h]\!] = \{\!\{\mathbb{C}e(\mathbf{u}) \cdot \nu\}\!\} \cdot [\![\mathbf{v}_h]\!] + \{\!\{\mathbf{v}_h\}\!\} \cdot [\![\mathbb{C}e(\mathbf{u}) \cdot \nu]\!]$$

holds and that by definition $[\![(\mathbb{C}e(\mathbf{u})\cdot\nu)\cdot\mathbf{v}_h]\!] = (\mathbb{C}e(\mathbf{u})\cdot\nu)\cdot\mathbf{v}_h$ on the boundary we thus get

$$\begin{aligned}
&\int_\Omega \left(\varphi^2+k_\varepsilon\right) e(\mathbf{u}) : \mathbb{C}e(\mathbf{v}_h)\,\mathrm{dx} \\
&\quad= \sum_{T\in\mathcal{T}} \int_T \left(\varphi^2+k_\varepsilon\right) e(\mathbf{u}) : \mathbb{C}e(\mathbf{v}_h)\,\mathrm{dx} \\
&\qquad- \sum_{F\in\mathcal{F}_{int}} \int_F \left(\varphi^2+k_\varepsilon\right) \left(\{\!\{\mathbb{C}e(\mathbf{u})\cdot\nu\}\!\}\cdot[\![\mathbf{v}_h]\!] + \{\!\{\mathbf{v}_h\}\!\}\cdot[\![\mathbb{C}e(\mathbf{u})\cdot\nu]\!]\right)\mathrm{ds} \\
&\quad= \sum_{T\in\mathcal{T}} \int_T \left(\varphi^2+k_\varepsilon\right) e(\mathbf{u}) : \mathbb{C}e(\mathbf{v}_h)\,\mathrm{dx} \\
&\qquad- \sum_{F\in\mathcal{F}_{int}} \int_F \left(\varphi^2+k_\varepsilon\right) \left(\{\!\{\mathbb{C}e(\mathbf{u})\cdot\nu\}\!\}\cdot[\![\mathbf{v}_h]\!] + \{\!\{\mathbb{C}e(\mathbf{v}_h)\cdot\nu\}\!\}\cdot[\![\mathbf{u}]\!]\right)\mathrm{ds}\,.
\end{aligned}$$

As $[\![\mathbf{u}]\!]=0$ on any $F\in\mathcal{F}_{int}$, comparison with equation (4.3) shows

$$\begin{aligned}
a_h^{DG}(\mathbf{u},\mathbf{v}_h) = &\int_\Omega \left(\varphi_h^2+k_\varepsilon\right) e(\mathbf{u}) : \mathbb{C}e(\mathbf{v}_h)\,\mathrm{dx} \\
&- \sum_{F\in\mathcal{F}_{ext}\cap\Gamma_D} \int_F \left(\varphi_h^2+k_\varepsilon\right) \left([\![\mathbf{u}]\!]\,\{\!\{\mathbb{C}e(\mathbf{v}_h)\cdot\nu\}\!\} + \{\!\{\mathbb{C}e(\mathbf{u})\cdot\nu\}\!\}\,[\![\mathbf{v}_h]\!]\right)\mathrm{ds} \\
&+ \sum_{F\in\mathcal{F}_{ext}\cap\Gamma_D} \frac{\eta}{h_h} \int_F \left(\varphi_h^2+k_\varepsilon\right) \left([\![\mathbf{u}]\!]\cdot\nu\right) : \mathbb{C}\left([\![\mathbf{v}_h]\!]\cdot\nu\right)\mathrm{ds}
\end{aligned}$$

for all $\mathbf{v}_h\in V_h$. A similar calculation shows

$$\int_\Omega (1-\alpha)\,\varphi_h p\nabla\cdot\mathbf{v}_h\,\mathrm{dx} = \sum_{T\in\mathcal{T}}\int_T (1-\alpha)\,\varphi_h p\nabla\cdot\mathbf{v}_h - \sum_{F\in\mathcal{F}_{int}}\int_F (1-\alpha)\,\varphi_h p\,[\![\mathbf{v}_h]\!]\cdot\nu.$$

Thus inserting the Dirichlet boundary condition we have

$$\begin{aligned}
&a_h^{DG}(\mathbf{u},\mathbf{v}_h) - F_h^{DG}\mathbf{v}_h \\
&\quad= \int_\Omega \left(\varphi_h^2+k_\varepsilon\right) e(\mathbf{u}) : \mathbb{C}e(\mathbf{v}_h)\,\mathrm{dx} - \int_{\Gamma_D} \left(\varphi_h^2+k_\varepsilon\right) \{\!\{\mathbb{C}e(\mathbf{u})\cdot\nu\}\!\}\,[\![\mathbf{v}_h]\!]\,\mathrm{ds} \\
&\qquad+ \int_\Omega (1-\alpha)\,\varphi_h p\nabla\cdot\mathbf{v}_h + \varphi_h\,\nabla p\cdot\mathbf{v}_h\,\mathrm{dx} + \int_{\Gamma_N} (\tau+p\nu)\cdot\mathbf{v}_h\,\mathrm{ds}\,.
\end{aligned} \tag{4.9}$$

Note that adding the term $-\int_{\Gamma_D}\left(\varphi_h^2+k_\varepsilon\right)\{\!\{\mathbb{C}e(\mathbf{u})\cdot\nu\}\!\}\,[\![\mathbf{v}]\!]\,\mathrm{ds}$ to equation (4.1) would not alter the weak solution. Indeed we test with $\mathbf{v}\in H_0^1(\Omega)$ and hence the terms would be zero. Thus equation (4.1) in combination with equation (4.9) yields the required Galerkin orthogonality. □

Proof of Theorem 4.1.3. Having collected Lemmata 4.1.4 to 4.1.6, the error estimate follows in the usual way, see for example [DPE12, Theorem 1.35]. Note that consistency of the discrete bilinear form is requested in the reference mentioned. Nevertheless in the proof only Galerkin orthogonality is used. □

4.1.2 TNNMG discretization of the phase-field equation

Let us now discretize the equation with respect to the phase field, assuming $\mathbf{u}_h = \mathbf{u}_{\text{previous}}$ given. Remember that $\mathbf{u}_h$ is the solution to equation (4.5), hence $\mathbf{u}_h \in V_h = \mathcal{P}_k(\mathcal{T})$. Thus we have $\|\mathbf{u}_h\|_{L^\infty(\Omega;\mathbb{R}^n)} < +\infty$ as well as $\|e(\mathbf{u}_h)\|_{L^\infty(\Omega;\mathbb{R}^{n\times n})} \leq \|\nabla \mathbf{u}_h\|_{L^\infty(\Omega;\mathbb{R}^{n\times n})} < +\infty$. The main challenge is now the nonlinearity in form of the function $\Phi(\cdot)$. To deal with this issue we apply the truncated non-smooth Newton multigrid (TNNMG) solver as described in [GSS09], see also [GK09]. This method is specialized in solving discrete problems of the general form

$$\text{Find } \varphi \in \mathbb{R}^n \text{ such that } J_h(\varphi) \leq J_h(\psi) \text{ for all } \psi \in \mathbb{R}^n. \tag{4.10}$$

The functional $J_h : \mathbb{R}^n \to \mathbb{R} \cup \{+\infty\}$ is composed of the smooth part $J_{h,0}$ and the non-smooth $\Phi_{h,\imath}$ as

$$J_h(\varphi) = J_{h,0}(\varphi) + \sum_{\imath=1}^{n} \Phi_{h,\imath}(\varphi_\imath). \tag{4.11}$$

If J_h is strictly convex, proper, lower semicontinuous and coercive, there exists a unique solution of equation (4.10) [ET76, Proposition II.1.2]. In the remainder of this chapter we thus define a discretization of our problem that fits into the framework of equation (4.10) and prove the aforementioned properties.

Let us begin with the discretization. Starting with equation (4.1) we approximate the space $H^1(\Omega)$ by the N-dimensional finite element space $W_h = \mathcal{P}_1(\mathcal{T}) \cap \mathcal{C}(\Omega) \subset H^1(\Omega)$ with basis $(\phi_\imath)_{\imath=0}^{N-1}$. A function $\varphi_h = \sum_{\imath=0}^{N-1} \varphi_{h,\imath}\phi_\imath \in W_h$ is represented by the coefficient vector $(\varphi_{h,\imath})_{\imath=0}^{N-1}$. The differentiable part of the functional J_h as in equation (4.11) is then given by

$$\begin{aligned}
J_{h,0}(\varphi_h) =& \frac{1}{2} a_h^\varphi(\varphi_h,\varphi_h) + b_h^\varphi(\varphi_h), \text{ where} \\
a_h^\varphi(\varphi_h,\psi_h) =& \int_\Omega \varphi_h \cdot \psi_h e(\mathbf{u}_h) : \mathbb{C}e(\mathbf{u}_h)\,\mathrm{dx} \\
&+ G_c \int_\Omega \varepsilon \nabla\varphi_h \cdot \nabla\psi_h + \frac{1}{\varepsilon}\varphi_h\cdot\psi_h\,\mathrm{dx} \\
=& \sum_{\imath=0}^{N-1}\sum_{\jmath=0}^{N-1} \int_\Omega (\varphi_{h,\imath}\phi_\imath)\cdot(\psi_{h,\jmath}\phi_\jmath)\, e(\mathbf{u}_h) : \mathbb{C}e(\mathbf{u}_h)\,\mathrm{dx} \\
&+ G_c \int_\Omega \varepsilon(\varphi_{h,\imath}\nabla\phi_\imath)\cdot(\psi_{h,\jmath}\nabla\phi_\jmath) + \frac{1}{\varepsilon}(\varphi_{h,\imath}\phi_\imath)\cdot(\psi_{h,\jmath}\phi_\jmath)\,\mathrm{dx} \text{ and} \\
b_h^\varphi(\psi_h) =& \int_\Omega ((1-\alpha)p\nabla\cdot\mathbf{u}_h + \nabla p\cdot\mathbf{u}_h)\psi_h\,\mathrm{dx} - \int_\Omega \frac{G_c}{\varepsilon}\psi_h\,\mathrm{dx} \\
=& \sum_{\imath=0}^{N-1} \int_\Omega ((1-\alpha)p\nabla\cdot\mathbf{u}_h + \nabla p\cdot\mathbf{u}_h)(\psi_{h,\imath}\phi_\imath)\,\mathrm{dx} - \int_\Omega \frac{G_c}{\varepsilon}(\psi_{h,\imath}\phi_\imath)\,\mathrm{dx}
\end{aligned}$$

$\forall \varphi_h, \psi_h \in W_h$.

In other words, defining the matrix $A = (a_{i,j})_{i,j=0}^{N-1}$ and the vector $b = (b_i)_{i=0}^{N-1}$ with

$$a_{i,j} = \int_\Omega \phi_i \cdot \phi_j e(\mathbf{u}_h) : \mathbb{C}e(\mathbf{u}_h)\,\mathrm{d}x + G_c \int_\Omega \varepsilon \nabla \phi_i \cdot \nabla \phi_j + \frac{1}{\varepsilon}\phi_i \cdot \phi_j \,\mathrm{d}x,$$
$$b_i = \int_\Omega (1-\alpha)\, p\nabla \cdot \mathbf{u}_h \phi_i + \nabla p \cdot \mathbf{u}_h \phi_i \,\mathrm{d}x - \int_\Omega \frac{G_c}{\varepsilon}\phi_i \,\mathrm{d}x$$

we have

$$J_{h,0}(\varphi_h) = \frac{1}{2} A\varphi_h \cdot \varphi_h + b \cdot \varphi_h.$$

The non-smooth part is given by

$$\Phi_{h,i}(\varphi_h) = \chi_{\varphi_{\text{previous},h,i}}(\varphi_{h,i}) = \begin{cases} 0 & \text{if } \varphi_{h,i} \leq \varphi_{\text{previous},h,i} \\ +\infty & \text{otherwise} \end{cases}$$

Lemma 4.1.7 (Properties of J_h)**:**
Let $J_h \colon W_h \to \mathbb{R} \cup \{+\infty\}$ be given as above. Then J_h is strictly convex, proper, lower semi-continuous and coercive.

Proof. **Strict convexity.** Let $\varphi_h, \psi_h \in W_h$ be arbitrary, $t \in (0,1)$ and write $\delta = \frac{t}{1-t}$. Then Young's inequality applied to the terms $t\varphi_h$ (respectively $t\nabla\varphi_h$) and $(1-t)\psi_h$ (respectively $(1-t)\nabla\psi_h$) yields

$$a_h^\varphi(t\varphi_h, (1-t)\psi_h) \leq \frac{t^2}{2\delta} a_h^\varphi(\varphi_h, \varphi_h) + \frac{\delta(1-t)^2}{2} a_h^\varphi(\psi_h, \psi_h).$$

Equality holds if and only if $t\varphi_h = \delta(1-t)\psi_h$. Plugging in our choice of δ we obtain equality if and only if $\varphi_h = \psi_h$. Further

$$\begin{aligned} &a_h^\varphi(t\varphi_h + (1-t)\psi_h, t\varphi_h + (1-t)\psi_h) \\ &\quad = t^2 a_h^\varphi(\varphi_h, \varphi_h) + 2a_h^\varphi(t\varphi_h, (1-t)\psi_h) + (1-t)^2 a_h^\varphi(\psi_h, \psi_h) \\ &\quad \leq \left(t^2 + t(1-t)\right) a_h^\varphi(\varphi_h, \varphi_h) + \left((1-t)^2 + t(1-t)\right) a_h^\varphi(\psi_h, \psi_h) \\ &\quad = t a_h^\varphi(\varphi_h, \varphi_h) + (1-t) a_h^\varphi(\psi_h, \psi_h). \end{aligned}$$

As b_h^φ is obviously convex by linearity, we conclude that $J_{h,0}$ is strictly convex.

To prove convexity of $\Phi_{h,i}$ for all i we consider

$$\Phi_{h,i}(t\varphi_{h,i} + (1-t)\psi_{h,i}) = \begin{cases} 0 & \text{if } 0 \leq (t\varphi_{h,i} + (1-t)\psi_{h,i}) \leq \varphi_{\text{previous},h,i} \\ +\infty & \text{otherwise}. \end{cases}$$

Now if $0 \leq \varphi_{h,i} \leq \varphi_{\text{previous},h,i}$ and $0 \leq \psi_{h,i} \leq \varphi_{\text{previous},h,i}$ are guaranteed it obviously also holds

$0 \leq (t\varphi_{h,i} + (1-t)\,\psi_{h,i}) \leq \varphi_{\text{previous},h,i}$, hence

$$\Phi_{h,i}\left(t\varphi_{h,i} + (1-t)\,\psi_{h,i}\right) = 0 = t\cdot 0 + (1-t)\cdot 0 = t\Phi_{h,i}\left(\varphi_{h,i}\right) + (1-t)\,\Phi_{h,i}\left(\psi_{h,i}\right).$$

On the other hand if either $\varphi_{h,i} \notin [0, \varphi_{\text{previous},h,i}]$ or $\psi_{h,i} \notin [0, \varphi_{\text{previous}}]$ then we have $\Phi_{h,i}\left(\varphi_{h,i}\right) = +\infty$ or $\Phi_{h,i}\left(\psi_{h,i}\right) = +\infty$ respectively, hence

$$\Phi_{h,i}\left(t\varphi_{h,i} + (1-t)\,\psi_{h,i}\right) \leq +\infty = t\Phi_{h,i}\left(\varphi_{h,i}\right) + (1-t)\,\Phi_{h,i}\left(\psi_{h,i}\right).$$

As the case distinction is exhaustive, $\Phi_{h,i}$ is convex for all i and thus we conclude that J_h is strictly convex by recalling the strict convexity of $J_{h,0}$.

Proper convexity. We obviously have $J_h\left(\varphi_h\right) > -\infty$ for all $\varphi_h \in \mathbb{R}^n$. Further there exists $\varphi_h = \varphi_{\text{previous},h}$ such that $J_h\left(\varphi_h\right) < +\infty$. Thus J_h is also proper convex.

Lower semicontinuity. Note that by Hölder's inequality

$$\begin{aligned} a_h^{\varphi}\left(\varphi_h, \psi_h\right) \leq & \left((2\mu + n\lambda)\left\| e\left(\mathbf{u}_h\right)\right\|_{L^\infty(\Omega;\mathbb{R}^n)} + \frac{G_c}{\varepsilon}\right) \|\varphi_h\|_{L^2(\Omega)} \|\psi_h\|_{L^2(\Omega)} \\ & + G_c\varepsilon \|\nabla\,\varphi_h\|_{L^2(\Omega)} \|\nabla\,\psi_h\|_{L^2(\Omega)} \\ & \leq c\left(\mu, \lambda, G_c, \varepsilon, \|\mathbf{u}_h\|_{W^{1,\infty}(\Omega;\mathbb{R}^n)}\right) \|\varphi_h\|_{H^1(\Omega)} \|\psi_h\|_{H^1(\Omega)}. \end{aligned}$$

Further

$$b_h^{\varphi}\left(\psi_h\right) \leq c\left(\alpha, \|p\|_{W^{1,\infty}(\Omega)}, \|\mathbf{u}_h\|_{H^1(\Omega;\mathbb{R}^n)}, G_c, \varepsilon\right) \|\psi_h\|_{H^1(\Omega)},$$

thus $J_{h,0}$ is continuous. Let us now show lower semicontinuity of Φ_h at $\varphi_h \in W_h$ arbitrary. If $\Phi_h\left(\varphi_h\right) = 0$ we obviously have $\Phi_h\left(\psi_h\right) \geq \Phi_h\left(\varphi_h\right)$ for all $\psi_h \in W_h$ and thus lower semicontinuity. On the other hand consider $\Phi_h\left(\varphi_h\right) = +\infty$. Noting that $W_h \setminus \{\psi_h : 0 \leq \psi_h \leq \varphi_{\text{previous},h} \text{ a. e.}\}$ is open, we have $\lim_{\psi_h \to \varphi_h} \Phi_h\left(\psi_h\right) = +\infty$ and lower semicontinuity is proven.

Coercivity. Applying Young's inequality with arbitrary $\delta_1, \delta_2 > 0$ we can estimate

$$\begin{aligned} J_{h,0}\left(\varphi_h\right) \geq & \frac{G_c\varepsilon}{2}\|\nabla\,\varphi_h\|_{L^2(\Omega)}^2 + \frac{G_c}{2\varepsilon}\|\varphi_h\|_{L^2(\Omega)}^2 \\ & - \frac{\|p^2\|_{W^{1,\infty}(\Omega)}\|\mathbf{u}_h\|_{H^1(\Omega;\mathbb{R}^n)}^2}{2\delta_1} - \frac{\delta_1}{2}\|\varphi_h\|_{L^2(\Omega)}^2 - \frac{G_c^2}{2\delta_2\varepsilon^2} - \frac{\delta_2}{2}\|\varphi_h\|_{L^2(\Omega)}^2. \end{aligned}$$

Thus for $\delta_1 = \delta_2 = \frac{G_c}{4\varepsilon}$ we get

$$J_{h,0}\left(\varphi_h\right) \geq \min\left(\frac{G_c}{4\varepsilon}, \frac{G_c\varepsilon}{2}\right)\|\varphi_h\|_{H^1(\Omega)}^2 - c, \tag{4.12}$$

where c depends on $\|p^2\|_{W^{1,\infty}(\Omega)}$, $\|\mathbf{u}_h\|_{H^1(\Omega;\mathbb{R}^n)}$, G_c and ε. Further for $\|\varphi_h\|_{H^1(\Omega)} \to +\infty$ at some

point in time $\varphi_h \leq \varphi_{\text{previous},h}$ $\mathcal{L}^n$-a. e. will no longer hold and thus

$$\lim_{\|\varphi_h\|_{H^1(\Omega)} \to +\infty} \Phi_h(\varphi_h) = +\infty. \tag{4.13}$$

Combining equations (4.12) and (4.13) yields

$$\lim_{\|\varphi_h\|_{H^1(\Omega)} \to +\infty} J_h(\varphi_h) = +\infty,$$

and thus coercivity is shown. □

We can now conclude the main result of this section.

Theorem 4.1.8 (Existence of a solution for the phase-field step)**:**
Let J_h be as in equation (4.11)*. Then equation* (4.10) *has a unique solution.*

Proof. The result follows immediately from Lemma 4.1.7 and the general existence result [ET76, Proposition II.1.2]. □

Thus our functional J_h is applicable for the TNNMG-Solver which according to [GSS09, Theorem 2] then converges to the solution of the minimization problem (4.10).

4.1.3 Adjustments for UDG

The unfitted Discontinuous Galerkin method has the advantage that it can handle interior domain boundaries without introducing as many degrees of freedom as a remeshing technique would require. We want to exploit this property, treating the crack as such an interior domain boundary. As described in Section 2.5.3, the main ingredient in the conversion from a DG to a UDG discretization is the inclusion of N sub-domains Ω^i and the corresponding sub-domain meshes $\mathcal{T}^i$ as well as their skeletons $\mathcal{F}^{i,i}_{int}$, $\mathcal{F}^i_{ext}$ and $\mathcal{F}^{i,j}_{int}$ for $0 \leq i < N$ and $0 \leq j < i$. For the moment let us assume that these are given satisfying two properties:

- it exists a subset $\mathcal{F}^c_{int} \subset \bigcup_{i=0}^{N-1} \bigcup_{j<i} \mathcal{F}^{i,j}_{int}$ which represents the crack and
- whenever an edge $F_{1,2} = \partial T_1^i \cap \partial T_2^j$ is part of $\mathcal{F}^c_{int}$ we have $i \neq j$, that is the two sides of $F_{1,2}$ belong to different domains.

We discuss the reconstruction of the crack and thus the creation of $\mathcal{F}^c_{int}$ in Section 4.2 and Section 5.2. The construction of the sub-domains with the corresponding meshes is described in more detail in Section 5.3.

A first adaptation of the SIPG discretization in the preceding chapter is then straightforward, following the lines of Section 2.5.3. The only difference to the discrete elasticity problem defined in equation (4.5) is that the summations in equation (4.3) and equation (4.4) are taken over all subdomain triangles and edges respectively. Nevertheless, having gained some additional information, namely an approximation of the crack $\mathcal{C}$ in form of $\mathcal{F}_{int}^c$, we want to make use of it. For this purpose we first omit weakly forcing continuity along the crack by simply not including skeleton terms along edges $F \in \mathcal{F}_{int}^c$. Second, recalling equation (2.9), we remember the formulation of the weak problem actually including surface terms along the crack. Skipping the application of Gauss' theorem that was used to get rid of the term $\int_{\partial\mathcal{C}} p\nu \cdot \mathbf{u}\,\mathrm{ds}$ we obtain the following energy minimization problem.

Definition 4.1.9 (Energy minimization problem for UDG)**:**
Find $\mathbf{u}$, $\mathcal{C}$ *such that*

$$\begin{aligned} &E^{UDG}(\mathbf{u},\mathcal{C}) \\ &\quad= \min_{\mathbf{v},K} E(\mathbf{v},K) \\ &\quad= \min_{\mathbf{v},K} \int_{\Omega\setminus K} \frac{1}{2} e(\mathbf{v}) : \mathbb{C}e(\mathbf{v}) \; - \alpha p\nabla\cdot\mathbf{v} - \int_{\Gamma_N} \tau\cdot\mathbf{v}\,\mathrm{ds} + \int_{\partial K} p\nu\cdot\mathbf{u}\,\mathrm{ds} + G_c\mathcal{H}^{n-1}(K)\,. \end{aligned} \tag{4.14}$$

Similar to Section 2.2.4, we obtain an approximative problem.

Definition 4.1.10 (Approximative energy minimization problem)**:**
Find $\mathbf{u} \in H_D^1(\Omega;\mathbb{R}^n)$ *and* $\varphi \in H^1(\Omega)$ *with* $0 \le \varphi \le 1$ *and* $\frac{\partial}{\partial t}\varphi \le 0$ *satisfying*

$$\begin{aligned} E_\varepsilon^{UDG}(\mathbf{u},\varphi) &= \min_{\mathbf{v},\psi} E_\varepsilon^{UDG}(\mathbf{v},\psi) \\ &= \min_{\mathbf{v},\psi} \left(\int_\Omega \frac{1}{2}\left(\psi^2 + k_\varepsilon\right) e(\mathbf{v}) : \mathbb{C}e(\mathbf{v}) - \alpha\psi p\nabla\cdot\mathbf{v}\,\mathrm{dx} \right. \\ &\qquad \left. - \int_{\Gamma_N} \tau\cdot\mathbf{v}\,\mathrm{ds} + \int_{\partial\mathcal{C}} p\nu\cdot\mathbf{u}\,\mathrm{ds} + G_c \int_\Omega \frac{1}{2\varepsilon}(1-\psi)^2 + \frac{\varepsilon}{2}|\nabla\psi|^2\,\mathrm{dx} \right). \end{aligned} \tag{4.15}$$

Note that the term $\int_{\partial\mathcal{C}} p\nu\cdot\mathbf{u}\,\mathrm{ds}$ is a continuous perturbation of the functional, thus the Γ-convergence results from Chapter 3 hold for this approximation as well.

The adapted approximative energy minimization problem leads to the following final UDG dis-

cretization for $\mathbf{u}_h, \mathbf{v}_h \in V_h$

$$
\begin{aligned}
a_h^{UDG}(\mathbf{u}_h, \mathbf{v}_h) = \sum_{i=0}^{N-1} \Bigg(& \sum_{T \in \mathcal{T}^i} \left(\int_T \left(\varphi_h^2 + k_\varepsilon\right) e(\mathbf{u}_h) : \mathbb{C} e(\mathbf{v}_h) \, \mathrm{dx} \right) \\
& - \sum_{F \in \mathcal{F}^i \setminus \left(\mathcal{F}^c_{int} \cup \Gamma_N\right)} \left(\int_F \left(\varphi_h^2 + k_\varepsilon\right) \left([\![\mathbf{u}_h]\!] \, \{\!\{ \mathbb{C} e(\mathbf{v}_h) \cdot \nu \}\!\} + \{\!\{ \mathbb{C} e(\mathbf{u}_h) \cdot \nu \}\!\} \, [\![\mathbf{v}_h]\!] \right) \mathrm{ds} \right) \\
& + \sum_{F \in \mathcal{F}^i \setminus \left(\mathcal{F}^c_{int} \cup \Gamma_N\right)} \frac{\eta}{h_F} \int_F \left(\varphi_h^2 + k_\varepsilon\right) \left([\![\mathbf{u}_h]\!] \cdot \nu \right) : \mathbb{C} \left([\![\mathbf{v}_h]\!] \cdot \nu \right) \mathrm{ds} \Bigg), \\
F_h^{UDG}(\mathbf{v}_h) = \sum_{i=0}^{N-1} \Bigg(& - \sum_{T \in \mathcal{T}^i} \int_T -\alpha \varphi_h p \nabla \cdot \mathbf{v}_h \, \mathrm{dx} \\
& + \sum_{F \in \mathcal{F}^i_{ext} \cap \Gamma_N} \int_F \tau \cdot \mathbf{v}_h \, \mathrm{ds} \\
& - \sum_{F \in \mathcal{F}^i_{ext} \cap \Gamma_D} \int_F \left(\varphi_h^2 + k_\varepsilon\right) \mathbf{u}_D \, \{\!\{ \mathbb{C} e(\mathbf{v}_h) \cdot \nu \}\!\} \, \mathrm{ds} \\
& + \sum_{F \in \mathcal{F}^i_{ext} \cap \Gamma_D} \frac{\eta}{h_F} \int_F \left(\varphi_h^2 + k_\varepsilon\right) \left(\mathbf{u}_D \cdot \nu \right) : \mathbb{C} \left([\![\mathbf{v}_h]\!] \cdot \nu \right) \mathrm{ds} \\
& - \sum_{F \in \mathcal{F}^i_{int} \setminus \mathcal{F}^c_{int}} \int_F \alpha \varphi_h p \, [\![\mathbf{v}_h]\!] \cdot \nu \, \mathrm{ds} + \sum_{F \in \mathcal{F}^c_{int}} \int_F p \nu \cdot \mathbf{v}_h \, \mathrm{ds} \Bigg).
\end{aligned}
$$

Note that the modification of the weak energy leads to a slightly different linear form for the TNNMG discretization of the phase-field equation as well. Namely, when solving the displacement problem with UDG, we define for all $\psi_h \in W_h$

$$
b_h^{\varphi, UDG}(\psi_h) = -\int_\Omega \alpha p \nabla \cdot \mathbf{u}_h \psi_h \, \mathrm{dx} - \int_\Omega \frac{G_c}{\varepsilon} \psi_h \, \mathrm{dx}.
$$

The bilinear form a_h^φ remains unchanged.

Reenacting the proofs of Section 4.1.2 we note that J_h still has the properties stated in Lemma 4.1.7 and thus Theorem 4.1.8 still holds. Concerning the analysis of the UDG discretization we note that going back to the term $\int_{\partial C} p\nu \cdot \mathbf{u} \, \mathrm{ds}$ does not alter the analysis. In fact, it has no influence on the bilinear form and the linear form is altered in a way that guarantees Galerkin orthogonality with respect to the corresponding weak problem. Nevertheless a rigorous analysis of the given formulation is not possible. As the crack can cut elements in an arbitrarily bad way, we cannot guarantee that standard assumptions on the grid are satisfied, such as shape regularity and quasi uniformity. For more details we refer the interested reader to [BE09].

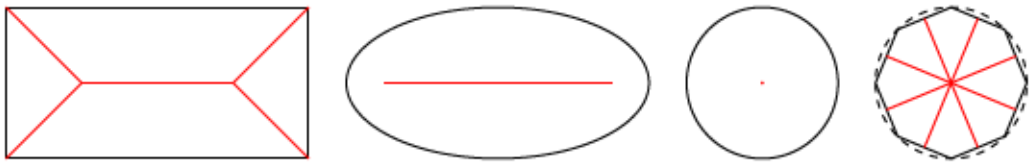

Figure 4.1: Skeletons (in red) of a rectangle, an ellipse, a circle and its polygonal approximation.

4.2 Reconstruction of the crack

As discussed in Section 4.1.3, in order to apply the UDG method we need an explicit representation of the crack. In recent years a couple of papers appeared, dealing with the combination of continuous methods for simulating crack propagation, as phase-field models or damage models, with discontinuous approaches, as for example the X-FEM method. Therein we can find numerous strategies for the reconstruction of the crack. In [GSF17] at every loading step the new crack tip is found and connected to the existing crack. Unfortunately to our knowledge this only works reliably in the case of an a-priori known crack path. Further they can not deal with branching at tip points. Other approaches introduce a discontinuity once a critical crack opening displacement is reached (e.g. [JZ01] and [SWS03]). It remains to determine the direction of the crack, which is done relying on the directions of maximum principal stress or maximum principal non-local strain. Note that [JZ01] allows for discontinuities in the crack path. In [SWS03] the introduced fracture segments always crack an entire element, their introduction of new crack tips relies on degrees of freedom on the boundary of elements. Thus both methods are not applicable in our case. Instead we follow a geometrical approach proposed in [TMRF15]. According to the theory, a crack would occur wherever φ is minimal. Unfortunately, the phase-field variable never reaches the value 0. We can not determine a discrete $(n-1)$-dimensional crack path but rather gain a path of elements, where φ is minimal. Nevertheless, intuitively one would expect the crack to be along "the middle" of the smeared region. Mathematically this can be described by the skeleton (or medial axis) of a level set $\varphi = \varphi^*$ for some threshold value φ^*.

The notion of a skeleton was first introduced by Blum [Blu67]. He describes what is known as the grass fire model. Starting a homogeneously spreading fire simultaneously at every boundary point, the skeleton is composed of those points where different fire fronts meet and quench. There exist many different ways to define a skeleton or similar structures. Blum additionally describes it as the set of all points with at least two closest points on the boundary. Calabi characterizes the skeleton or medial axis as being composed of the centers of maximal inscribed disks [Cal65, CH68]. See Figure 4.1 for some examples of skeletons of simple geometrical shapes.

There exists an enormous amount of literature on skeleton generation, a fairly recent overview is given by Saha et al. in [SBdB16]. The different approaches to skeletonization can be roughly grouped into three categories. The main ideas derive from the different definitions of a skeleton or medial axis. We distinguish

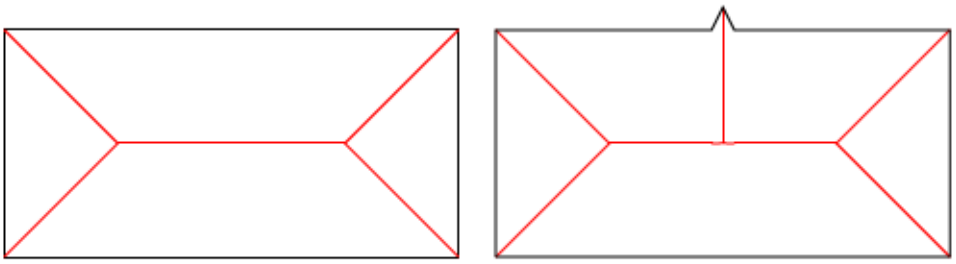

Figure 4.2: Example for the sensitivity of a skeleton to noisy boundary: the rectangle was slightly modified at the boundary resulting in a completely new skeleton branch.

- thinning algorithms,
- algorithms trying to detect ridges in the discrete distance transform and
- algorithms based on Voronoi diagrams.

Any such algorithm has one major challenge, the sensitivity of a skeleton to noisy boundary data, see Figure 4.2. A further difficulty is working with discrete data. Given a smooth geometric shape and its discrete approximation their skeletons might differ dramatically, as seen in the case of the circle and its approximation in Figure 4.1. Additional properties of skeletons that are often desired but difficult to achieve are

- connectivity i.e. the skeleton should be connected and have the same topological structure as the underlying shape,
- rotation invariance and
- reversibility i. e. by storing in addition the distance from the boundary at the centers of maximal disks, the original shape should be reconstructible.

Obviously the most important property for us, besides insensitivity to noisy boundary data, is connectivity of the skeleton, which amounts to connectivity of the crack.

Let us give a short overview of existing algorithms, their advantages and disadvantages. Thinning algorithms are a common choice when working with pixel data, for example in the field of pattern recognition. An extensive overview of the first two-dimensional algorithms can be found in [LLS92]. For the extension to three-dimensional cases see for example [TF81, GB90, MFV98]. Thinning algorithms usually work iteratively. Starting from the boundary they remove "simple cells", that is cells whose removal does not change the topology of the object. The process is repeated until no further "simple cells" remain. Some further geometrical restrictions are usually necessary to keep the endpoints of branches. The criterion for simple cells is usually a local one, depending only on the neighborhood of a cell. Thus they have two major drawbacks for our application. First, they produce a band of cells as the skeleton, not an $(n-1)$-dimensional crack. Second, as they must take into account the neighborhood of a cell, they mainly work on structured, hexahedral grids. More recently a couple of papers extended the principle to cell complexes and thus simplicial grids

[WM08, LCLJ10, KP12, DS14]. While some of these algorithms still rely on structured grids or are affected by the grid orientation, others only produce a band of elements as skeleton. Thus these methods are not suitable for our application.

The second widely used approach to find the skeleton is the detection of ridges (local maxima) in the distance map of the boundary. They first solve the Eikonal equation to compute the distance. Afterwards the ridges of the distance map are detected. The interested reader can find examples for algorithms of these types in [LL92, AdB92, SP95, GF96, SBTZ02, TvW02, RT02]. These algorithms suffer from similar disadvantages as the thinning methods, most of them rely on structured, hexahedral grids. Some of them even rely on a thinning process to detect the ridges. Further they need to detect regions of high curvature and treat them separately, thus they depend on a smooth boundary. Finally they sometimes only approximate the Euclidean distance, which leads to skeletons that are no longer rotation-invariant.

The third class of algorithms generating a skeleton relies on the concept of Voronoi diagrams. In our case they have the main advantage to directly work on a polygonal representation of the boundary. Using this representation either the edges or the nodes or both are taken as so-called set of Voronoi sites $\mathcal{S}$. The Voronoi region V_s corresponding to a site $s \in \mathcal{S}$ is then defined as all points closer to s than to any other site $s' \in \mathcal{S}$ with respect to a metric d. The Voronoi diagram VD consists of the boundaries of all these regions. In mathematical terms that reads

$$\begin{aligned} V_s &= \{x \in \mathbb{R}^n : \forall s' \in \mathcal{S},\, s' \neq s : d(x,s) \leq d(x,s')\} \\ VD &= \bigcup_{s \in \mathcal{S}} \partial V_s. \end{aligned} \tag{4.16}$$

In most applications the skeleton is restricted to the inside of the shape. Obviously this results in a branch of the Voronoi diagram for every pair of neighboring nodes in the polygonal representation of the boundary. The main parts of the skeleton, corresponding to a skeleton of the continuous boundary, are obtained by applying some pruning methods distinguishing between "important" skeleton branches and minor parts. This approach was first introduced in [OI92]. It was expanded to create a hierarchic structure of skeleton branches in [OK95]. Many other authors discussed the usage of Voronoi diagrams for skeletonization, see for example [LWH+12, MR96]. Their relation to other methods computing the medial axes is studied in [FEC02]. See [ABE09] for an overview of the stability of the generated medial axes. As mentioned before a main ingredient in skeleton generation using Voronoi diagrams is the pruning method. While several methods relying on the distance of Voronoi sites s and s' along the boundary are proposed in [OI92], a method additionally taking the angle between s and s' into account is proposed in [BLyL07].

In summary we see three big problems with most methods for our use case. The first problem is that many approaches start with a continuous representation of the shape boundary, which is not given in our case. Indeed, numerically we only obtain a piecewise linear approximation of the boundary. They use information such as curvature maxima. Second, most of the algorithms use a pixel based representation of the shape, relying heavily on the structured grid setting. Finally many

algorithms represent the skeleton in form of pixels or elements and not in form of a one-dimensional interface as we would like to do.

Analyzing the existing literature under these aspects, a skeletonization approach based on Voronoi diagrams was implemented in the present thesis. The major advantage is that the algorithm works directly with the polygonal approximation of the boundary. This is exactly what is represented by our piecewise linear level set and thus the natural starting point for us. In addition using pruning methods we can extract the important branches of the crack. More details on the algorithms employed and their implementation can be found in Section 5.2.

5 Implementation

5.1 Distributed and Unified Numerics Environment (DUNE)

All numerical tests in the present thesis were implemented using the software toolbox DUNE, short for Distributed and Unified Numerics Environment. An archive of the complete source code and instructions to reproduce the results shown in Chapter 6 are published in [Som19]. DUNE is a free software aiming at the solution of partial differential equations with grid-based methods. Its implementation follows three main principles: flexibility, efficiency and extensibility. Abstract interfaces are used to separate algorithms and data structures. They also enable the flexible integration of external libraries for example for grid integration. For more information on the basic concepts of DUNE we refer to its website[1].

The basis for the implementation of PDE solvers with DUNE are the so-called core modules, namely `dune-common`, `dune-geometry`, `dune-grid` ([BDE+05, BBD+08b, BBD+08a]), `dune-istl` ([BB07, BB08]) and `dune-localfunctions`. They provide a stable foundation for any application using DUNE. On top of these a wide range of other modules are available. There exist grid, discretization, extension and user modules as well as tutorial modules. The present thesis highly relies on the discretization module `dune-pdelab` [BHM10]. We employ the grid modules `dune-uggrid`, providing a grid implementation, and `dune-grid-glue` ([BBS09, EM16]) to cut one-dimensional slices into a grid for the evaluation of line integrals. Further, our code takes advantage of some functionalities implemented in the extension modules `dune-functions` ([EGMSb, EGMSa]) and `dune-typetree`. For the UDG discretization and the TNNMG solver mentioned in Section 4.1.1 and Section 4.1.2, we heavily rely on `dune-udg` [EH12] and `dune-tnnmg`, respectively. For the TNNMG module we additionally need `dune-solvers`. The UDG discretization module itself makes use of `dune-tpmc` [EN17] and is supplemented in the course of this thesis with a new way of constructing a subtriangulation described in Section 5.3. For profiling purposes we used some functionality from `dune-xt` [MSL17].

[1] `https://www.dune-project.org/`

5.2 Construction of the skeleton

The reconstruction of the crack as the medial axis of some level set $\varphi = \varphi^*$ of the phase field consists of five steps. First we extract the level set of φ and sort the points found along the boundary. Afterwards the Voronoi diagram corresponding to the obtained points is computed. In the post-processing all Voronoi edges are restricted to the inside of $\varphi = \varphi^*$ and a pruning algorithm is applied to remove unimportant branches. In the following the individual steps are described in more detail.

The level set extraction is done by a topology preserving marching cubes algorithm. We use an implementation already integrated in the `DUNE` framework [EN17]. It can be used to generate a list of points and the connecting interfaces of a multilinear approximation of the level set. Sorting the points along the boundary according to the connecting interfaces, we obtain a list of point sites suitable for the generation and pruning of the Voronoi diagram.

The algorithm of choice to compute the Voronoi diagram of a given set of point sites is the sweep line algorithm [For87]. For a good overview on the algorithm and some implementational details see for example [dBvKOS00, Chapter 7] and [Sch13]. The algorithm has optimal complexity and many reference implementations exist. Unfortunately none of these fit our needs perfectly, hence we re-implemented it. Some of the implementations demand for integer coordinates of the sites [Boo]. Furthermore, many implementations do not keep track of the generating sites of a Voronoi edge, which we need for the subsequent pruning.

Having successfully created a Voronoi diagram as defined in equation (4.16), many of its edges are half-infinite. To overcome this difficulty a bounding box is used and half-infinite or infinite Voronoi edges are cut by the bounding box. Applying the algorithm for crack reconstruction, the computational domain is naturally chosen as the bounding box. In our case we can restrict the Voronoi diagram to an even smaller region. As we are only interested in the crack inside of the domain described by $\varphi = \varphi^*$, we cut the Voronoi edges by this boundary as well.

Our final task is pruning the Voronoi diagram to remove unimportant branches. We implemented pruning according to the potential residual as introduced in [OK95] as described below. The alternative pruning based on discrete curve evolution as proposed in [BLyL07] has the property that it does not prune the principal branch of the skeleton. While this might be a desired property in many applications, it would result in the crack tip lying on the chosen level set $\varphi = \varphi^*$. This is obviously not realistic and increases the dependence of the reconstructed crack on the chosen value of φ^*, hence it is a major disadvantage for our application.

Let $s_1, s_2 \in \mathcal{S}$ be the two Voronoi sites corresponding to an edge e of the Voronoi diagram. In other words $d(x, s_1) = d(x, s_2) = \min_{s \in \mathcal{S}} d(x, s)$ for all points $x \in e$. Following [OK95] we then define the potential residual of e as the distance of s_1 and s_2 along the level set $\varphi = \varphi^*$,

writing $r(e) = d^{LS}(s_1, s_2)$. If the level set consists of multiple connected components, we define $r(e) = +\infty$ if s_1 and s_2 lie on different components. The skeleton is then pruned with a simple thresholding. A branch is more significant, the more distant its two generating sites are. Thus we erase any edge with a residual smaller than a given threshold r^*. To render r^* independent of the scaling of an object we apply a relative criterion. That means we prune a branch if and only if its potential residual $r(e)$ is smaller than r^* times the total length of the component of the level set, where its generating sites lie on. An example of skeleton generation is shown in Figure 6.3.

5.3 Creation of sub-domains

Let us suppose we have reconstructed the crack as described in the previous section. Thus we assume that we have given a pruned Voronoi diagram and we wish to introduce the Voronoi edges into our domain. As we want to apply the UDG method it is not necessary to remesh the grid. It is sufficient to find a separation of the elements $T \in \mathcal{T}$ cut by one or more Voronoi edges into sub-domains $T^i \in \mathcal{T}^i$ with domain index $i \in \mathbb{N}$. We start this section by a short description of the `DUNE` module `dune-udg`. Afterwards we describe the way we integrate the creation of sub-domains generated from a Voronoi diagram. Finally the creation process and arising problems are described in more detail.

The module `dune-udg` is an extension of `dune-pdelab` providing the infrastructure to implement cut-cell methods as for example the UDG method applied in this thesis. Its main ingredient is to provide a sub-triangulation of a grid, such that integration over sub-domains and boundaries of sub-domains becomes possible. In the classical approach the sub-domains are separated by the zero level set of a given function. A marching cubes algorithm is applied to find a multi-linear approximation of the zero level set. Subsequently, a hash can be computed to identify the case of cutting through an element. Afterwards the sub-elements for integration are constructed according to this unambiguous case. For more details see [EH12] and [EN17]. The most important methods provided to the user by the sub-triangulation are `create_entity_parts` and `create_intersection_parts`. They take as input an element $T \in \mathcal{T}$, called entity in `DUNE`, and provide the user with a set of entity parts and intersection parts, respectively. These represent a subdivision of the entity into simplices and hypercubes, on which it is easy to implement quadrature rules, as well as the corresponding boundaries. In the following we describe how to construct this subdivision when the sub-domain boundary is not given by a zero level set of a function but rather by a Voronoi diagram. The construction must satisfy the following two main requirements,

- the crack must stay exactly connected and
- on different sides of the crack the entity parts must belong to different sub-domains.

The first approach that comes to mind is to adapt the ideas of a marching cubes algorithm. That is for a given pair (T, e) of an element $T \in \mathcal{T}$ and a Voronoi edge e one would calculate a hash that

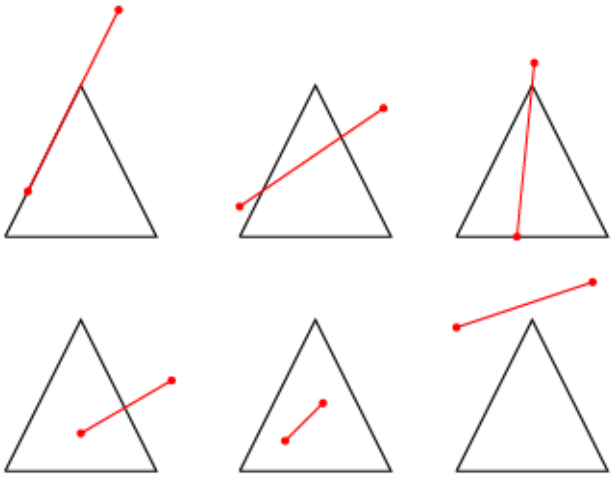

Figure 5.1: Example configurations of a Voronoi edge cutting through a triangular grid element.

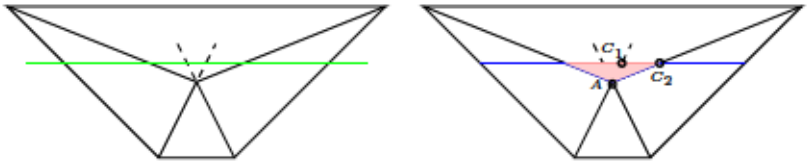

Figure 5.2: Example of a situation where numerical comparison of the cut point between a Voronoi edge and the edges of triangles with the common corner of the triangles fails.
The triangles (black) are cut by the skeleton edge (green). Assuming that the numerical ε is chosen such that the cut point C_1 is closer to the center A than ε, but the cut point C_2 is not, the topmost triangle reconstructs the skeleton as depicted in red, the others see the blue reconstruction. Thus a very small, completely disconnected triangle (red) is generated.

symbolizes how e cuts through T. Possible cases include going along an edge of T and cutting (or ending at) an edge of T or at a corner of T as well as ending inside of T or not touching T at all. See Figure 5.1 for some exemplary configurations. Unfortunately this gives rise to problems due to numerical inexactness. If we compare cuts with corners of T exactly, we encounter problems as the numerical calculation of a cut between two edges can never be computed exactly [She97]. Alternatively, if we merely compare the corner of T with the cut point between an edge of T and the Voronoi edge e numerically, the topology of the crack might change. An example of these special cases is shown in Figure 5.2, where due to the inexact comparison a small hole is introduced. Thus finding the cut geometry for any pair (T, e) separately will not work. Instead we need to follow a different approach to guarantee topological correctness of the resulting crack.

We apply an advancing front technique, inspired by [GJ09, GJ13]. The authors describe how non-matching grids of dimension two or three are projected on each other using advancing fronts. We adapt their approach to the situation where a grid consisting of one-dimensional elements, namely the Voronoi diagram, is cut into a higher dimensional one. We start with an arbitrary Voronoi node P_1 and find the grid element it lies in by a brute force search. Next, we consider all edges starting at P_1 consecutively. Therefore we put them into an event queue of tuples of the form (element, edge). Computing the cut configuration of a Voronoi edge e with the current element T we either

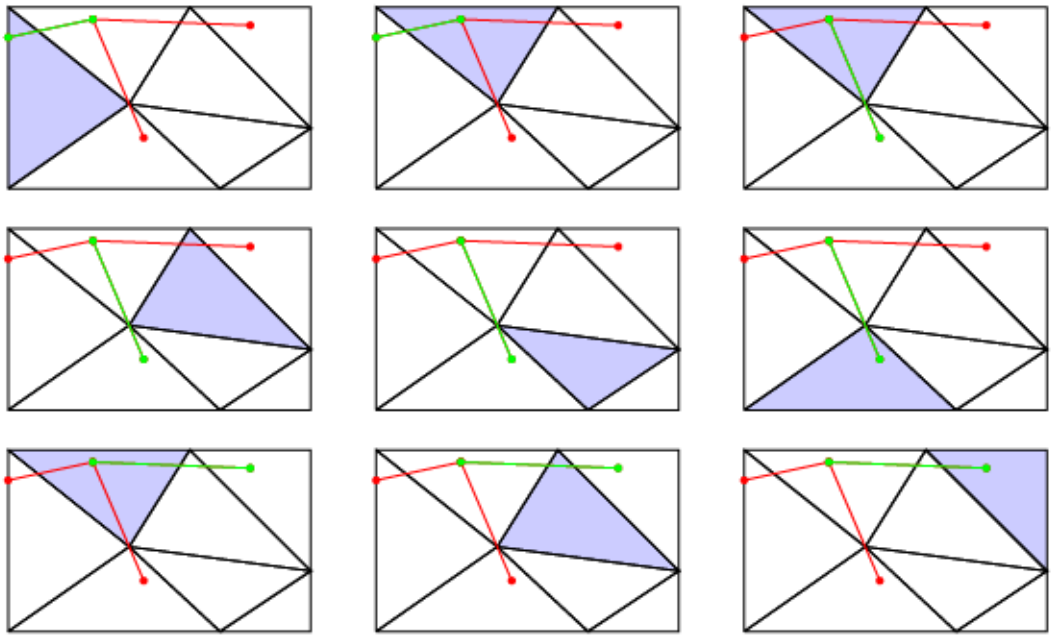

Figure 5.3: Advancing front algorithm to find the intersections between a grid (black) and a Voronoi diagram (red). The currently treated triangle and the currently treated Voronoi edge are colored in blue and green, respectively.

reach the end of e inside of T or e cuts through one side or corner of T. In the first case the ending node P_2 of e is reached and we are finished calculating the cut of e with T. We add all non-treated edges starting (or ending) at P_2 with T as start element to the event queue of (edge, element) pairs and continue with the next pair from this queue. In the second case, when e leaves T through a side s, we also obtain the cut configuration of e with T. We continue with the algorithm by cutting e into the neighbor element T' of T across s. This ensures that both triangles, T and T', see the same cut point with the common edge s. If e leaves T through a corner C, there does not exist a single neighbor. In this case we move around C as long as the neighboring triangle merely touches e in the corner C. When we reach a new element T' that intersects with e in more than the corner C we continue with the pair (T', e). If we reach the boundary of the domain before finding such an element we go all the way around the corner until we reach the other boundary element and start over from there. If e ends exactly at C we simply add the two neighbors of T at C to the queue with all non-treated edges starting at C. A small example of how a Voronoi diagram consisting of three edges is introduced into a small grid consisting of seven triangles is given in Figure 5.3.

Having obtained a list of cut configurations for any pair (element, edge) where a cut exists in a preprocessing step, the main work in `create_entity_parts` is to actually compute the entity parts resulting from these cuts. This is especially difficult in the case of multiple, possibly not directly connected edges cutting through an element as shown in Figure 5.4. To avoid any numerical difficulties we use the Triangle[2] library, "A Two-Dimensional Quality Mesh Generator and Delaunay Triangulator" [She96, She02]. For an element T we insert the corners of T and any cut points stored for the tuple (T, e) for any Voronoi edge e cutting through T into Triangle and

[2] `https://www.cs.cmu.edu/~quake/triangle.html`

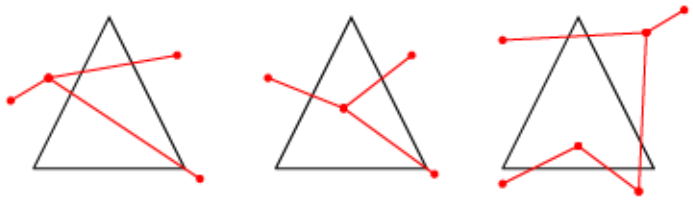

Figure 5.4: Examples of multiple Voronoi edges cutting through the same grid element. In the right-hand case some of them are not directly connected.

gain a triangular mesh of sub entities of T. Triangle is also capable of constructing constrained Delaunay triangulations, thus we can force the edges e to be part of the resulting mesh. Moreover it is possible to assign segment markers to the inserted edges, such that any segment in the output of Triangle can be distinguished between crack and non-crack. The output of Triangle thus provides us with the desired entity parts. At the same time it also yields the intersection parts needed for `create_intersection_parts`. The only remaining problem is to find the neighboring entity part for intersection parts on the boundary of an element. This is done by constructing the entity and intersection parts of the neighboring element followed by a geometrical matching. The advancing front algorithm described earlier guarantees that the intersection parts in the neighboring element will have the same coordinates and we can compare them exactly. Noticing that `create_entity_parts` and `create_intersection_parts` are often called consecutively on the same element, we can optimize a bit. To avoid double computation, we always store the entity parts and intersection parts for the lastly treated element in the cache. Storing all configurations for the whole grid would be too memory intensive.

Finally the question of domain indices remains. In other words we have to sort the entity parts into sub-domains satisfying our requirements. The easiest way of doing that is to assign a consecutive domain index to every sub-domain. Obviously this guarantees different indices on different sides of the crack inside an element. While this approach works, it is awfully slow. It would result in a new set of basis functions for every entity part in the construction of the UDG basis. Hence we would loose the benefit that cut-cell methods have over remeshing techniques. To reduce the computational costs of solving PDEs we would thus like to reduce the number of sub-domains. To combine entity parts on the same side of the crack essentially is a graph coloring problem. We take the entity parts as graph vertices $\mathcal{V}$ and the connecting intersections as graph edges $\mathcal{E}$. Partitioning $\mathcal{E} = \mathcal{E}_1 \cup \mathcal{E}_2$ we can assume that exactly the edges in $\mathcal{E}_1$ belong to the crack. We want to color the resulting graph in a way that vertices connected by an edge in $\mathcal{E}_1$ must obtain different colors. Vertices connected by an edge in $\mathcal{E}_2$ should obtain the same color if this is possible without violating the first rule. Note that there might occur situations where it is not possible due to crack tips, see Figure 5.5 for such an example and the corresponding graph. If it is not important to guarantee the optimal coloring (i.e. to use the smallest possible number of colors), the standard algorithm for a graph coloring is a greedy algorithm as described for example in [MMI72]. Assume a sufficient number of colors equipped with some ordering given. We start with an arbitrary vertex and color it with the *first available color*. Then we follow all edges in $\mathcal{E}_2$ starting at this vertex and color the neighboring vertices. If we reach a vertex $V \in \mathcal{V}$ that is not connected to any already colored

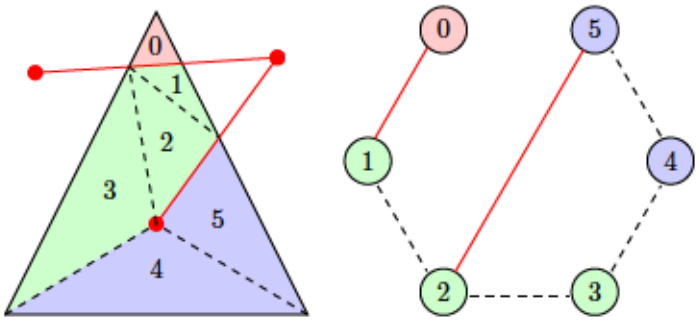

Figure 5.5: Example coloring for a triangle containing a crack tip. Although entity part 5 is connected to entity part 2 via 3 and 4, they lie on opposite sides of the crack. Thus they must have different colors. On the right the corresponding graph is depicted.

vertex by an edge from $\mathcal{E}_1$, we choose the first color not taken. If otherwise V is connected to at least one already treated vertex by an edge from $\mathcal{E}_1$, we have to choose more carefully. In this case we search all neighbors connected to V through edges in $\mathcal{E}_1$ for the first missing color. V is then assigned the maximum of this color and the *first available color* for this connected component. We continue this procedure through all vertices connected by edges in $\mathcal{E}_2$ until none are left.

If the graph is not connected only considering edges in $\mathcal{E}_2$, we start over with the next component. The *first available color* for this subsequent component will be the first color not assigned to any node so far. An example of a coloring gained this way is shown in Figure 6.4.

In contrast to former implementations of UDG the resulting partitioning in sub-domains has a dynamically changing size. More precisely, the number of sub-domains is not only unknown a-priori but can also change during crack propagation. Thus it was necessary to implement a new representation of a finite element that can handle a basis of dynamic size.

6 Numerical experiments

Let us now validate our model with some studies. Examining three different examples we show its capability to numerically simulate the propagation of fluid-filled pressurized fractures.

6.1 Pure mode I loading

We first consider an example without pressure to validate our code in the pure elasticity setting. Further we use this example to discuss the results of crack reconstruction. As in [KM10] crack propagation is initiated by a pure mode I loading. Considering a square of length b with an initial crack of length a along the line $[b-a, b] \times \left\{\frac{b}{2}\right\}$, we tear at top and bottom simultaneously with an increasing tension $|\sigma| = 6\text{N}/\left(\text{mm}^2\text{s}\right) \cdot t$. For the setup and the initial crack choosing $b = 1\text{mm}$ and $a = 0.25\text{mm}$ see Figure 6.1. We apply Neumann boundary conditions for the displacement in y-direction. The displacement in x-direction is equipped with homogeneous Dirichlet boundary conditions at $\{0\} \times [0,1]$ and homogeneous Neumann boundary conditions on the other boundaries. For the phase field we choose homogeneous Neumann boundary conditions at $\{0\} \times [0,1]$ and $\{1\} \times [0,1]$. On the upper and lower boundary we implement Dirichlet boundary conditions. The material parameters are $G_c = 1.0\text{N/mm}$ and $\mu = \lambda = 22\text{kN/mm}^2$. All computations in this section are executed with $k = 10^{-10}$ and $\eta = 10$.

This model problem allows for an analytical solution for the critical load σ_{crit} at which the crack starts to propagate. Having $\lambda = \mu$ and a and b as above, the formula given in [GS11] simplifies to

$$\sigma_{crit} = \sqrt{\frac{4\lambda}{3\text{mm}\tan\left(\frac{\pi}{8}\right)} G_c} \cdot C^{-1} \quad \text{with} \quad C = \frac{1.257 + 0.37\left(1 - \sin\left(\frac{\pi}{8}\right)\right)^3}{\cos\left(\frac{\pi}{8}\right)}. \tag{6.1}$$

The critical time t_{crit}, at which crack propagation starts, is obtained from the critical load via $t_{crit} = \sigma_{crit} \cdot \left(6\frac{\text{N}}{\text{mm}^2}\right)^{-1}$. Figure 6.2 plots the time at which the crack starts propagating. It also shows an example of the phase field at this time step. As can be seen the numerical solution is in very good agreement with the analytical one given by equation (6.1). Numerically t_{crit} is taken as the first time step, at which φ at the first node in front of the initial crack becomes lower than 0.003. Looking at Table 6.1 there is a very sharp decline of the values of φ at this time, indicating that the threshold $\varphi < 0.003$ is sufficient.

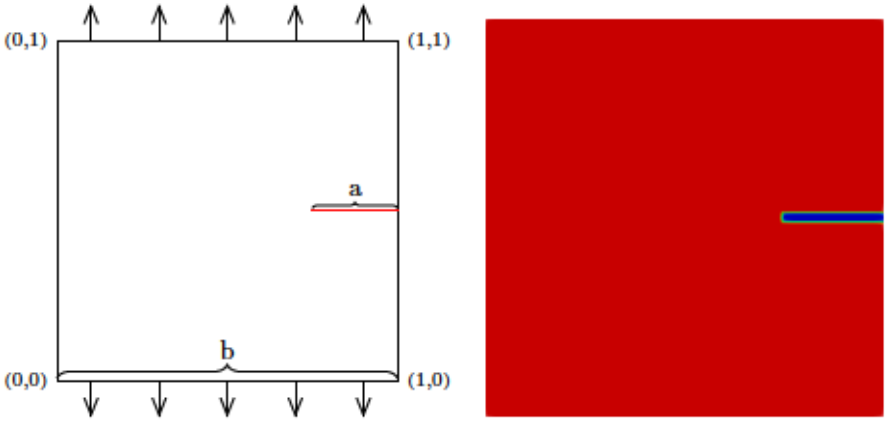

Figure 6.1: Symmetric load example: Setup on the left and initial crack for $h = 0.0078125$ on the right.

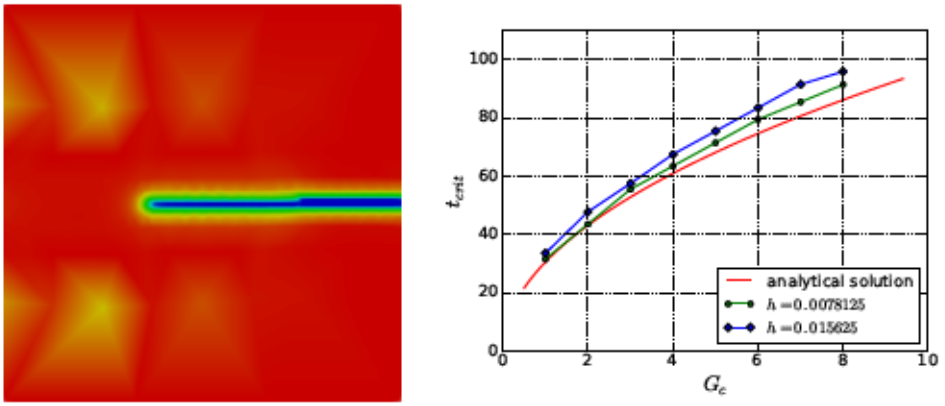

Figure 6.2: Symmetric load example: Left: Example of φ at t_{crit} for $h = 0.0078125$. Right: Starting time of crack propagation for $\varepsilon = 0.05h^{1/4}$ and different values of G_c compared to the analytical solution.

t	0	7.5	15.5	23.5	31.5	39.5	47.5	55.5
φ	1.0	0.9926	0.99063	0.98717	0.98202	0.97483	0.96497	0.95124
t	63.5	67.5	71.5	71.50001526	71.502	71.5117	71.5205	71.535
φ	0.9308	0.89231	0.83801	7.8454e-4	7.8454e-4	7.8454e-4	7.8454e-4	7.8454e-4

Table 6.1: Values of φ at the node in front of the initial crack for exemplary times t and $G_c = 5$.

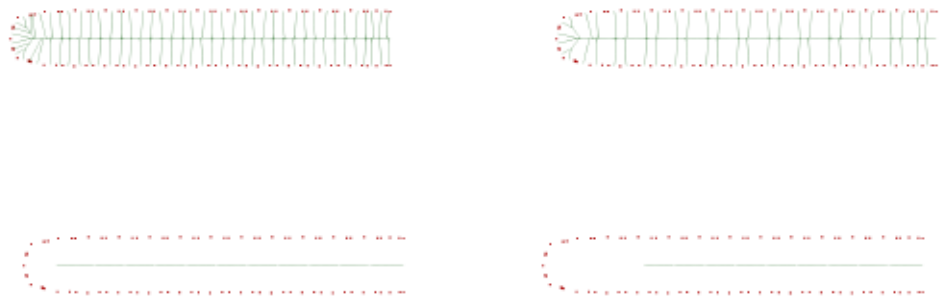

Figure 6.3: Symmetric load example: Skeleton reconstruction as the medial axis (green) of the level set $\varphi = \varphi^*$ (red). First we show the Voronoi diagram for $\varphi^* = 0.5$ at $t = 0.5$, then the pruned Voronoi diagram for the pruning parameters 0.01, 0.1 and 0.3.

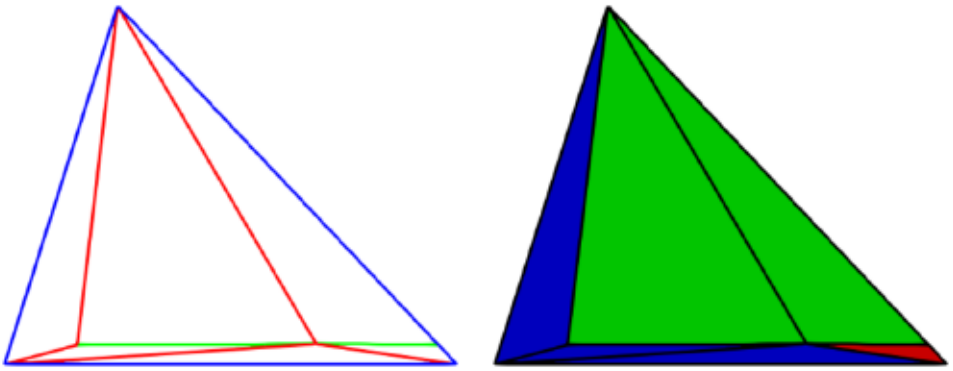

Figure 6.4: Symmetric load example: Construction of the sub-triangulation. On the left the mesh is shown, edges that are part of the skeleton are depicted in green. On the right the partition in sub-domains is depicted. Note that on opposite sides of the crack we always have different colors.

Let us now study the reconstruction of the crack as the skeleton of the level set $\varphi = \varphi^*$ for some threshold value φ^*. In Figure 6.3 we show the process of reconstructing the skeleton in more detail. First, the level set $\varphi = \varphi^*$ is constructed. Second, its Voronoi diagram is computed. Finally the skeleton is pruned to delete unnecessary branches as described in Section 5.2. Note that the pruning factor has to be chosen sufficiently large as to avoid *false* branches. On the other hand, the larger the pruning factor, the more the tip is pruned as well. Once the crack is reconstructed, it has to be included in the grid as described in Section 5.3. An example of the resulting sub-triangulation for one triangle is shown in Figure 6.4.

In Figure 6.5 we study the influence of the threshold value φ^*. As can be seen, there is almost no visible difference between the different reconstructions. Hence the influence of the choice of φ^* on the result is negligible. This is confirmed again looking at the starting times of crack propagation with respect to φ^* as shown in Table 6.2.

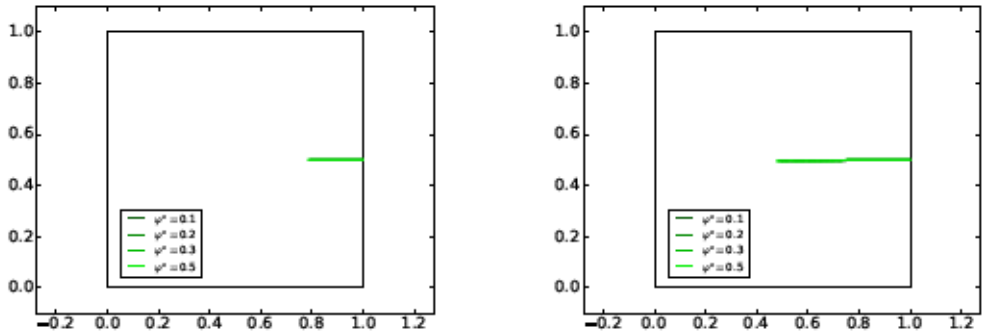

Figure 6.5: Symmetric load example: Skeleton reconstruction as the medial axis of the level set $\varphi = \varphi^*$ for different thresholds φ^* at initial time (left) and after crack propagation started (right).

threshold φ^*	0.1	0.2	0.3	0.5
t_{crit}	71.5	71.5	71.5001	71.5

Table 6.2: Values of t_{crit} for different thresholds φ^* and $G_c = 5$.

6.2 Constant pressure

Let us now consider an example with a non-zero pressure in the crack. The configuration we choose was also studied in [WWW14, MWW15b]. We choose $\Omega = (0, 4) \times (0, 4)$ as computational domain and prescribe homogeneous Dirichlet boundary conditions for the displacement. The Dirichlet boundary condition $\varphi = 1$ is set for the phase field and the initial configuration includes a crack $\mathcal{C} = (1.8, 2.2) \times \{2.0\}$. We use a mesh adapted to the initial crack, see Figure 6.6.

The crack is forced to open by a constant pressure $p = 10^{-3}\text{N/m}^2$. The material parameters are $\lambda = 0.277778\text{N/m}^2$, $\mu = 0.416667\text{N/m}^2$ and $G_c = 1.0\text{N/m}$. This example corresponds to Sneddon's benchmark example for which he gave an analytic solution for the crack opening displacement (COD) in [Sne46]. The COD is defined by

$$\text{COD} = \int_{-\infty}^{+\infty} \mathbf{u}(x, y) \cdot \nabla \varphi(x, y) \, \mathrm{d}y \, .$$

In this setup Sneddon provides an analytical solution for the COD as

$$\text{COD} = 4 l_0 p \frac{1 - \nu^2}{E} \sqrt{\left(1 - \frac{x^2}{l_0^2}\right)}, \tag{6.2}$$

where $2l_0$ is the initial crack length and E and ν are Young's modulus and Poisson's ratio, respectively.

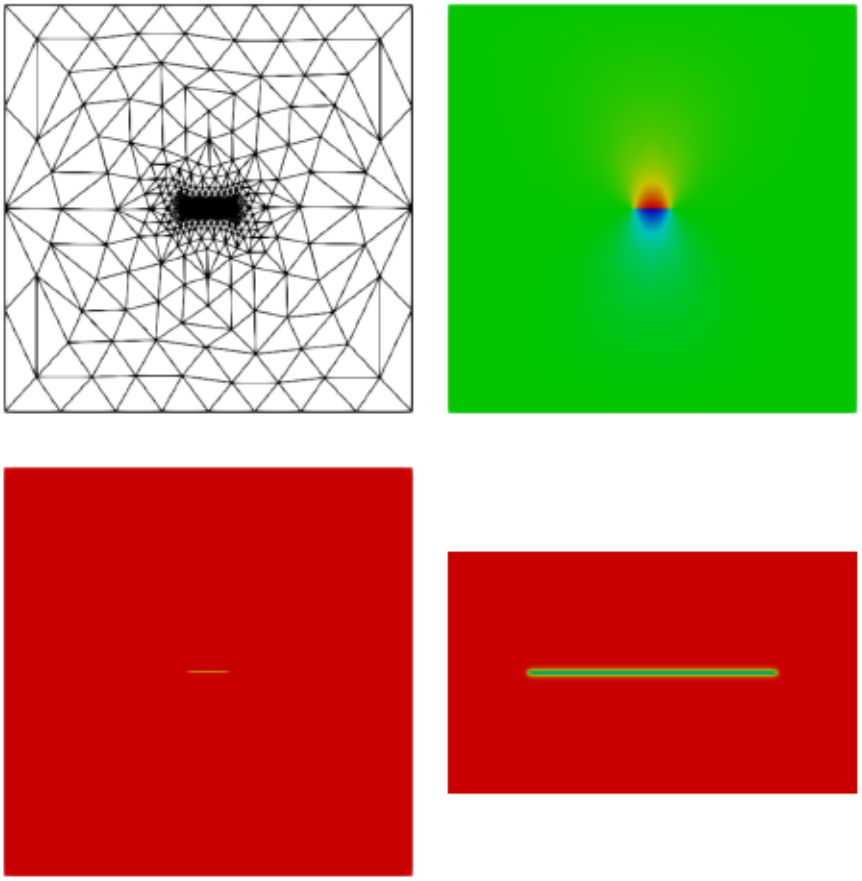

Figure 6.6: Constant pressure example: Mesh, solution $\mathbf{u}_y$ for the displacement in y-direction and solution φ for the phase field for $h = 0.00004882$, $\varepsilon = 0.003125$ and $k = 10^{-7}$.

Figure 6.6 shows a computed solution of the displacement in y-direction and of the phase field. In Figure 6.7 we compare the solution obtained with a DG discretization with the one obtained for UDG for fixed parameters. Namely we fixed $h = 0.00004882$, $\varepsilon = 0.003125$ and $k = 10^{-7}$. Warping the solution by the displacement vector it is obvious that the UDG solution allows for an actual discontinuity at the crack. In addition we note that the weakly enforced continuity in the DG case leads to a slightly smaller peak displacement. Indeed the maximal u_Y is $3.1 \cdot 10^{-4}$ for DG and $4.2 \cdot 10^{-4}$ for UDG. This observation is backed up by the smaller COD obtained with the fitted discontinuous Galerkin discretization as shown in Figure 6.8.

In the following we study the influence of the parameters ε, k, the DG penalty parameter η and the mesh size h, comparing the numerically computed solution for the COD with the analytical one given by equation (6.2). In Figure 6.8 we fix $h = 0.00004882$, $\varepsilon = 0.003125$ and $k = 10^{-7}$. Varying η we notice that as soon as η is sufficiently large its influence is negligible. Therefore all other simulations are carried out with fixed $\eta = 10$. Next, Figure 6.9 studies the influence of the coercivity parameter k. To this end, we study two configurations, a coarse one with $h = 0.00078125$ and $\varepsilon = 0.01397542$ and a fine one with $h = 0.00004882$ and $\varepsilon = 0.003125$. Obviously as soon as we choose k smaller than 10^{-3} it has no further influence on the solution. Hence it seems justified to run all further simulations with $k = 10^{-7}$.

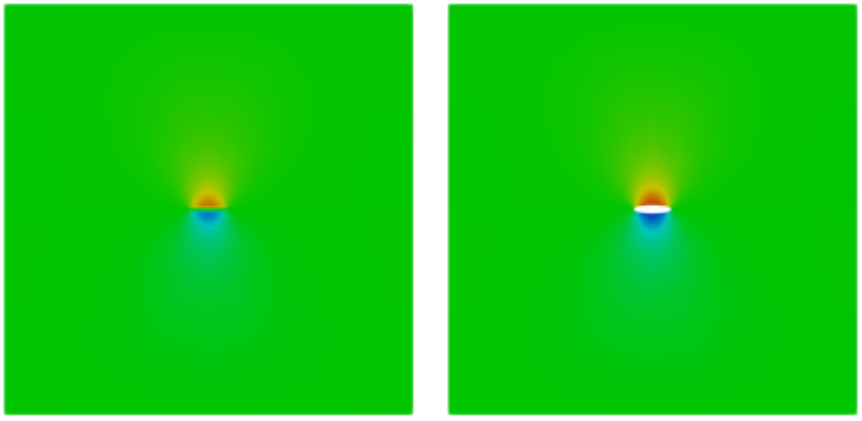

Figure 6.7: Constant pressure example: Comparison of the solution for the displacement warped by 100**u** for DG (left) and UDG (right) for $\varepsilon = 0.003125$, $h = 0.00004882$ and $k = 10^{-7}$.

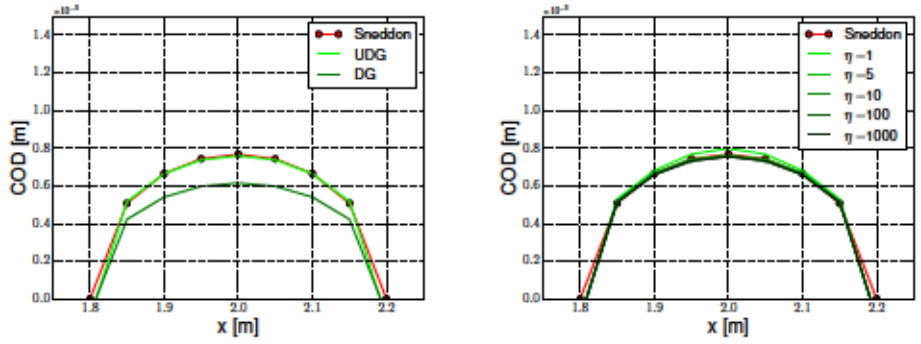

Figure 6.8: Constant pressure example: Comparison of the COD for DG and UDG on the left and convergence with respect to η on the right, both for $\varepsilon = 0.003125$, $h = 0.00004882$ and $k = 10^{-7}$.

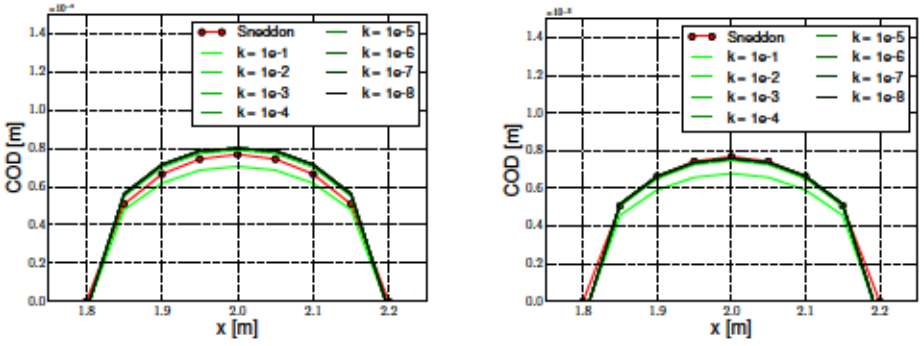

Figure 6.9: Constant pressure example: Convergence with respect to the coercivity parameter k for $h = 0.00078125$, $\varepsilon = 0.01397542$ (left) and for $h = 0.00004882$, $\varepsilon = 0.003125$ (right).

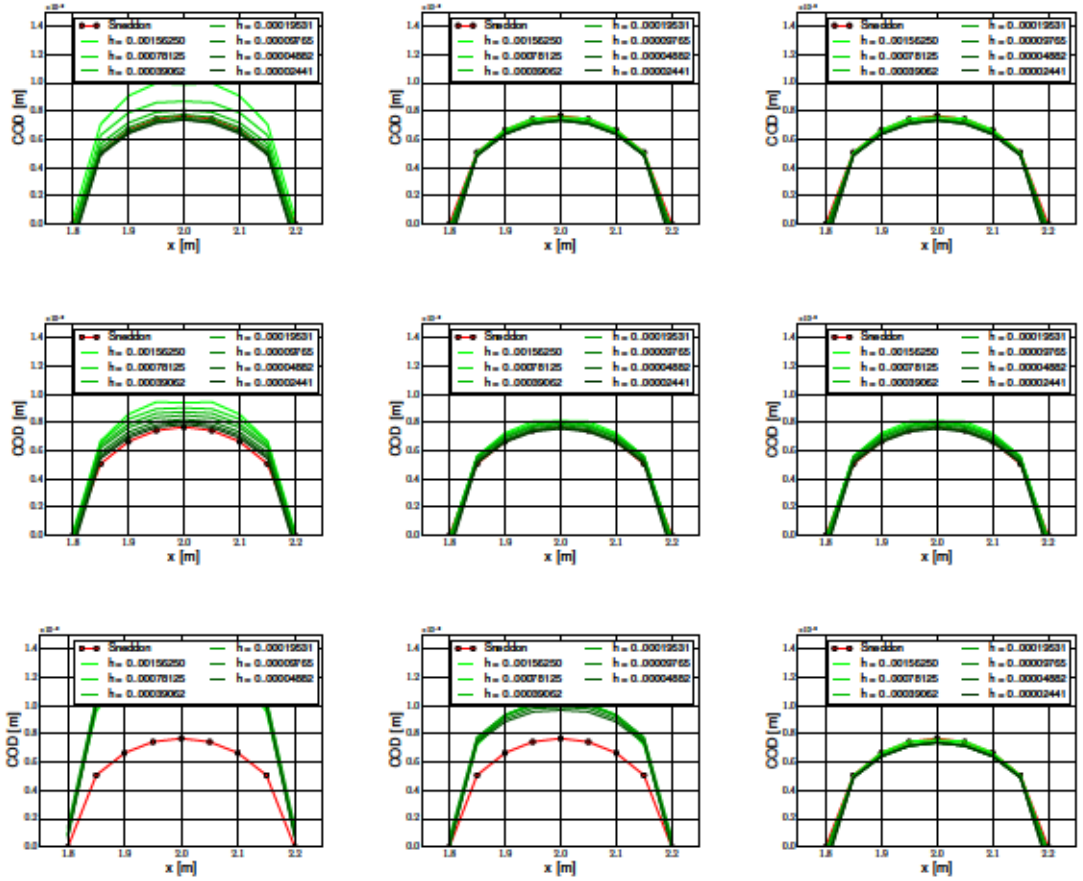

Figure 6.10: Constant pressure example: Convergence with respect to ε and h. First row $\varepsilon = 30h$, $\varepsilon = 2h$ and $\varepsilon = h$, second row $\varepsilon = h^{1/2}$, $\varepsilon = 0.5h^{1/2}$ and $\varepsilon = 0.1h^{1/2}$, third row $\varepsilon = 0.5h^{1/4}$, $\varepsilon = 0.25h^{1/4}$ and $\varepsilon = 0.01h^{1/4}$.

Let us finally analyze the relationship of ε and h in more detail and study the convergence with respect to these parameters. We consider three regimes:

- $\varepsilon = ch$,
- $\varepsilon = ch^{1/2}$ and
- $\varepsilon = ch^{1/4}$,

each for three different constants c. As can be seen in Figure 6.10 we achieve convergence in any of them. Nevertheless we notice that not in all cases the convergence approaches the analytical solution for the COD. In fact, the smaller c, the better we approximate Sneddon's solution. For a sufficiently small c, that is sufficiently small ε, a rather large mesh size h suffices to get good results. In Figure 6.11 we study the convergence in h and ε separately. For $h = 0.0004882$ we obtain good convergence for decreasing ε. For a rather large $\varepsilon = 0.03125$ no convergence in h can be observed. On the other hand, if we choose ε sufficiently small, a good agreement with equation (6.2) can be reached even for large values of h.

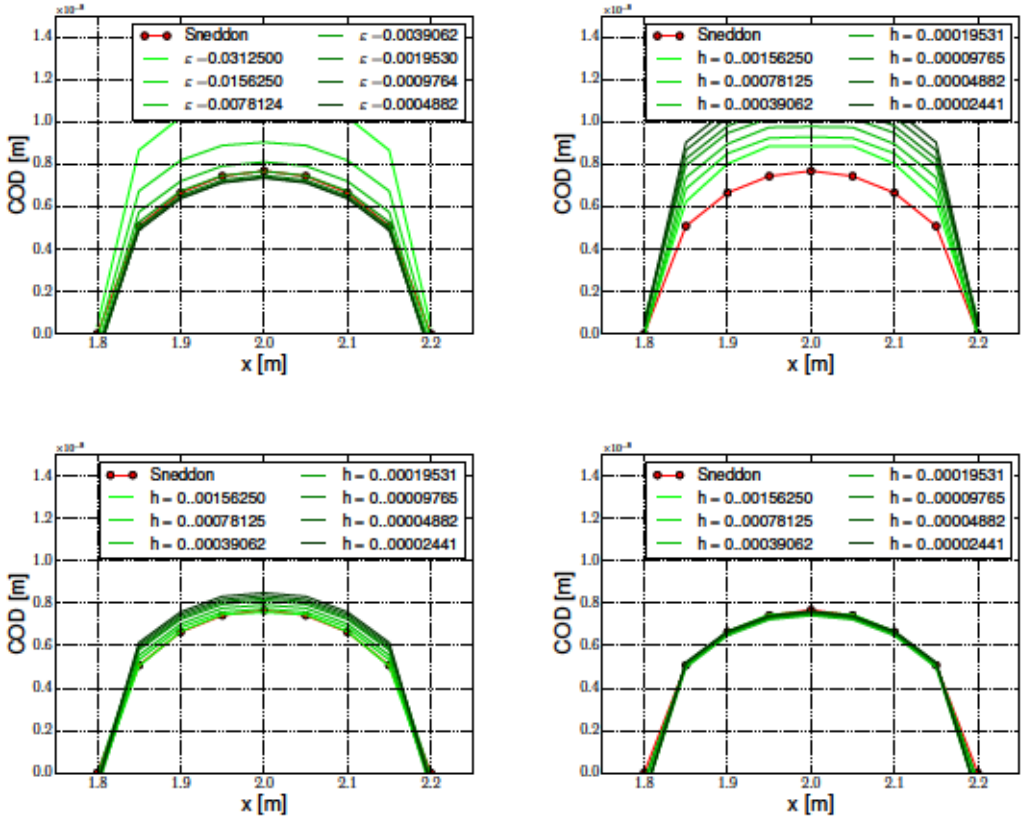

Figure 6.11: Constant pressure example: Convergence with respect to ε for fixed $h = 0.0004882$ and with respect to h for fixed $\varepsilon = 0.03125$, $\varepsilon = 0.01$ and $\varepsilon = 0.003125$, respectively.

6.3 Two cracks joining

In the final example we show the capability of the method combining UDG with a phase-field approach to handle topological changes in the fractures as the joining of two cracks. Starting with the same domain configuration and boundary conditions as in Section 6.2 we add an additional initial crack along the line $\{2.6\}\times[1.0, 3.0]$. As before we set $\lambda = 0.277778\text{N/m}^2$, $\mu = 0.416667\text{N/m}^2$ and $G_c = 1.0\text{N/m}$, but increase the applied pressure in every time-step. Namely we force the cracks open by applying $p = 0.1t$. This leads to crack propagation and joining as shown in Figure 6.12 where the phase field is depicted at different times. The reconstructed crack starts out with two connected components that also join.

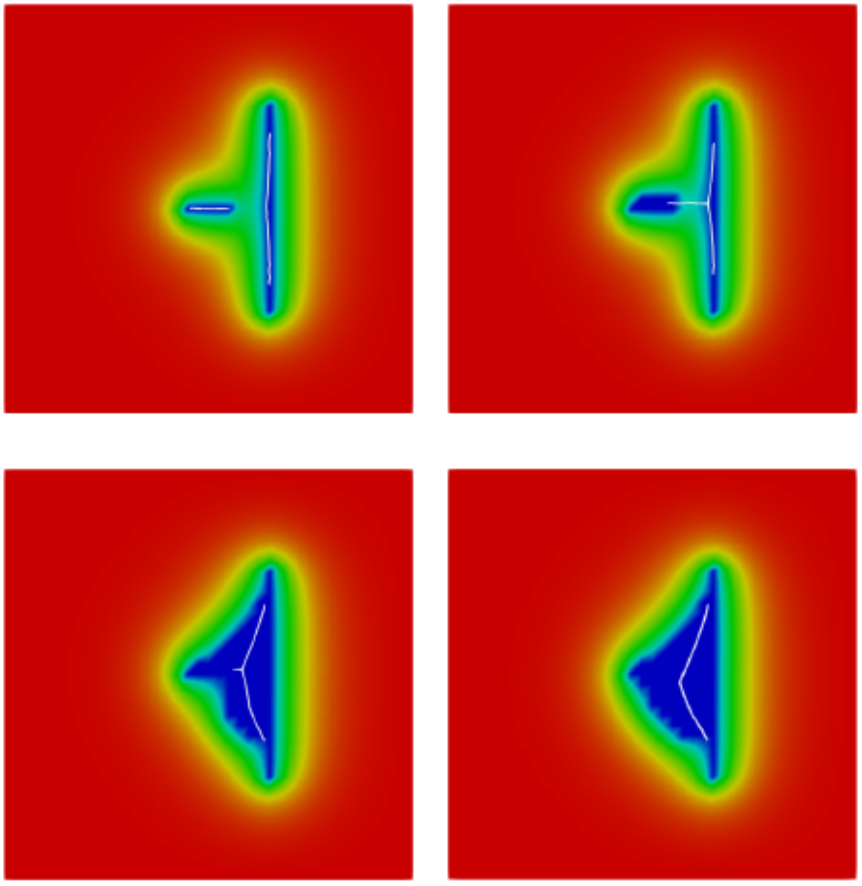

Figure 6.12: Joining cracks example: Solution for the phase field and the reconstructed crack (white) at $t = 0.5$, $t = 0.875$, $t = 0.882812$ and $t = 0.883301$. The residual threshold is $r^* = 0.15$, the level set is $\varphi = 0.3$ and $\varepsilon = 0.26$.

We remark that in this case the choice of the level set $\varphi = \varphi^*$ plays a more important role than it did previously. Depending on φ^* the level sets will join earlier than the cracks and thus the skeletons join before the cracks, too. The strong influence of φ^* is also illustrated in Figure 6.13. A similar effect can be observed for large values of ε, see Figure 6.14. If ε is chosen large, the smearing zone is rather large as well. Thus the level set for a given threshold moves away from the cracks and already joins at an earlier time, leading to a connected crack reconstruction.

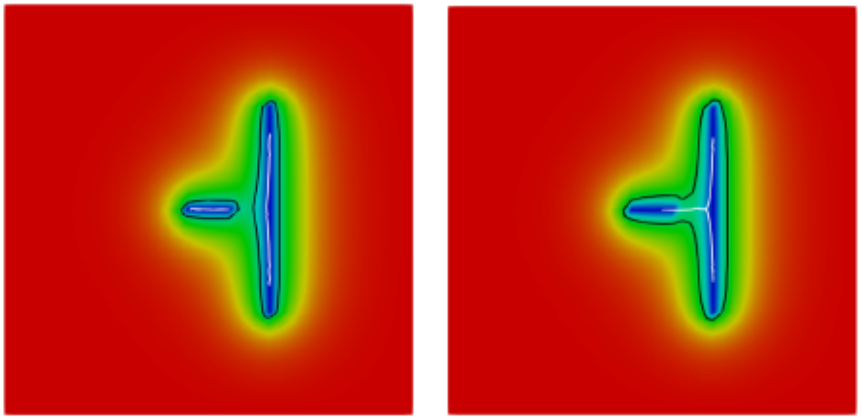

Figure 6.13: Joining cracks example: Solution for the phase field and the reconstructed crack (white) at $t = 0.5$ as medial axis of the level set (black) at $\varphi^* = 0.3$ and $\varphi^* = 0.4$. The residual threshold is $r^* = 0.15$ and $\varepsilon = 0.26$.

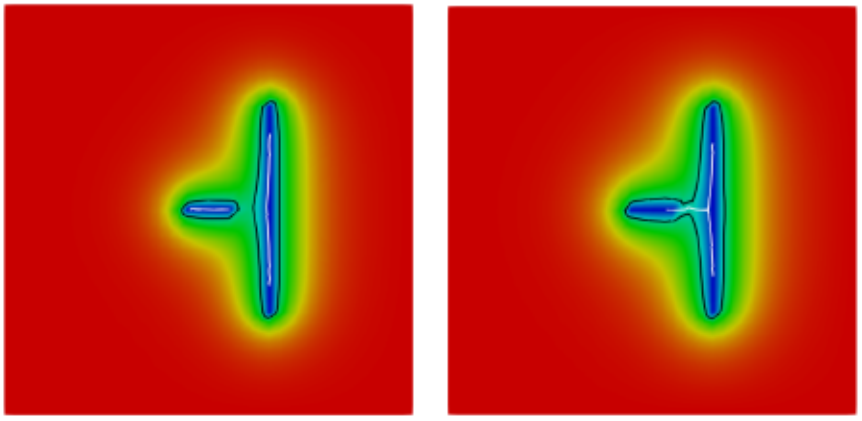

Figure 6.14: Joining cracks example: Solution for the phase field and the reconstructed crack (white) at $t = 0.5$ for $\varepsilon = 0.26$ and $\varepsilon = 0.3$. The residual threshold is $r^* = 0.15$ and the level set (black) is taken at $\varphi^* = 0.3$.

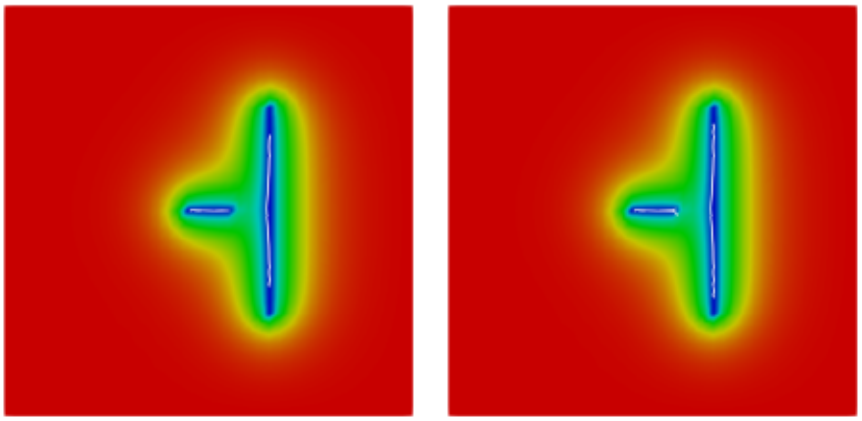

Figure 6.15: Joining cracks example: Solution for the phase field and the reconstructed crack (white) at $t = 0.5$ for $r^* = 0.15$ and $r^* = 0.1$. The level set is taken at $\varphi^* = 0.3$ and $\varepsilon = 0.26$.

Finally let us show the influence of the residual threshold r^*. In Figure 6.15 one notes that on the right side, for smaller residual threshold, the vertical crack is less pruned. On the other hand, unimportant, branching parts of the horizontal crack are not pruned. Thus the choice of r^* has an important influence on the resulting reconstruction.

7 Summary and outlook

This thesis is concluded by summarizing the achievements and providing an outlook towards potential further developments. In Section 3.1 we were able to prove Γ-convergence of the regularized energy functionals in a one-dimensional setting with respect to convergence in L^1. The key ingredient was Young's inequality that allowed us to reuse the corresponding properties from the case without pressure terms. The result was generalized to a setting with Dirichlet boundary conditions. Relying on recent work on the properties of the space $GSBD(\Omega;\mathbb{R}^n)$ we were able to generalize our findings to higher dimensions in Section 3.2. Under some geometrical constraints we were able to include Dirichlet and homogeneous Neumann boundary conditions into the proof of Γ-convergence. The question how to include non-homogeneous Neumann boundary conditions still remains open and could be the subject of future work. To answer it one would need to study the properties of traces in the case of functions in $GSBD(\Omega;\mathbb{R}^n)$ in more detail. There are already some results in that direction, especially dealing with functions in $BD(\Omega;\mathbb{R}^n)$ [Bab15]. One can also deduce some properties of truncations of $GSBD(\Omega;\mathbb{R}^n)$-functions as in [Iur14]. However, to our knowledge no general results are known for $GSBD(\Omega;\mathbb{R}^n)$. The analytical part of this thesis was concluded in Section 3.3 by showing convergence of minimizers of the regularized functionals to minimizers of the Γ-limit functional in the presence of a fidelity term. Crucial to this proof was the equi-coercivity of the included functionals. Unfortunately, in the context of fracture propagation the fidelity term guaranteeing equi-coercivity is rather artificial. Thus it would be interesting to study other requirements under which convergence of minimizers can be shown. One possibility might be to benefit from fixed Dirichlet boundary data. Some steps in that direction can be found in the recent literature [FS18, CC18]. As they rely on a Γ-convergence result with respect to convergence in measure, at present they are not applicable to the situation with pressure terms.

In Section 4.1 we derived a discretization scheme to numerically solve the minimization problem for the regularized energies. We followed a split approach, alternatingly solving for the displacement and the phase field in a fixed-point iteration. The irreversibility constraint for the phase field was treated as a non-smooth obstacle, allowing us to apply the truncated non-smooth Newton multigrid method to solve for the phase field. For the displacement we derived a DG discretization. Assuming a given reconstruction of the crack we adapted it to construct an unfitted DG discretization that allows for actual discontinuities of the displacement along fractures. Section 4.2 discussed how to reconstruct the crack from a given regularization, that is from a given phase-field representation. Based on geometric considerations we reconstructed the crack as skeleton of a level set of the phase field. Numerically, the skeleton was computed as pruned Voronoi diagram of point sites.

The numerical challenges of the construction of the skeleton and its integration into the grid were solved in Chapter 5. In particular, an advancing front algorithm ensured that the connectivity of the skeleton, and thus its topology, remains unchanged even if numerical inaccuracies occur. A graph coloring algorithm reduced the number of sub-domains in cut grid cells and thereby the number of newly introduced degrees of freedom along the crack. Finally, in Chapter 6 we showed that our method is capable of simulating crack propagation. In a first example we showed that in the presence of a single crack the reconstruction of the skeleton seems to be robust with respect to the chosen level set of φ. A second example, including pressure terms, was used to show convergence with respect to the mesh size h and the regularization parameter ε. Finally, we proved the capability of our method to handle topological changes in a third example, where two initially disconnected fractures join due to an applied increasing pressure. In the case of multiple fractures the chosen level set of φ and the residual threshold r^* can have a strong influence on the reconstructed crack.

Nevertheless there remains room for improvements. One major numerical challenge is that a proper initialization of the phase field requires having element boundaries along initial cracks. As at the moment the phase field and the displacement are defined on the same grid this leads to having many Voronoi edges very close to element edges. Thus we obtain very small sub-domains compromising stability. A possible solution to this problem would be the decoupling of the grids for displacement and phase field. This would need to be done very carefully. As the two subproblems are coupled to each other, an interpolation of the solution for the displacement and the phase field onto the respective other grid would be necessary in every iteration of the fixed-point scheme. To avoid the computational costs getting out of hand, choosing hierarchical grids seems reasonable. Thus the phase-field grid would be a refinement of the displacement grid. Preferably one would try to construct grids where initial cracks are along edges of the refined grid, but not included in the coarse grid. An additional advantage of separate grids would be the reduction of computational costs due to the substantial reduction of degrees of freedom for the displacement, benefiting even more from the advantages of an unfitted method.

A second possibility to improve the method is to limit the phase-field representation to areas around the tip of fractures. Similar to [GSF17], one could fix the already reconstructed crack and only determine new parts of it as soon as propagation is indicated by the phase field. Besides the reduction of computational costs due to far fewer degrees of freedom for the phase field, this method also has the benefit of explicitly including the irreversibility condition for the crack in its reconstruction. So far we only guarantee irreversibility for the phase field. On the other hand the method has a major disadvantage. As described in [GSF17], to present it is not capable of tracking crack initiation, that is finding new crack tips. Thus also merging and branching of cracks can not be handled to the present. Hence while this approach inherits the accurate prediction of propagation path and velocity from phase-field methods, it looses the further advantage of implicitly handling topological changes. Finally, we note that stability of the numerical scheme might be improved using ghost penalties.

Bibliography

[ABCM02] D. N. Arnold, F. Brezzi, B. Cockburn, and L. D. Marini. Unified analysis of discontinuous Galerkin methods for elliptic problems. *SIAM Journal on Numerical Analysis*, 39(5):1749–1779, 2001/02. (pages 27, 28).

[ABE09] D. Attali, J.-D. Boissonnat, and H. Edelsbrunner. *Mathematical Foundations of Scientific Visualization, Computer Graphics, and Massive Data Exploration*, chapter Stability and Computation of Medial Axes - a State-of-the-Art Report, pages 109–125. Springer Berlin Heidelberg, Berlin, Heidelberg, 2009. (page 80).

[ACDM97] L. Ambrosio, A. Coscia, and G. Dal Maso. Fine properties of functions with bounded deformation. *Archive for Rational Mechanics and Analysis*, 139(3):201–238, 1997. (pages 20, 21, 22, 23).

[AdB92] C. Arcelli and G. S. di Baja. Ridge points in euclidean distance maps. *Pattern Recognition Letters*, 13(4):237 – 243, 1992. (page 80).

[AFP00] L. Ambrosio, N. Fusco, and D. Pallara. *Functions of bounded variation and free discontinuity problems*, volume 254. Clarendon Press Oxford, 2000. (pages 14, 15, 47, 63).

[Amb89] L. Ambrosio. A compactness theorem for a new class of functions of bounded variation. *Bollettino della Unione Matematica Italiana*, 3(4):857–881, 1989. (pages 2, 18).

[Amb90] L. Ambrosio. Existence theory for a new class of variational problems. *Archive for Rational Mechanics and Analysis*, 111(4):291–322, 1990. (page 18).

[Arn82] D. N. Arnold. An interior penalty finite element method with discontinuous elements. *SIAM Journal on Numerical Analysis*, 19(4):742–760, 1982. (page 28).

[AT90] L. Ambrosio and V. M. Tortorelli. Approximation of functionals depending on jumps by elliptic functionals via Γ-convergence. *Comm. Pure Appl. Math.*, 43(8):999–1036, 1990. (pages 10, 36).

[Bab15] J.-F. Babadjian. Traces of functions of bounded deformation. *Indiana University Mathematics Journal*, pages 1271–1290, 2015. (page 103).

[BB07] M. Blatt and P. Bastian. The iterative solver template library. In B. Kågström, E. Elmroth, J. Dongarra, and J. Waśniewski, editors, *Applied Parallel Computing. State of the Art in Scientific Computing*, pages 666–675, Berlin, Heidelberg, 2007. Springer Berlin Heidelberg. (page 83).

[BB08] M. Blatt and P. Bastian. On the generic parallelisation of iterative solvers for the finite element method. 4:56, 2008. (page 83).

[BBD+08a] P. Bastian, M. Blatt, A. Dedner, C. Engwer, R. Klöfkorn, R. Kornhuber, M. Ohlberger, and O. Sander. A generic grid interface for parallel and adaptive scientific computing. II. Implementation and tests in DUNE. *Computing. Archives for Scientific Computing*, 82(2-3):121–138, 2008. (page 83).

[BBD+08b] P. Bastian, M. Blatt, A. Dedner, C. Engwer, R. Klöfkorn, M. Ohlberger, and O. Sander. A generic grid interface for parallel and adaptive scientific computing. I. Abstract framework. *Computing. Archives for Scientific Computing*, 82(2-3):103–119, 2008. (page 83).

[BBS09] P. Bastian, G. Buse, and O. Sander. Infrastructure for the coupling of dune grids, 2009. (page 83).

[BCDM98] G. Bellettini, A. Coscia, and G. Dal Maso. Compactness and lower semicontinuity properties in $SBD(\Omega)$. *Mathematische Zeitschrift*, 228(2):337–351, 1998. (page 20).

[BCXZ03] T. Belytschko, H. Chen, J. Xu, and G. Zi. Dynamic crack propagation based on loss of hyperbolicity and a new discontinuous enrichment. *Int. J. Numer. Meth. Eng.*, 58(12):1873–1905, 2003. (page 2).

[BDE+05] P. Bastian, M. Droske, C. Engwer, R. Klöfkorn, T. Neubauer, M. Ohlberger, and M. Rumpf. Towards a unified framework for scientific computing, 2005. (page 83).

[BE09] P. Bastian and C. Engwer. An unfitted finite element method using discontinuous Galerkin. *International Journal for Numerical Methods in Engineering*, 79(12):1557–1576, 2009. (pages 3, 25, 29, 77).

[BFM00] B. Bourdin, G. A. Francfort, and J.-J. Marigo. Numerical experiments in revisited brittle fracture. *J. Mech. Phys. Solids*, 48(4):797–826, 2000. (pages 2, 6, 10).

[BFM08] B. Bourdin, G. A. Francfort, and J.-J. Marigo. The variational approach to fracture. *J. Elasticity*, 91(1-3):5–148, 2008. (pages 2, 6).

[BHM10] P. Bastian, F. Heimann, and S. Marnach. Generic implementation of finite element methods in the distributed and unified numerics environment (DUNE). *Kybernetika*, 46(2):294–315, 2010. (page 83).

[Bio55] M. A. Biot. Theory of elasticity and consolidation for a porous anisotropic solid. *J. Appl. Phys.*, 26:182–185, 1955. (page 8).

[Blu67] H. Blum. A transformation for extracting new descriptors of shape. In W. Wathen-Dunn, editor, *Proc. Models for the Perception of Speech and Visual Form*, pages 362–380, Cambridge, MA, November 1967. MIT Press. (page 78).

[BLyL07] X. Bai, L. J. Latecki, and W. y. Liu. Skeleton pruning by contour partitioning with discrete curve evolution. *IEEE Transactions on Pattern Analysis and Machine Intelligence*, 29(3):449–462, March 2007. (pages 80, 84).

[BM97] I. Babuska and J. M. Melenk. The partition of unity method. *Int. J. Numer. Meth. Eng.*, 40(4):727–758, 1997. (page 2).

[Boo] `https://www.boost.org/doc/libs/1_60_0/libs/polygon/doc/voronoi_main.htm`. Accessed: April 09, 2019. (page 84).

[Bra98] A. Braides. *Approximation of Free-Discontinuity Problems*. Springer-Verlag, Berlin, 1998. (pages 14, 15, 16, 18, 34, 35, 36, 37, 38, 40, 49).

[Bra02] A. Braides. Γ-*Convergence for Beginners*. Oxford University Press, Oxford, 2002. (pages 11, 13, 42, 47).

[Bra07] D. Braess. *Finite elements*. Cambridge University Press, Cambridge, third edition, 2007. Theory, fast solvers, and applications in elasticity theory, Translated from the German by Larry L. Schumaker. (page 25).

[BS08] S. C. Brenner and L. R. Scott. *The mathematical theory of finite element methods*, volume 15 of *Texts in Applied Mathematics*. Springer, New York, third edition, 2008. (page 25).

[BS19] A. Bach and L. Sommer. A γ-convergence result for fluid-filled fracture propagation, 2019. (page 42).

[BZMB04] E. Budyn, G. Zi, N. Moës, and T. Belytschko. A method for multiple crack growth in brittle materials without remeshing. *Int. J. Numer. Meth. Eng.*, 61(10):1741–1770, 2004. (page 2).

[Cal65] L. Calabi. *A Study of the Skeleton of Plane Figures*. Scientific Report // Parke Mathematical Laboratories. Parke Mathematical Laboratories, 1965. (page 78).

[CC18] A. Chambolle and V. Crismale. Compactness and lower semicontinuity in *GSBD*. *arXiv preprint arXiv:1802.03302*, 2018. (pages 64, 103).

[CC19] A. Chambolle and V. Crismale. A density result in GSBDp with applications to the approximation of brittle fracture energies. 232:1329–1378, 2019. (pages 20, 23, 42, 49, 55, 56, 57, 58, 59, 60, 61).

[CH68] L. Calabi and W. E. Hartnett. Shape recognition, prairie fires, convex deficiencies and skeletons. *The American Mathematical Monthly*, 75:335–342, 1968. (page 78).

[Cha04] A. Chambolle. An approximation result for special functions with bounded deformation. *J. Math. Pures Appl. (9)*, 83(7):929–954, 2004. (page 50).

[Cha05] A. Chambolle. Addendum to: "An approximation result for special functions with bounded deformation" [J. Math. Pures Appl. (9) **83** (2004), no. 7, 929–954; mr2074682]. *J. Math. Pures Appl. (9)*, 84(1):137–145, 2005. (page 50).

[Cia88] P. G. Ciarlet. *Mathematical elasticity. Vol. I*, volume 20 of *Studies in Mathematics and its Applications*. North-Holland Publishing Co., Amsterdam, 1988. Three-dimensional elasticity. (page 66).

[Cia02] P. G. Ciarlet. *The finite element method for elliptic problems*, volume 40 of *Classics in Applied Mathematics*. Society for Industrial and Applied Mathematics (SIAM), Philadelphia, PA, 2002. Reprint of the 1978 original [North-Holland, Amsterdam; MR0520174 (58 #25001)]. (pages 25, 26).

[Cor97] G. Cortesani. Strong approximation of GSBV functions by piecewise smooth functions. *Annali dell'Università di Ferrara*, 43(1):27–49, 1997. (page 19).

[CT99] G. Cortesani and R. Toader. A density result in SBV with respect to non-isotropic energies. *Nonlinear Analysis. Theory, Methods & Applications. An International Multidisciplinary Journal*, 38(5, Ser. B: Real World Appl.):585–604, 1999. (page 19).

[dBvKOS00] M. de Berg, M. van Kreveld, M. Overmars, and O. C. Schwarzkopf. Computational geometry, 2000. (page 84).

[DG75] E. De Giorgi. Sulla convergenza di alcune successioni d'integrali del tipo dell'area. *Ennio De Giorgi*, 414, 1975. (page 11).

[DG77] E. De Giorgi. γ-convergenza e g-convergenza. *Ennio De Giorgi*, page 437, 1977. (page 11).

[DGF75] E. De Giorgi and T. Franzoni. Su un tipo di convergenza variazionale. *Atti Accad. Naz. Lincei Rend. Cl. Sci. Fis. Mat. Natur.(8)*, 58(6):842–850, 1975. (page 11).

[DM12] G. Dal Maso. *An introduction to Γ-convergence*, volume 8. Springer Science & Business Media, 2012. (pages 11, 13).

[DM13] G. Dal Maso. Generalised functions of bounded deformation. 2013. (pages 16, 20, 22, 23, 42).

[DPE12] D. A. Di Pietro and A. Ern. *Mathematical Aspects of Discontinuous Galerkin Methods*. Springer, Heidelberg, 2012. (pages 25, 27, 28, 29, 30, 68, 69, 70, 71).

[DS14] P. Dłotko and R. Specogna. Topology preserving thinning of cell complexes. *IEEE Transactions on Image Processing*, 23(10):4486–4495, 2014. (page 80).

[EG92] L. C. Evans and R. F. Gariepy. *Measure theory and fine properties of functions*. Studies in Advanced Mathematics. CRC Press, Boca Raton, FL, 1992. (pages 14, 15).

[EGMSa] C. Engwer, C. Gräser, S. Müthing, and O. Sander. Function space bases in the dune-functions module. (page 83).

[EGMSb] C. Engwer, C. Gräser, S. Müthing, and O. Sander. The interface for functions in the dune-functions module. (page 83).

[EH12] C. Engwer and F. Heimann. Dune-udg: A cut-cell framework for unfitted discontinuous galerkin methods, 2012. (pages 83, 85).

[EM16] C. Engwer and S. Müthing. Concepts for flexible parallel multi-domain simulations. In *Domain decomposition methods in science and engineering XXII*, volume 104 of *Lect. Notes Comput. Sci. Eng.*, pages 187–195. Springer, Cham, 2016. (page 83).

[EN17] C. Engwer and A. Nüßing. Geometric reconstruction of implicitly defined surfaces and domains with topological guarantees. *Association for Computing Machinery. Transactions on Mathematical Software*, 44(2):Art. 14, 20, 2017. (pages 83, 84, 85).

[Eng09] C. Engwer. *An unfitted discontinuous Galerkin scheme for micro-scale simulations and numerical upscaling.* PhD thesis, 2009. (pages 29, 31).

[ES17] C. Engwer and L. Schumacher. A phase field approach to pressurized fractures using discontinuous galerkin methods. *Mathematics and Computers in Simulation*, 137:266–285, 2017. (pages 33, 65).

[ET76] I. Ekeland and R. Temam. *Convex analysis and variational problems.* North-Holland Publishing Co., Amsterdam-Oxford; American Elsevier Publishing Co., Inc., New York, 1976. Translated from the French, Studies in Mathematics and its Applications, Vol. 1. (pages 72, 75).

[Eva10] L. C. Evans. *Partial differential equations*, volume 19 of *Graduate Studies in Mathematics.* American Mathematical Society, Providence, RI, second edition, 2010. (page 26).

[FB10] T.-P. Fries and T. Belytschko. The extended/generalized finite element method: an overview of the method and its applications. *Int. J. Numer. Meth. Eng.*, 84(3):253–304, 2010. (page 2).

[FEC02] R. Fabbri, L. Estrozi, and F. L. D. Costa. On voronoi diagrams and medial axes. *Journal of Mathematical Imaging and Vision*, 17(1):27–40, 2002. (page 80).

[Fed14] H. Federer. *Geometric measure theory.* Springer, 2014. (page 14).

[FM98] G. A. Francfort and J.-J. Marigo. Revisiting brittle fracture as an energy minimization problem. *J. Mech. Phys. Solids*, 46(8):1319–1342, 1998. (pages 2, 6, 10).

[Foc01] M. Focardi. On the variational approximation of free-discontinuity problems in the vectorial case. *Math. Models Methods Appl. Sci.*, 11(4):663–684, 2001. (pages 34, 36, 42, 44, 47, 50).

[For87] S. Fortune. A sweepline algorithm for Voronoi diagrams. *Algorithmica. An International Journal in Computer Science*, 2(2):153–174, 1987. (page 84).

[FR60] W. H. Fleming and R. Rishel. An integral formula for total gradient variation. *Archiv der Mathematik*, 11:218–222, 1960. (page 16).

[Fri14] T.-P. Fries. Overview and comparison of different variants of the XFEM. *PAMM*, 14(1):27–30, 2014. (page 2).

[FS18] M. Friedrich and F. Solombrino. Quasistatic crack growth in 2d-linearized elasticity. In *Annales de l'Institut Henri Poincare (C) Non Linear Analysis*, volume 35, pages 27–64. Elsevier, 2018. (pages 64, 103).

[GB90] W. Gong and G. Bertrand. A simple parallel 3d thinning algorithm. In *[1990] Proceedings. 10th International Conference on Pattern Recognition*, volume 1, pages 188–190. IEEE, 1990. (page 79).

[GF96] Y. Ge and J. M. Fitzpatrick. On the generation of skeletons from discrete euclidean distance maps. *IEEE Trans. Pattern Anal. Mach. Intell.*, 18(11):1055–1066, November 1996. (page 80).

[GJ09] M. J. Gander and C. Japhet. An algorithm for non-matching grid projections with linear complexity. In *Domain decomposition methods in science and engineering XVIII*, pages 185–192. Springer, 2009. (page 86).

[GJ13] M. J. Gander and C. Japhet. Algorithm 932: Pang: software for nonmatching grid projections in 2d and 3d with linear complexity. *ACM Transactions on Mathematical Software (TOMS)*, 40(1):6, 2013. (page 86).

[GK09] C. Gräser and R. Kornhuber. Multigrid methods for obstacle problems. *Journal of Computational Mathematics*, 27(1):1–44, 2009. (page 72).

[GM] C. Gürkan and A. Massing. A stabilized cut discontinuous galerkin framework: I. elliptic boundary value and interface problems. (page 31).

[GR07] C. Grossmann and H.-G. Roos. *Numerical treatment of partial differential equations.* Universitext. Springer, Berlin, 2007. Translated and revised from the 3rd (2005) German edition by Martin Stynes. (pages 24, 25).

[Gri21] A. A. Griffith. The phenomena of rupture and flow in solids. *Phil. Trans. R. Soc. A*, 221:pp. 163–198, 1921. (pages 2, 6, 9).

[GS11] D. Gross and T. Seelig. *Bruchmechanik.* Springer, Berlin, Heidelberg, 2011. (page 91).

[GSF17] B. Giovanardi, A. Scotti, and L. Formaggia. A hybrid XFEM –phase field (Xfield) method for crack propagation in brittle elastic materials. *Computer Methods in Applied Mechanics and Engineering*, 320:396–420, jun 2017. (pages 2, 78, 104).

[GSS09] C. Gräser, U. Sack, and O. Sander. Truncated nonsmooth Newton multigrid methods for convex minimization problems. In *Domain Decomposition Methods in Science and Engineering XVIII*, volume 70 of *Lect. Notes Comput. Sci. Eng.*, pages 129–136. Springer, Berlin, 2009. (pages 72, 75).

[Hal13] P. R. Halmos. *Measure theory*, volume 18. Springer, 2013. (page 15).

[HCB05] T. J. R. Hughes, J. A. Cottrell, and Y. Bazilevs. Isogeometric analysis: CAD, finite elements, NURBS, exact geometry and mesh refinement. *Computer Methods in Applied Mechanics and Engineering*, 194(39-41):4135–4195, 2005. (page 26).

[Iur14] F. Iurlano. A density result for GSBD and its application to the approximation of brittle fracture energies. *Calculus of Variations and Partial Differential Equations*, 51(1-2):315–342, 2014. (pages 49, 50, 61, 62, 103).

[JZ01] M. Jirásek and T. Zimmermann. Embedded crack model. part ii: Combination with smeared cracks. *International Journal for Numerical Methods in Engineering*, 50(6):1291–1305, 2001. (page 78).

[KM10] C. Kuhn and R. Müller. A continuum phase field model for fracture. *Eng. Fract. Mech.*, 77(18):3625 – 3634, 2010. Computational Mechanics in Fracture and Damage: A Special Issue in Honor of Prof. Gross. (pages 2, 6, 7, 91).

[Koh79] R. V. Kohn. *New estimates for deformations in terms of their strains*. PhD thesis, Princeton University, 1979. (pages 20, 21).

[KP12] P. Kardos and K. Palágyi. *Combinatorial Image Analaysis: 15th International Workshop, IWCIA 2012, Austin, TX, USA, November 28-30, 2012. Proceedings*, chapter On Topology Preservation for Triangular Thinning Algorithms, pages 128–142. Springer Berlin Heidelberg, Berlin, Heidelberg, 2012. (page 80).

[LCLJ10] L. Liu, E. W. Chambers, D. Letscher, and T. Ju. A simple and robust thinning algorithm on cell complexes. *Computer Graphics Forum*, 29(7):2253–2260, 2010. (page 80).

[LeV02] R. J. LeVeque. *Finite volume methods for hyperbolic problems*. Cambridge Texts in Applied Mathematics. Cambridge University Press, Cambridge, 2002. (page 24).

[LL92] F. Leymarie and M. D. Levine. Simulating the grassfire transform using an active contour model. *IEEE Transactions on Pattern Analysis and Machine Intelligence*, 14(1):56–75, Jan 1992. (page 80).

[LLS92] L. Lam, S.-w. Lee, and C. Y. Suen. Thinning methodologies—a comprehensive survey, 1992. (page 79).

[LNSO04] A. Lew, P. Neff, D. Sulsky, and M. Ortiz. Optimal BV estimates for a discontinuous Galerkin method for linear elasticity. *AMRX Appl. Math. Res. Express*, (3):73–106, 2004. (page 66).

[LWH+12] H. Liu, Z. Wu, D. F. Hsu, B. S. Peterson, and D. Xu. On the generation and pruning of skeletons using generalized voronoi diagrams. *Pattern Recognition Letters*, 33(16):2113 – 2119, 2012. (page 80).

[MDB99] N. Moës, J. Dolbow, and T. Belytschko. A finite element method for crack growth without remeshing. *Int. J. Numer. Meth. Eng.*, 46(1):131–150, 1999. (page 2).

[Mer16] A. Merxhani. An introduction to linear poroelasticity. 2016. (page 8).

[MFV98] G. Malandain and S. Fernández-Vidal. Euclidean skeletons. *Image and Vision Computing*, 16(5):317 – 327, 1998. (page 79).

[MHW10] C. Miehe, M. Hofacker, and F. Welschinger. A phase field model for rate-independent crack propagation: robust algorithmic implementation based on operator splits. *Comput. Methods Appl. Mech. Engrg.*, 199(45-48):2765–2778, 2010. (pages 2, 6, 7).

[MMI72] D. W. Matula, G. Marble, and J. D. Isaacson. Graph coloring algorithms. In R. C. Read, editor, *Graph Theory and Computing*, pages 109 – 122. Academic Press, 1972. (page 88).

[MR96] N. Mayya and V. T. Rajan. Voronoi diagrams of polygons: A framework for shape representation. *Journal of Mathematical Imaging and Vision*, 6(4):355–378, 1996. (page 80).

[MS89] D. Mumford and J. Shah. Optimal approximations by piecewise smooth functions and associated variational problems. *Comm. Pure Appl. Math.*, 42(5):577–685, 1989. (pages 2, 10).

[MSC79] H. Matthies, G. Strang, and E. Christiansen. The saddle point of a differential program, in "energy methods in finite element analysis", volume dedicated to professor fraeijs de veubeke; glowinski, r., rodin, e., zienkiewicz, oc, eds, 1979. (page 20).

[MSL17] R. Milk, F. Schindler, and T. Leibner. Extending dune: The dune-xt modules. *Archive of Numerical Software*, 5(1):193–216, 2017. (page 83).

[MWW15a] A. Mikelić, M. F. Wheeler, and T. Wick. Phase-field modeling of a fluid-driven fracture in a poroelastic medium. *Computational Geosciences*, 19(6):1171–1195, 2015. (pages 7, 8).

[MWW15b] A. Mikelić, M. F. Wheeler, and T. Wick. A quasi-static phase-field approach to pressurized fractures. *Nonlinearity*, 28(5):1371, 2015. (pages 2, 6, 8, 10, 65, 66, 67, 94).

[Nit71] J. Nitsche. über ein Variationsprinzip zur Lösung von Dirichlet-Problemen bei Verwendung von Teilräumen, die keinen Randbedingungen unterworfen sind. *Abhandlungen aus dem Mathematischen Seminar der Universität Hamburg*, 36:9–15, 1971. Collection of articles dedicated to Lothar Collatz on his sixtieth birthday. (page 28).

[Nit81] J. A. Nitsche. On Korn's second inequality. *RAIRO Analyse Numérique*, 15(3):237–248, 1981. (page 67).

[OI92] R. Ogniewicz and M. Ilg. Voronoi skeletons: theory and applications. In *Computer Vision and Pattern Recognition, 1992. Proceedings CVPR '92., 1992 IEEE Computer Society Conference on*, pages 63–69, Jun 1992. (page 80).

[OK95] R. L. Ogniewicz and O. Kübler. Hierarchic voronoi skeletons. *Pattern Recognition*, 28(3):343 – 359, 1995. (pages 80, 84).

[Red17] J. N. Reddy. *Energy principles and variational methods in applied mechanics*. John Wiley & Sons, 2017. (page 6).

[Riv08] B. Rivière. *Discontinuous Galerkin methods for solving elliptic and parabolic equations*, volume 35 of *Frontiers in Applied Mathematics*. Society for Industrial and Applied Mathematics (SIAM), Philadelphia, PA, 2008. Theory and implementation. (pages 66, 68).

[RLS15] S.-N. Roth, P. Léger, and A. Soulaïmani. A combined XFEM–damage mechanics approach for concrete crack propagation. *Computer Methods in Applied Mechanics and Engineering*, 283:923–955, 2015. (page 3).

[RT02] M. Rumpf and A. Telea. A continuous skeletonization method based on level sets. In *Proceedings of the symposium on Data Visualisation 2002*, pages 151–ff. Eurographics Association, 2002. (page 80).

[SBdB16] P. K. Saha, G. Borgefors, and G. S. di Baja. A survey on skeletonization algorithms and their applications. *Pattern Recognition Letters*, 76:3–12, 2016. (page 78).

[SBTZ02] K. Siddiqi, S. Bouix, A. Tannenbaum, and S. W. Zucker. Hamilton-jacobi skeletons. *International Journal of Computer Vision*, 48(3):215–231, 2002. (page 80).

[Sch13] K. Schaal. Havoc - here's another voronoi code. Master's thesis, Eberhard-Karls-Universität Tübingen, 4 2013. (page 84).

[SdBH04] E. Stein, R. de Borst, and T. J. R. Hughes, editors. *Encyclopedia of computational mechanics. Vol. 1.* John Wiley & Sons, Ltd., Chichester, 2004. Fundamentals. (pages 24, 25).

[She96] J. R. Shewchuk. Triangle: Engineering a 2d quality mesh generator and delaunay triangulator. In *Workshop on Applied Computational Geometry*, pages 203–222. Springer, 1996. (page 87).

[She97] J. R. Shewchuk. Adaptive precision floating-point arithmetic and fast robust geometric predicates. *Discrete & Computational Geometry. An International Journal of Mathematics and Computer Science*, 18(3):305–363, 1997. ACM Symposium on Computational Geometry (Philadelphia, PA, 1996). (page 86).

[She02] J. R. Shewchuk. Delaunay refinement algorithms for triangular mesh generation. *Computational geometry*, 22(1-3):21–74, 2002. (page 87).

[Sne46] I. N. Sneddon. The distribution of stress in the neighbourhood of a crack in an elastic solid. *Proc. R. Soc. Lond. A Math. Phys. Sci.*, 187(1009):229–260, 1946. (page 94).

[Som19] L. Sommer. Code supplementing the PhD thesis of Liesel Sommer. `https://doi.org/10.5281/zenodo.3241247`, 2019. (page 83).

[SP95] F. Y. Shih and C. C. Pu. A skeletonization algorithm by maxima tracking on euclidean distance transform. *Pattern Recognition*, 28(3):331 – 341, 1995. (page 80).

[Suq78] P. Suquet. *Existence et régularité des solutions des équations de la plasticité parfaite.* PhD thesis, 1978. (page 20).

[SWS03] A. Simone, G. N. Wells, and L. J. Sluys. From continuous to discontinuous failure in a gradient-enhanced continuum damage model. 192:4581–4607, 2003. (page 78).

[TF81] Y. F. Tsao and K. S. Fu. A parallel thinning algorithm for 3-d pictures. *Computer graphics and image processing*, 17(4):315–331, 1981. (page 79).

[TMRF15] E. Tamayo-Mas and A. Rodríguez-Ferran. A medial-axis-based model for propagating cracks in a regularised bulk. *International Journal for Numerical Methods in Engineering*, 101(7):489–520, feb 2015. (pages 3, 78).

[Tru92] C. A. Truesdell. *A first course in rational continuum mechanics*, volume 1. Academic Press, 1992. (page 7).

[TS80] R. Temam and G. Strang. Functions of bounded deformation. *Archive for Rational Mechanics and Analysis*, 75(1):7–21, 1980. (page 20).

[TvW02] A. Telea and J. J. van Wijk. An augmented fast marching method for computing skeletons and centerlines. In *Proceedings of the Symposium on Data Visualisation 2002*, VISSYM '02, pages 251–ff, Aire-la-Ville, Switzerland, Switzerland, 2002. Eurographics Association. (page 80).

[Was74] K. Washizu. *Variational methods in elasticity and plasticity.* Pergamon Press, Oxford,New York, 1974. (page 8).

[WM08] P. Wiederhold and S. Morales. Thinning on quadratic, triangular, and hexagonal cell complexes. In *International Workshop on Combinatorial Image Analysis*, pages 13–25. Springer, 2008. (page 80).

[WWW14] M. F. Wheeler, T. Wick, and W. Wollner. An augmented-Lagrangian method for the phase-field approach for pressurized fractures. *Comput. Methods Appl. Mech. Engrg.*, 271:69–85, 2014. (page 94).